Alma Mater Studiorum · University of Bologna

School of Science
Department of Physics and Astronomy
Master Degree in Physics

N-Body Model of Black Holes with Quantum Dust Cores

Supervisor:
Prof. Roberto Casadio

Submitted by:
Tommaso Bambagiotti

Academic Year 2022/2023

Abstract

Gravitational collapses are natural laboratories where observable signatures of a quantum theory of gravity may be produced and may be hidden in detectable astrophysical phenomena. A rooted theoretical description of a spherically symmetric gravitational collapse in General Relativity is given by the Oppenheimer-Snyder model. However, General Relativity is expected to break down at the very late stages of the collapse, and the classical dynamics to be affected by quantum gravitational effects. An effective quantum description of the Oppenheimer-Snyder model is provided by means of a bound-state quantisation procedure, where the areal radius of a single layer of dust is quantised in analogy to the position of the electron in the hydrogen atom [1]. In this work, the same procedure has been extended to an isotropic distribution of dust, which is discretised into an arbitrary number N of nested layers, each containing ν_i dust particles. The final state of the collapsed matter is represented by the global ground state of a core of quantum dust of average areal radius $R_s \approx 3/2G_N M$, where M is the total ADM mass, which naturally reproduces the area quantisation of a black hole. Then, macroscopic properties of the core have been investigated assuming that a fraction of dust particles is in an arbitrary excited state. Furthermore, a more accurate description of the ground state dust distribution has been explicitly determined. Near the centre, the mass function is shown to grow linearly with the areal radius, and the central singularity is replaced by an integrable singularity. The core surface is instead described by a non-linear fifth-order polynomial in the transitional shell $16/9\, R_H \lesssim r \lesssim 3/4\, R_H$ and matches smoothly the outer Schwarzschild solution and the inner bulk matter. Finally, observational signatures of quantum gravitational effects provided by this model has been addressed.

Contents

Introduction

Today, there are strong evidences that our universe is populated by a copious number of black holes [2]. In General Relativity, black holes are described by asymptotically flat, stationary, vacuum solutions to Einstein's field equations, and identified as regions in spacetime causally disconnected from the rest. Their boundaries are called *event horizons*[1]. Because of the very few parameters through which they are identified, namely their mass, charge and angular momentum, black holes are said to have almost "no-hair". Astronomers have discovered two populations of astrophysical black holes: stellar-mass black holes, with masses in the range $5M_\odot \lesssim M \lesssim 10^2 M_\odot$, and supermassive black holes, with masses $10^5 M_\odot \lesssim M \lesssim 10^{10} M_\odot$. In particular, the formers are thought to be created during the gravitational collapse of heavy stars [4]. When a star exhausts its nuclear fuel, thermonuclear reactions sustaining the inner pressure of the body stop and no forces can any more balance its own gravitational attraction. The inner heaviest core starts contracting, while an enormous fraction of energy and matter is expelled in few seconds, and if the collapsing core has approximately mass $M \gtrsim 5M_\odot$, nothing will be able to end the collapse and to prevent the creation of a black hole. In General Relativity, an unbounded compression of matter would curve spacetime to the point that the theory itself is expected to break down, and to be replaced by a more fundamental description. Therefore, the compression of matter into "ultra-high" density regions opens up to new scenarios, where quantum effects could significantly modify the classical dynamics of a gravitational collapse.

Most semiclassical models of the collapse of a spherically symmetric distribution of dust predict that a non-singular spacetime is left behind a re-expanding matter core [5, 6, 7]. These are *minisuperspace* model, where the system is usually reduced to describe only few degrees of freedom. With a canonical analysis of an effective action constructed from the Einstein-Hilbert action adapted to the symmetries of the system, usually it is possible to construct a quantum theory of gravitational systems using a Dirac's quantisation prescription, an approach which is usually called *quantum geometrodynamics* or *canonical quantisation* of gravity. The same qualitative picture emerges from another not totally independent approach to quantum collapse models, which is Loop Quantum Cosmology (LGC), an application of Loop Quantum Gravity (LQG) techniques to cosmology and big bang models [8, 9, 10].

Particularly interesting for our discussion is the scale at which matter stops contracting. From a Quantum Field Theory (QFT) perspective, gravity can be consistently described by an effective field theory of spin-2 vacuum fluctuations over a background vacuum solution. The

[1] There exist more general definitions in terms of dynamical horizons, which does not even require spacetime to be asymptotically flat [3].

length scale at which the theory is expected to lose a connection with experimental observations is commonly set to be the Planck length

$$\ell_p = \sqrt{\hbar G_N}. \tag{0.0.1}$$

Working in units of $\hbar = 1$, the Planck length corresponds to the inverse of the Planck mass

$$m_p = \sqrt{\frac{\hbar}{G_N}}, \tag{0.0.2}$$

through which the energy cut-off of the effective theory of gravity is equivalently set to m_p. In agreement with this picture are many collapse models, in which quantum dynamics deviate significantly from classical trajectories at energy $E \approx m_p$ [11, 5, 6]. However, in LQG models a quantum-gravitational repulsion may appear well before the Planck scale, in that the bounce could occur when the matter density ρ reaches a *critical density* ρ_c estimated to be,

$$\rho_c \sim \frac{m_p}{\ell_p^3}. \tag{0.0.3}$$

For a spherically symmetric and homogeneous source, the linear dimension ℓ of the quantum region is simply given by

$$\ell \approx \left(\frac{M}{\rho_c}\right)^{1/3} \sim \left(\frac{M}{m_p}\right)^{1/3} \ell_p, \tag{0.0.4}$$

where M is the Arnowitt-Deser-Misner (ADM) mass of the system. For solar-mass black holes, ℓ is larger than ℓ_p of tens of orders of magnitude, which open up the possibility of detecting quantum gravitational effects at scales far from the Planck scale. Furthermore, if quantum gravitational effects are not confined to some experimentally inaccessible scale, features of a quantum theory of gravity could influence the spacetime geometry up to the horizon and beyond. Disagreement with classical solutions to Einstein's equation would suggest that actually black holes have *quantum hair*.

A serious limitation of a canonical analysis is that technical complications make it impractical for any model with many degrees of freedom. All previous quantum mechanical models have as only dynamical degree of freedom the areal radius of a collapsing shell, whose dynamics will hardly reproduce a realistic collapse of a massive star.

Recently, an alternative quantisation procedure [1] to the canonical approach was shown to reproduce the picture of a spherically symmetric black holes as a final end state of the Oppenheimer-Snyder collapse. The Hamiltonian constraint of General Relativity is ensured by the radially free-falling dust, which here is described by a single shell whose areal radius satisfy the constraint equation, name the geodesic equation for radially in-falling matter. Then, the quantisation of the areal radius of a single shell provided an effective quantum mechanical description in analogy to the hydrogen atom, where the position of the electron is quantised. As a result, a highly degenerate spectrum of bound states is produced, where the ground state is characterised by a large surface area quantised accordingly to Bekenstein's area law [12]. The problem of the hairy geometry is naturally addressed in this model, since the presence of a macroscopic quantum core with width $R_s \approx R_H = 2G_N M$ should be reflected into the quantum state of the outer geometry, by producing deviations from the classical Schwarzschild

solution. The avoidance of the classical singularity is realised by showing that quantum states with wavelengths arbitrarily smaller than the gravitational radius are not physical states.

If self-consistency of new theoretical models is the only way to ensure the reliability of a model in absence of any possible experimental test, it is common practise to leave the last word only to their agreement with real experiments. To make contact with observations, one must find testable predictions within a theory which reasonably describes a realistic physical system. One main advantage from more traditional semiclassical models based on quantum geometrodynamics is that, the present approach can be easily extended to describe more realistic systems where matter degrees of freedom are included. As the mathematical complexity of the problem forbid even in this case to represent matter particles from the fundamental point of view of the Standard Model, their existence should be encoded in some entropies, which in principle could be computed from the effective quantum description. For these reasons, this work is aimed to extend this fruitful quantisation procedure to a more refined system. The content of this master thesis is organised in three Chapters:

Chapter 1

The framework of General Relativity is set up to investigate gravitational collapse scenarios. In particular, spherically symmetric collapses are analysed in the most general setting, to understand all possible dynamical behaviours predicted by Einstein's theory. After that, the Tolman-Bondi-Lemaître and Oppenheimer-Snyder collapse models has been solved analytically and all solutions determined. In particular, the OS model is shown to produce a singular solution of Einstein's field equations describing a black hole.

Chapter 2

The Hamiltonian theory of gravity is reviewed to understand, and it is addressed the problem of the quantisation of gravitational systems. After introducing the main tools for quantisation, three semiclassical models of a gravitational collapse in the canonical approach will be reviewed. In particular, the collapse of a null shell of dust and the quantum LTB and OS models. The scale at which the contraction stops is showed to be approximately at the Planck scale for the null and LTB collapses, while the canonical quantum theory of the OS model does not reproduce the expected picture of the classical model.

Chapter 3

a bound-state quantisation procedure has been extended to an isotropic distribution of dust, which is discretised into an arbitrary number N of nested layers, each containing a number ν_i of dust particles. This corresponds to the Oppenheimer-Snyder model, where dust particles fall along radial time-like geodesics in the Schwarzschild spacetime manifold. The areal radius of each shell has been quantised with a standard canonical prescription, and solutions to the Schrödinger equations has been proved to describe a discrete spectrum of bound states. The quantisation has been extended to dust particles as in [13], and the full Hilbert space of the theory has been determined. The global ground state of the collapsed ball describes a macroscopic quantum core with width $R_s \lesssim R_H$, and naturally reproduces the area quantisation of a black hole [14, 12]. After that, the properties of macroscopic core have been investigated assuming that a fraction $1 - x$ of particles is

excited, addressing the possibility to provide an effective framework to the production of gravitational waves. At the end, a more accurate description of the surface core has been proposed. In the innermost region, a linear approximation of the Misner-Sharp-Hernandez mass function replaces the central singularity with an integrable singularity. However, this approximation is shown to break down at the surface and must be replaced by a non-linear function interpolating the dust density distribution $|\psi_{N_s}|^2$ in the outermost layer.

Chapter 1

Classical dynamics of a spherically symmetric gravitational collapse

J. Robert Opphenheimer and his student Hartland Snyder pioneered in 1939 the theoretical understanding of a gravitational collapse, publishing a seminal work [15] which described the creation of a black hole in a collapse scenario. In this chapter, a general theoretical framework will be developed to describe the collapse of a spherically symmetric body. Then, the inhomogeneous dust model, called Lemaĭtre-Tolman-Bondi model, and the special case of homogeneous dust, namely the Oppenheimer-Snyder model, will be discussed.

1.1 General model

The most general spherically symmetric metric is given by the line element,

$$\mathrm{d}s^2 = -e^{2\nu(t,r)}\mathrm{d}t^2 + e^{2\psi(t,r)}\mathrm{d}r^2 + R(t,r)^2\mathrm{d}\Omega^2, \tag{1.1.1}$$

where $\mathrm{d}\Omega^2 = \mathrm{d}\theta^2 + \sin^2\theta\mathrm{d}\phi^2$ is the line element of a two-sphere. Let us consider the collapse of an anisotropic distribution of matter described by energy-momentum tensor[1]

$$T^{tt} = \rho(t,r), \quad T^{rr} = p_r(t,r), \quad T^{\theta\theta} = T^{\phi\phi} = p_\theta(t,r). \tag{1.1.2}$$

The function $\rho(t,r)$ represents the energy density as measured by a local observer instantaneously moving with matter, while $p_r(t,r)$ and $p_\theta(t,r)$ are principal pressures measured from the same observer, whose velocity field is

$$\vec{u} = (e^{-\nu}, 0, 0, 0). \tag{1.1.3}$$

In general, all possible final states of a collapsing ball are determined by classes of solutions to the Einstein's equations given the initial matter profiles

$$\rho_0(r) = \rho(t_0,r), \quad p_{r,0}(r) = p_r(t_0,r), \quad p_{\theta,0}(r) = p_\theta(t_0,r), \tag{1.1.4}$$

[1] In literature, $\{t, r, \theta, \phi\}$ are called synchronous-comoving coordinates for obvious reasons.

at the initial Cauchy hypersurface $\Sigma_0 = \Sigma(t_0)$ [16]. From (1.1.1), any hypersurface Σ_t is foliated by two-spheres of areal radius $R(t,r)$ labelled by the comoving coordinate r. To ensure that the collapse will start from a physically well-defined initial state, we have to require regularity conditions on ρ, p_r and p_θ at Σ_0. Moreover, in order to have a well-posed Cauchy problem, spacetime $(\mathcal{M}, \mathbf{g})$ is assumed to be globally hyperbolic, and the metric functions

$$\nu(t_0, r), \quad \psi(t_0, r), \quad R(t_0, r), \tag{1.1.5}$$

to be at least C^2 at the initial time, $\forall r \in [0, r_b]$.

By solving Einstein's field equations [2] [17],

$$G_{\mu\nu} = 8\pi G_N T_{\mu\nu}$$

for the metric field (1.1.1), we explicitly get from G_{00}, G_{01}, G_{11} and $G_{22} = G_{33}$ a system of four second-order partial differential equations,

$$4\pi\rho = \frac{m'}{R^2 R'} \tag{1.1.6}$$

$$4\pi p_r = -\frac{\dot{m}}{R^2 \dot{R}} \tag{1.1.7}$$

$$\nu' = 2\frac{p_\theta - p_r}{\rho + p_r}\frac{R'}{R} - \frac{p_r'}{\rho + p_r} \tag{1.1.8}$$

$$\dot{R}' = \frac{1}{2}\Big(R'\frac{\dot{G}}{G} + \dot{R}\frac{H'}{H}\Big), \tag{1.1.9}$$

where

$$m(t,r) := \frac{R}{2G_N}\big(1 - G + H\big), \tag{1.1.10}$$

and $G(t,r)$ and $H(t,r)$ are expressed by

$$H(t,r) := \dot{R}^2 e^{-2\nu(t,r)}, \quad G(t,r) := R'^2 e^{-2\psi(t,r)}. \tag{1.1.11}$$

The shorthand notations $\dot{f} = \partial_t f$ and $f' = \partial_r f$ will be adopted in the rest of this chapter. At the late stages of the collapse, the divergence of matter density $\rho(t,r)$ will signal the presence of a singularity in spacetime (a curvature singularity), as follows from (1.1.6) if either $R(t_s, r) = 0$ or $R(t_s, r)' = 0$. The vanishing of $R' = 0$ with $R \neq 0$ corresponds to a shell-crossing singularity, which occurs when two nearby matter shells cross each other at a finite comoving radius r. However, since they don't correspond to the divergence of curvature scalars, they will be disregarded assuming $R' > 0$ everywhere, Moreover, even the first condition $R(t_s, r) = 0$ fails to uniquely identify the singularity, in that for any $t_0 \leq t < t_s$, the areal radius $R(t, r = 0)$ vanishes "at the centre" (degenerate two-sphere of zero areal radius labelled by $r = 0$) of the

[2] In units $c = 1$.

collapsing ball. This issue can be solved by fixing the radial coordinate gauge; since r is still only a label, introducing a scale function $a(t,r)$ defined by

$$R(t,r) = a(t,r)r, \quad \text{with} \quad a(t_0,r) = 1, \quad a(t_s,r) = 0, \quad \forall r \in [0,r_b] \tag{1.1.12}$$

t_s will be uniquely identified by $a(t_s,r) = 0$, since $a(t,r)$ is everywhere non-vanishing on Σ_t for $t_0 \leq t < t_s$. The system of five differential equations (1.1.6), (1.1.7), (1.1.8), (1.1.9) and (1.1.10) do not fix uniquely the evolution of the seven unknown functions ρ, p_r, p_θ, ν, R, m and ψ, and that give us the freedom to choose two free functions. If an accurate description of matter inside the collapsing ball is known, the equations of state

$$p_r = p_r(\rho,\alpha), \quad p_\theta = p_\theta(\rho,\alpha),$$

will fix the two degrees of freedom and determine a unique solution to the Einstein's equation, provided more equations [3] for the additional variables α. More in general, the two free functions can be constraint if we require regularity conditions on initial data and during the dynamical evolution, and if we assume broad energy conditions on matter. In both cases, to solve analytically the Einstein's equations is almost impossible, and relevant information about the dynamics and the final state of the collapse can be extracted easily if we follow the second more general analysis. Finally, equation (1.1.10) provides the equation of motion for each shell labelled by r, which can be written more explicitly as

$$\dot{R}^2 = e^{2\nu}\Big(\frac{2G_N m}{R} + G - 1\Big), \tag{1.1.13}$$

or for the scale function $a(t,r)$,

$$\dot{a} = e^{2\nu}\Big(\frac{2G_N m}{r^3 a} + \frac{G-1}{r^2}\Big). \tag{1.1.14}$$

Before discussing the regularity and energy conditions, (1.1.9) can be solved in G, and the family of solutions expressed as

$$G(a,r) = b(r)e^{2rA(a,r)}, \tag{1.1.15}$$

where $A(a,r)$ is a solution to the first order partial differential equation

$$\partial_a A(a,r) = \frac{\nu'}{R'}. \tag{1.1.16}$$

1.1.1 Regularity and energy conditions

Einstein's equations by themselves do not provide any information about the physical properties of the collapsing matter. In classical models, restrictions on matter distribution are usually introduced to rule out "exotic" systems, which cannot be as yet reproduced in a laboratory with well-know repeatable procedures. These restrictions are typically expressed in the form

[3] For a barotropic fluid there is no additional variable α, and equations of state reduce to $p_r = p_r(\rho)$ and $p_\theta = p_\theta(\rho)$.

of energy conditions for the components of the energy-momentum tensor, and the three most common conditions which a classical distribution is required to satisfy are:

Weak energy condition (**WEC**):

$$T_{\mu\nu}Y^\mu Y^\nu \geq 0 \quad \text{for any time-like vector} \quad Y^\mu,$$

or

$$\rho \geq 0, \quad \rho + p_r \geq 0, \quad \rho + p_\theta \geq 0.$$

Dominant energy condition (**DEC**):

$$J^\mu = T^\mu{}_\nu Y^\nu,$$

is time-like and future directed for any time-like and future directed vector Y^μ, or

$$\rho \geq 0, \quad \rho \geq |p_r|, \quad \rho \geq |p_\theta|.$$

Strong energy condition (**SEC**):

$$T_{\mu\nu}Y^\mu Y^\nu + \frac{1}{2}T \geq 0 \quad \text{for any time-like vector} \quad Y^\mu,$$

or

$$\rho + p_r + 2p_\theta \geq 0, \quad \rho + p_r \geq 0, \quad \rho + p_\theta \geq 0.$$

Regular centre

The energy density, which is assumed to be $\rho \geq 0$ as part of the energy conditions[4], must be regular at the core of the ball, and (1.1.6) requires that M must behave as r^3 near the regular centre, before that the singularity is formed. Therefore, the function $m(t, r)$ must have the general form

$$m(t, r) = r^3 M(t, r), \tag{1.1.17}$$

where $M(t, r)$ is a positive regular function for $t_0 \leq t < t_s$ and $r \geq 0$. From equation (1.1.6), $m(t, r)$ as defined in (1.1.10) represents the total mass within a shell of comoving radius r at time t, and it is usually called Misner-Sharp-Hernandez *mass function*. At the regular centre, the net gravitational pull exerted on spherically distributed matter vanishes, thus also every pressure gradient will vanish in the same region. This implies that,

$$p_r'(t, 0) = 0, \quad p_\theta'(t, 0) = 0, \quad \forall t \in [t_0, t_s[. \tag{1.1.18}$$

Moreover, from (1.1.8), at $r = 0$ the derivative ν' could diverge, unless we require that

$$p_r(t, r) - p_\theta(t, r) = 0 \tag{1.1.19}$$

[4]As will be showed, for dust this requirement is satisfied by all energy conditions.

Clearly, this condition forces the core of the star to behave as a perfect fluid during the late stages of the collapse, and allow us to express ν near $r = 0$ as

$$\nu(t, r) = r^2 g(t, r), \tag{1.1.20}$$

since under condition (1.1.18) $p_r' \sim r$ for $r << 1$. Furthermore, by looking at (1.1.14), the scale factor will be regular at $r = 0$ only if $G - 1 \sim r$ for $r << 1$, which allows us to write $b(r)$ as

$$b(r) = 1 + r^2 f(r), \tag{1.1.21}$$

where $f(r)$ is a regular function at $r = 0$.

Initial conditions

Regularity conditions at the initial data Cauchy surface Σ_0 ensure that the collapse does not start in a singular state and that the initial configuration is not trapped. Once all of them are specified and the free functions fixed, the dynamical evolution of the system is completely determined. The set of initial data to be specified is

$$\rho(t_0, r) = r_0(r), \quad p_r(t_0, r) = p_{r,0}(r), \quad p_\theta(t_0, r) = p_{\theta,0}(r), \tag{1.1.22}$$

$$R(t_0, r) = R_0(r), \quad \nu(t_0, r) = \nu_0(r), \quad \psi(t_0, r) = \psi_0(r), \tag{1.1.23}$$

and

$$m(t_0, r) = m_0(r). \tag{1.1.24}$$

Since the initial values must be solution of the Einstein's equations, they will not be all independent and some of them cannot be chosen arbitrary. As later some of this initial conditions will be used, it is useful to observe that for ν and A the initial values can be expressed in terms of the only function $g(t_0, r)$,

$$\nu_0(r) = r^2 g(t_0, r) = r^2 g_0(r) \tag{1.1.25}$$

$$\partial_a A(r, a(t_0, r)) = \partial_a A\big|_0 = 2 g_0 r^2 + g_0' r^3. \tag{1.1.26}$$

Trapped configuration

In general, theoretical models describing gravitational collapses are useful to understand how and when each shell could be trapped during the collapse. A trapped surface can be defined from a two-dimensional submanifold $\mathcal{S}$ embedded in $\mathcal{M}$. There exist two future-directed null vectors orthogonal to $\mathcal{S}$, $\vec{l}$ usually called outgoing null normal, and $\vec{k}$ called *ingoing* null normal. To be more precise, they are properly outgoing and ingoing if $\mathcal{S}$ is *orientable*, i.e. we can define the *interior* and *exterior* of $\mathcal{S}$. For a trapped surface it is not necessary to require $\mathcal{S}$ being orientable, but indeed it is if we would characterise locally the boundary of a black hole. We denote $h_{\mu\nu}$ the components of the pulled-back metric in $\mathcal{S}$ from $\mathcal{M}$, where $\sqrt{h} = \sqrt{\det(h_{\mu\nu})}$. The metric tensor $\mathbf{h}$ is usually called *induced* metric in $\mathcal{S}$.

Def. 1.1.1: Trapped surface

A closed, (i.e. compact without boundary) two-dimensional spacelike submanifold $\mathcal{S}$ is a *future trapped surface* if, for both families of outgoing and ingoing future-directed null geodesics, the expansion is negative on $\mathcal{S}$,

$$\theta^{(\vec{x})}|_{\mathcal{S}} < 0 \quad \text{for} \quad \vec{x} \in \{\vec{l}, \vec{k}\}, \quad \text{where} \quad \theta^{(\vec{x})} = \frac{1}{\sqrt{h}} \pounds_{\vec{x}} \sqrt{h}$$

If $\theta^{(\vec{l})} = 0$ and $\theta^{(\vec{k})} < 0$, then $\mathcal{S}$ is called *marginally trapped surface.*

In a spherically symmetric spacetime, natural candidates for $\mathcal{S}$ are two-spheres parametrised by coordinates $\{\theta, \phi\}$, whose area is

$$A(t,r) = \int_0^{\pi} d\theta sin\theta \int_0^{2\pi} d\phi \sqrt{h} = 4\pi R(t,r)^2. \tag{1.1.27}$$

Therefore, $\nabla_\mu R$ are the components of a one-form normal to two-spheres of constant area A, and can be used to describe null geodesics [18]. Then, a shell labelled by r becomes trapped at time t_{ah} when

$$\theta^{(\vec{l})}\theta^{(\vec{k})} \propto g^{\mu\nu}\nabla_\mu R \nabla_\nu R = 0, \tag{1.1.28}$$

which using (1.1.1) simplifies to

$$g^{\mu\nu}\nabla_\mu R \nabla_\nu R = -e^{-2\nu}\dot{R}^2 + e^{-2\psi}R'^2 = 1 - \frac{2G_N m(t_{ah}, r)}{R(t_{ah}, r)} = 0.$$

The condition that every regular initial configuration must be not trapped is readily

$$\frac{2G_N m_0(r)}{R_0(r)} < 1, \tag{1.1.29}$$

and it clearly shows that the initial matter configuration $m_0(r)$ must be related to the initial boundary of the collapsing ball.

Boundary conditions

The metric tensor field (1.1.1) describes the spacetime manifold $\mathcal{M}$ only inside the collapsing ball. To have a globally defined metric $\mathbf{g}$ on $\mathcal{M}$, we have to identify the outer metric tensor and match it with the interior metric on the surface of the ball. If there is no outward flux of energy, as in dust collapse or in the presence of only transverse pressures, the field equation (1.1.7) ensures that the Misner-Sharp-Hernandez mass function is conserved during the contraction, i.e. $\dot{m} = 0$. In this case, if outside the collapsing configuration there is only empty space, Birkhoff's theorem [19] dictates that the exterior solution is locally equivalent to part of the maximally extended Schwarzschild solution, which for a collapse is uniquely identified. More care is needed if the mass function is not conserved during collapse, i.e. $\dot{m} \neq 0$, in which case a spherically symmetric solution to the field equations for a radiating source can be described by the Vaydia solution [20, 21].

1.1.2 Dynamical Evolutions

Now, it is clear that in the even in General Relativity, for a set of regular initial data at Σ_0, there are more possible dynamical evolutions for each shell of a collapsing ball:

- If $\dot{a}(t,r) < 0$, $\forall t \in [t_0, t_s[$ and $r \in [0, r_b]$. Each shell procede towards a singularity.
- If $\dot{a}(t,r) = 0$ at $t = t_{bounce}$, while at the same time $\ddot{a} \neq 0$. The collapse of the shell r halts at a finite comoving time and bounce back.
- If $\dot{a}(t,r) = \ddot{a}(t,r) = 0$ at $t = t_{eq}$. The collapse halts and the shell reaches an equilibrium configuration.

In the most general scenario, shells corresponding to an inner core $0 \leq r < \bar{r}$ will collapse and form a singularity, while the outer shells $\bar{r} \leq r \leq r_b$ may halt and bounce back, or eventually end in static configurations. Pressure-less collapsing matter like dust can never bounce or reach the equilibrium from a continuos collapse; in fact, it is possible to show that in this case, choosing suitable initial conditions at Σ_0, (1.1.14) reduces to

$$\dot{a}^2 = \frac{M(r)}{a} + f(r), \tag{1.1.30}$$

and if $\dot{a}(t,r) < 0$ at any time, it will be negative at any later time [22]. On the opposite, any kind of realistic matter distribution with non-vanishing pressures can stop collapsing and bouncing back or reaching an asymptotic equilibrium configuration, in that the gravitational attraction could be balanced by those pressures. Of great astrophysical interest are static configurations, since they could represent stable and compact remnants (with a regular core).

1.2 LTB and OS collapse models

At this point, the toolbox required to study the simplest collapse scenarios is filled up with all the essential theoretical instruments needed. Of great interests are models of spherically symmetric collapses, where any interaction other than gravity is neglected. Even if they do not accurately represent any realistic situation, since every star is known to be composed of rotating distributions of elementary interacting particles, it is generally accepted that they would encode all the relevant features to describe the mechanism through which black holes form. In fact, in these situations, the Einstein's field equations can be analytically solved, and the global structure of spacetime is explicitly revealed. Furthermore, their simple mathematical structure make them appealing to investigate deviations from classical predictions produced by a more fundamental quantum theory of gravity.

For these reasons, the models presented are the Lemaître-Tolman-Bondi (LTB) model [23, 24, 25], where the collapsing mass distribution is assumed to be inhomogeneous dust, and the simpler particular case of the Oppenheimer-Snyder (OS) homogeneous collapse [15].

1.2.1 Dust

Generically, the name *dust* denotes any kind of matter which interacts only through gravity. More precisely, for this system it is assumed that energy can only be transferred through a mass inviscid flow, while neither heat or electric current conduction is possible, nor particles have random motion. The energy momentum tensor for a dust volume element with velocity $\vec{u}$ can be written in any coordinate system $\{x^0, x^i\}$ as

$$T^{\mu\nu} = \rho\, u^\mu u^\nu, \quad g(\vec{u}, \vec{u}) = -1, \tag{1.2.1}$$

where ρ is the mass distribution as measured by an observer which instantaneously moves with dust. In the limit in which the proper mass of dust particles vanishes, this system gives a good description of radiation in the geometric-optics (high frequency) limit. In this case, the energy-momentum tensor for *null dust* with energy density ϵ will be

$$T^{\mu\nu} = \epsilon\, l^\mu l^\nu, \quad g(\vec{l}, \vec{l}) = 0, \tag{1.2.2}$$

where $\vec{l}$ is a null vector tangent to null trajectories followed by massless dust. A remarkable property of dust is that it always falls along geodesics [17].

1.2.2 LTB model - Inhomogeneous dust

For dust, the absence of random motion provides the equations of state,

$$p_r = 0, \quad p_\theta = 0, \tag{1.2.3}$$

which fix the evolution of the remaining five unknown functions by means of the field equations. In fact, now (1.1.8) becomes

$$\nu' = 0, \tag{1.2.4}$$

and requiring the initial condition $\nu(t_0) = 0$, from the continuity of the metric field we get $\nu = 0$ identically[5]. Then, (1.1.15) simplifies to

$$G(r) = R'^2 e^{-2\psi} = 1 + r^2 f(r) \tag{1.2.5}$$

while from (1.1.7) the mass function $m = m(r)$ is now independent on time. The equation of motion (1.1.13) for the areal radius R becomes,

$$\dot{R}^2 = \frac{2G_N m}{R} + 2E(r), \tag{1.2.6}$$

where we have re-defined the arbitrary function $2E(r) = r^2 f(r)$. This equation is formally identical to the equation of conservation of energy for the motion of a unit mass particle in a Newtonian potential, where $m(r)$ corresponds to the Newtonian mass within a shell labelled by

[5]Otherwise, it is possible to do a change of coordinates $t \to t' = \int e^\nu dt$ which leads to $\nu = 0$ in the new coordinates

r, and $E(r)$ play the role of the total energy within the same shell. Then, the solutions to the field equations are

$$\mathrm{d}s^2 = -\mathrm{d}t^2 + \frac{R'^2}{1+2E(r)}\mathrm{d}r^2 + R^2\mathrm{d}\Omega^2, \tag{1.2.7}$$

where R is determined by (1.2.6), and $E(r) > -1/2$ for all $r \in [0, r_b]$. The integration of (1.2.6) gives three family of solutions which depends on the sign $\varepsilon = \mathrm{sgn}(E)$ of E: for $\varepsilon \neq 0$ the solutions are parametrised by $\eta \geq 0$,

$$\begin{cases} R(t,r) = K\partial_\eta h_\varepsilon \\ t - t_s(r) = \pm \dfrac{K}{\sqrt{|2E|}} h_\varepsilon \end{cases} \tag{1.2.8}$$

where the function h_ε is defined as

$$h_\epsilon(\eta) := \begin{cases} \eta - \sin\eta, & \varepsilon = -1 \\ \sinh\eta - \eta, & \varepsilon = +1 \end{cases} \tag{1.2.9}$$

and the functions $K(r)$ and $\tilde{K}(r)$ as

$$K(r) := \frac{G_N m(r)}{|2E(r)|}, \tag{1.2.10}$$

while for $\varepsilon = 0$ the integration is trivial,

$$t - t_s = \pm\frac{\sqrt{2}}{3}\frac{R^{3/2}}{\sqrt{G_N m}} \tag{1.2.11}$$

The same solutions for the scale factor can be written using the regularity of $m(r) = r^3 M(r)$ around $r = 0$ in (1.1.17), with whom the previous equations (1.2.8), (1.2.11) for $\varepsilon \neq 0$ become

$$\begin{cases} a(t,r) = \tilde{K}\partial_\eta h_\varepsilon, \\ t - t_s(r) = \pm \dfrac{\tilde{K}}{\sqrt{|f|}} h_\varepsilon \end{cases} \tag{1.2.12}$$

whereas for $\varepsilon = 0$,

$$t(a,r) - t_s(r) = \pm\frac{\sqrt{2}}{3}\frac{a^{3/2}}{\sqrt{G_N M}}, \tag{1.2.13}$$

where the function $\tilde{K}(r)$ is defined as

$$\tilde{K}(r) = \frac{G_N M(r)}{|f(r)|}. \tag{1.2.14}$$

These solutions are expressed in parametric form in the time variable defined by

$$\eta(t,r) = \sqrt{|f(r)|}\int^t \frac{r}{R}dt', \tag{1.2.15}$$

whose physical interpretation will be clear in the homogeneous model. The arbitrary function $t_s(r)$ coming out of the integration defines the time at which the shell r reaches the singularity during a collapse, which is given by $t(a=0,r)=t_s(r)$ by imposing the initial condition (1.1.12) $a(t_0,r)=1$,

$$t_s(r) = t_0 \pm \frac{\sqrt{2}}{3}\frac{1}{\sqrt{G_N M(r)}}. \tag{1.2.16}$$

1.2.3 OS model - Homogeneous dust

Up to this point, each solution depends on three arbitrary function $m(r)$, $E(r)$ and $t_s(r)$, while the energy density ρ is determined by (1.1.6). The special case of homogeneous dust is determined requiring the mass density being a constant function of time

$$\partial_r \rho = 0. \tag{1.2.17}$$

This condition is equivalent to require that in (1.1.17) and (1.2.5),

$$M = M_0 > 0, \quad f = \frac{2E}{r^2} = -k, \tag{1.2.18}$$

where $M_0 \in \mathbb{R}_+$ and $k \in \mathbb{R}$ are constants[6] [17]. Since the collapsing configuration is homogeneous, each shell at the same comoving time will be equally pulled by gravity towards the centre of symmetry of the matter distribution; thus, the scale factor a will now depend only on time and R factorises as

$$R(t,r) = a(t)r, \tag{1.2.19}$$

while the solutions to the field equations simplifies to

$$\mathrm{d}s^2 = -\mathrm{d}t^2 + a^2(t)\Big[\frac{\mathrm{d}r^2}{1-kr^2} + r^2\mathrm{d}\Omega^2\Big], \tag{1.2.20}$$

where $a(t)$ is determined by the same solutions (1.2.12), (1.2.13), if R is expressed as (1.2.19) and $\varepsilon = -\mathrm{sgn}(k)$. Therefore, the region of spacetime filled with homogeneous dust has the topological structure determined by the Friedmann-Robertson-Walker-Lemaître (FRWL) solutions. The dynamical evolutions of $a(t)$ governed by (1.2.12) and (1.2.13) for homogeneous dust are the well-known solutions to the Friedmann's equations, which are represented in Figure 1.1. In a gravitational collapse, only the trajectories where $\dot{a} < 0$ represent a real contraction of an initial distribution of matter. For all solutions labelled by $k \in \mathbb{R}$, the final configuration will be singular, in that from (1.1.6),

$$\rho = \frac{M_0}{\frac{4\pi}{3}a^3} \to +\infty \quad \text{for} \quad a \to 0^+. \tag{1.2.21}$$

The time at which each shell reaches the singular region is now constant and does not depend on r, since t_s as determined by (1.2.16) depends only on the arbitrary constants t_0 and M_0.

[6] For dust, $M_0 > 0$ follows from any energy conditions.

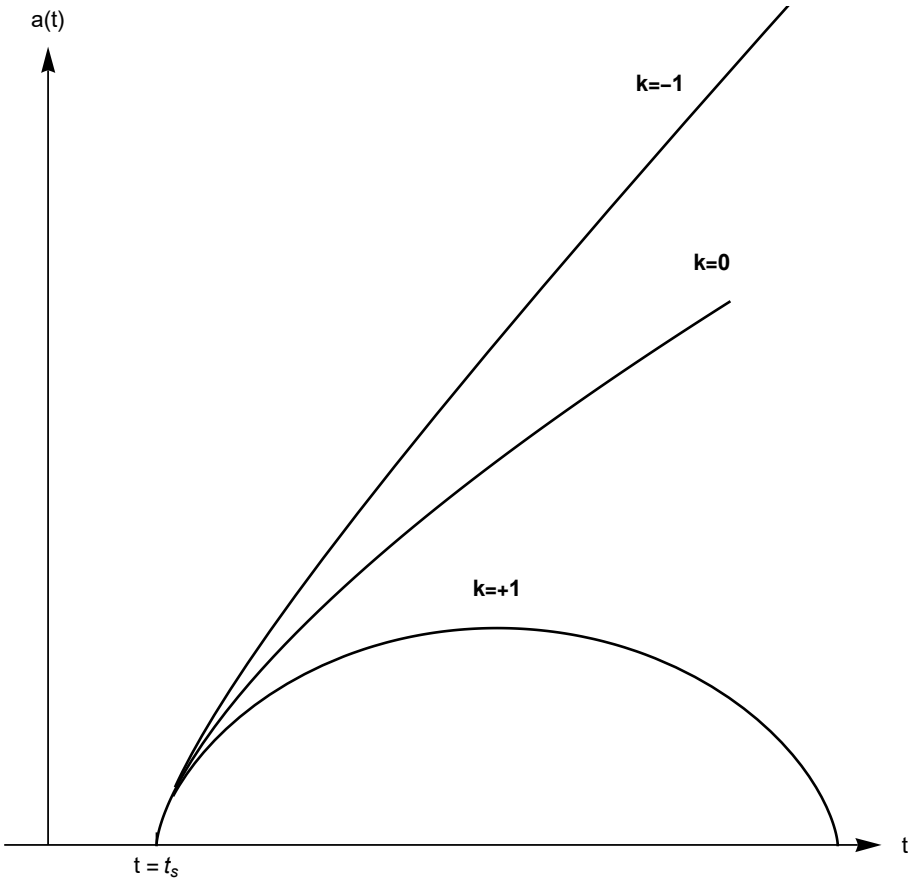

Figure 1.1: Time evolution of the scale factor $a(t)$ for values $k = 0, +1, -1$.

1.2.4 Matching with the Schwarzschild solution

What is still missing is the time,

$$t_{ah} = t(a(t_{ah}), r), \tag{1.2.22}$$

as measured by an observer radially infalling with dust, at which each shell becomes trapped, and which is implicitly determined by (1.1.29). At an intermediate stage of the collapse, it may be possible to neglect gravitational effects of the emitted radiation or matter, and to consider the outer space as empty. In this case, the global solution to the field equations will be given by the FRWL manifold for $r \leq r_b$, and by the Schwarzschild manifold for $r \geq r_b$, where both solutions match smoothly at time $t = t(a(t, r_b), r_b)$ representing the external shell. This requires that each shell moves along geodesics of both spacetimes [17, 26], and specifically, if ρ is the Schwarzschild radial coordinate,

$$\rho = R(t, r_b), \quad m(r_b) = M_s, \tag{1.2.23}$$

where M_s is the mass parameter of the Schwarzschild solution. The first shell to become trapped will be the outermost one, and that at time t_{ah} at which (1.1.29) holds,

$$2G_N m(r_b) = R(r_b, t_H), \quad t_H = t(a(t_{ah}, r_b), r_b). \tag{1.2.24}$$

Therefore, from time $t \geq t_H$, the whole dust distribution will be hidden behind an event horizon, whose equation is expressed in the Schwarzschild radial coordinate by

$$\rho_H = R(r_b, t_H) = 2G_N M_s, \tag{1.2.25}$$

which is the so called *Schwarzschild radius* of the collapsing ball [15]. Therefore, the Oppenheimer-Snyder model describes the creation of a black hole as a final end state of the collapse of an isotropic distribution of homogeneous dust.

1.2.5 Singularity

The conclusion that a collapse of homogeneous dust, and more in general every pressureless body, will always end in a singular final state is a simple consequence of the singularity theorems.

The singularity theorems[7] provide a set of sufficient conditions under which a spacetime manifold $\mathcal{M}$ must be geodesically null or/and timelike incomplete [19]. Rather than giving the general statements, they can be presented in a threefold structure.

Th. 1.2.1: Singularity theorem(s)

A spacetime $(\mathcal{M}, g)$ cannot be timelike or/and null geodesically complete if:

1. Timelike or/and null convergence conditions are satisfied,

$$R_{\mu\nu} Y^\mu Y^\nu \geq 0 \quad \text{for all timelike or/and null vectors} \quad Y^\mu;$$

2. Causality violations are ruled out by some assumptions about the causal structure of spacetime;

3. A region of "no escape" $\mathcal{S}$ exist in spacetime.

The idea behind these theorems is that, if Einstein's field equations hold and matter satisfies some energy condition, then the focusing theorem ensures that null geodesics emanating from these "no escape" regions will focus on a finite interval of the affine parameter. If M is assumed to be complete in the future (past), then the future (past) light-cone of $\mathcal{S}$ will have a topology which turns out to be inconsistent with the imposed causal structure of spacetime. In a gravitational collapse, the "no escape" region is a trapped surface [27]. In the OS model, conditions (1.2.18) ensures the timelike converge condition, global hyperbolicity is assumed to have a well-defined Cauchy problem and trapped surfaces forms at the time which each shell crosses the event horizon, whose equation for the outermost shell is given by (1.2.25). This result makes clear that, to prevent this class of spherically symmetric dust configurations from ending

[7] Historically, more than one singularity theorem were developed.

into a singularity in space-time, we have to, or violate energy conditions, or reject assumptions about the causal structure, or modify General Relativity. In any of these possibilities we do not need to introduce necessarily quantum effects, and if we rule out the most dramatic choice of rejecting General Relativity (or even the mathematical framework of differential geometry), non-singular final configurations could be in principle realised and are usually called *regular black holes* (if hidden behind an event horizon).

Chapter 2

Quantum dynamics of a spherically symmetric gravitational collapse

The dynamics of a spherically symmetric system, which undergoes a gravitational collapse, is considerably modified by quantum effects. A well-established framework which allows a quantum description of space-time is *quantum geometrodynamics*, which can be employed to quantise a Schwarzschild black hole. In this chapter, a review of the Hamiltonian formulation of General Relativity, also called *geometrodynamics*, will be given. Then, the problem of the quantisation of General Relativity will be addressed, in particular by inspecting some mini-superspace models of spherical collapses.

2.1 Canonical quantisation of black holes

2.1.1 Globally hyperbolic spacetime

In a hyperbolic spacetime $(\mathcal{M}, g)$, there exist a global 'time' function $t : \mathcal{M} \to \mathbb{R}$ such that each level set $t =$ constant is a Cauchy surface. Therefore, $\mathcal{M}$ can be foliated in Cauchy hypersurfaces Σ_t, where Σ_t are all homeomorphic, thus identified only by Σ, and its topology is $\mathcal{M} \cong \Sigma \times \mathbb{R}$.

2.1.2 Arnowitt-Deser-Misner 3+1 decomposition

The dynamics of a general relativistic system can be reduced to an initial-value problem, in particular to the time-evolution of the metric field and additional matter fields on an initial-data Cauchy surface Σ. In the Arnowitt, Deser and Misner (ADM) construction, the dynamics is generated by the Hamiltonian constraints, and the Hamilton equations of motion for the spatial metric h_{ij} are determined by the action principle given by the functional action S,

$$S = \int dt \int_\Sigma d^3x \left(P^{ij}(x)\dot{h}_{ij}(x) - N(x)\mathcal{H}_0(x) - N^i(x)\mathcal{H}_i(x)\right), \tag{2.1.1}$$

where $\mathcal{H}_0(x; h_{ij}, P^{ij}]$ and $\mathcal{H}_i(x; h_{ij}, P^{ij}]$ are the Hamiltonian constraints, $N(x)$ and $N^i(x)$ are Lagrange multipliers, and P^{ij} are the momenta conjugated to h_{ij}. The odd notation $(x; h_{ij}, P^{ij}]$

is only used there to highlight the functional dependence of the constraints on the metric field and momenta.

The configuration space of the system is a manifold $\mathcal{S}$ called *superspace*, and the constraints define the submanifold $\Gamma \subset \mathcal{S}$ of the physical states. Actually, the set Γ of physical field configurations fail to have a manifold structure at those points corresponding to isometric metric fields, in that they are singular points for Γ. The fundamental striking consequences is that General Relativity is not equivalent to a parameterised theory, thus there can never be a completely successful deparameterisation of Einstein's theory of gravity, with the only exception for a theory without any symmetry [28]. However, in very special cases, it has been proved that a (non-global and non-unique) identification of a gravitational model with a parameterised theory is possible, as prescribed by the Kuchař decomposition [29].

2.2 Kuchař decomposition

A parameterised theory can be formally constructed from any field theory by promoting to dynamical variables the spacelike embeddings. The real advantages of putting a theory in this form is to have a clear separation between kinematical (or *pure gauge*) variables with truly dynamical variables. To identify GR (or any system described by GR) with a parameterised theory, we could attempt a canonical transformation from the ADM phase space

$$(h_{ij}(x), P^{ij}(x)) \to (X^\mu(x), P_\mu(x), q^\alpha(x), p_\alpha(x)), \tag{2.2.1}$$

such that the action (2.1.1) transforms into

$$S = \int dt \int_\Sigma d^3x \, (p_\alpha(x)\dot{q}^\alpha(x) + P_\mu(x)\dot{X}^\mu(x) - N^\mu(x)\mathcal{H}_\mu(x)). \tag{2.2.2}$$

Variables $X^\mu(x)$ are the parametric equations of any embedding $X : \Sigma \to \mathcal{M}$ of the three-dimensional Cauchy surface Σ into the four-dimensional manifold $\mathcal{M}$, where $\{X^\mu\}$ are coordinates on $\mathcal{M}$ and $\{x^k\}$ are coordinates on Σ. These are purely kinematic variables, unlike the 'true' physical degrees of freedom, which we group in the canonical variables q^α and momenta p_α. Now we can eliminate 4 of the 8 kinematical degrees of freedom $X^\mu(x)$ and $P_\mu(x)$ if we do a second canonical transformation, which cast the Hamiltonian constraints in the form

$$\mathcal{H}_\mu = P_\mu + h_\mu(x; X^\mu, q^\alpha, p_\alpha] \approx 0, \tag{2.2.3}$$

and the remaining 4 by replacing (2.2.3) into (2.2.2),

$$S = \int dt \int_\Sigma d^3x \, (p_\alpha(x)\dot{q}^\alpha(x) - h_\mu(x)\dot{X}^\mu_t(x)), \tag{2.2.4}$$

where we imposed the constraint equations $\mathcal{H}_\mu \approx 0$, and $\dot{X}^\mu_t(x)$ corresponds to a choice of an embedding, i.e. they are fixed functions of (t, x^i) and must not be varied. The final action describes a physical system with an unconstrained Hamiltonian

$$H(t) = \int_\Sigma d^3x \, h_\mu(x)\dot{X}^\mu_t(x), \tag{2.2.5}$$

from which we can derive the equation of motions for q^α and p_α

$$\dot{q}^\alpha = \{q^\alpha, H\}, \quad \dot{p}_\alpha = \{p_\alpha, H\}. \tag{2.2.6}$$

Then the construction of a quantum theory is straightforward, as the constraint equation (2.2.3) can be now transformed into a functional Schrödinger equation for a wave functional $\Psi[q^\alpha]$,

$$i\hbar \frac{\delta \Psi[q^\alpha(x)]}{\delta X^\mu(x)} = h_\mu[\hat{q}^\alpha, \hat{p}_\beta]\Psi[q^\alpha(x)]. \tag{2.2.7}$$

Moreover, every observable in the quantum theory now would be function of the operators $\hat{q}^\alpha$ and $\hat{p}_\alpha$, which represents dynamical degrees of freedom, while X^μ are not turned into operators.

However, this decomposition faces many serious problems. The most important issues have been reported at the end of Section 2.1.2: transformation (2.2.1) may be non-global, which means that it could fail in some region of the ADM phase-space, may be non-unique, and can be implemented only in few lucky cases. In the quantisation of a null shell a different method from the standard canonical quantisation will be employed, because of the non-trivial boundary of the phase-space of the system.

2.2.1 Covariant gauge fixing

In this model, we would like to construct the dynamical theory of a null shell over a fixed manifold $\mathcal{M}$. However, since points of $\mathcal{M}$ are not by itself distinguishable, active displacement of points, hence a proper time evolution, cannot be disentangled from passive coordinate transformations. A possible way out for this problem is loosely to "choose a gauge", which is implemented by a *covariant gauge fixing*. A covariant gauge fixing is a purely geometric way to identify uniquely points on a background manifold $\mathcal{M}$, and can be formally described defining $\mathrm{Riem}(\mathcal{M})$ as the space of all four-dimensional Lorentian metrics on $\mathcal{M}$ and $\mathrm{Diff}(\mathcal{M})$ as the group of all spacetime diffeomorphism of $\mathcal{M}$. In general, the gauge group of a general-relativistic theory is a subgroup of $\mathrm{Diff}(\mathcal{M})$; for example, this is always the case for a system with asymptotically flat solutions, where the *asymptotic structures* $\mathcal{I}^+$ and $\mathcal{I}^-$ are common to all solutions and can be used to define asymptotical reference of frames at $\partial_\infty \mathcal{M}$[1]. An element of the quotient space $\mathrm{Riem}(\mathcal{M})/\mathrm{Diff}(\mathcal{M})$ [2] will be called a *geometry* on $\mathcal{M}$. A covariant gauge fixing is a choice of a representative metric for each geometry, that is a section

$$\sigma : U \subset \mathrm{Riem}(\mathcal{M})/\mathrm{Diff}(\mathcal{M}) \to \mathrm{Riem}(\mathcal{M}), \tag{2.2.8}$$

such that $\pi \circ \sigma = id$, where $\pi : \mathrm{Riem}(\mathcal{M}) \to \mathrm{Riem}(\mathcal{M})/\mathrm{Diff}(\mathcal{M})$ is the natural projection for the quotient space. It is called *covariant,* since each representative metric and section can be explicitly written in any coordinate system (a section will be represented by coordinates on $\mathrm{Riem}(\mathcal{M})$).

The separation between pure gauge degrees of freedom and physical variable, which will be

[1] This asymptotical reference of frame will be associated to physical observers.

[2] The quotient space $\mathrm{Riem}(\mathcal{M})/\mathrm{Diff}(\mathcal{M})$ should not be confused with the superspace $\mathcal{S}$, which instead is composed of all Euclidean three-dimensional geometries. For convenience, we consider the space of configuration for only gravity.

implemented in the shell model, now can be made more precise. In fact, a Kuchař decomposition is possible if the canonical transformation (2.2.1) can be constructed starting from a map

$$\tilde{\Gamma} \to \mathrm{Riem}(\mathcal{M})/\mathrm{Diff}(\mathcal{M}) \times \mathrm{Emb}(\Sigma, \mathcal{M}), \tag{2.2.9}$$

where $\tilde{\Gamma}$ is the constraint surface in the ADM phase-space and $\mathrm{Emb}(\Sigma, \mathcal{M})$ denotes the space of embeddings of the initial data surface Σ into $\mathcal{M}$. A general result is that, given a covariant gauge fixing σ on U, it can be used to construct the inverse map

$$\mathrm{Riem}(\mathcal{M})/\mathrm{Diff}(\mathcal{M}) \times \mathrm{Emb}(\Sigma, \mathcal{M}) \to \tilde{\Gamma}, \tag{2.2.10}$$

and that map is well-defined only if singular points are removed from $\tilde{\Gamma}$ (metric field with isometries). This construction is possible since, fixed a geometry $\gamma \in U$ and a representative metric $\sigma(\gamma)$ in $\mathcal{M}$, there exist a unique embedding $X : \Sigma \to \mathcal{M}$ of a Cauchy surface Σ in $(\mathcal{M}, \sigma(\gamma))$ determined by the gauge fixing. Then, this map has been shown to be invertible and can be extended outside the constraint surface in a neighbourhood of $\tilde{\Gamma}$ and $\mathrm{Riem}(\mathcal{M})/\mathrm{Diff}(\mathcal{M}) \times \mathrm{Emb}(\Sigma, \mathcal{M})$, where the constraint surface is given by the vanishing of the momenta conjugated to X^μ, namely $P_\mu \approx 0$, which implements the full Kuchař decomposition.

2.3 Null dust shell quantum model

For convenience, the full Hamiltonian theory and its quantisation is presented only for the gravitational collapse of a shell of massless, or *null*, dust [30]. In fact, for this system, while a mathematically consistent quantum theory with respect to asymptotic observers can be explicitly constructed, the formalism will not be burden with too technical details, which are daily bread in the canonical approach.

2.3.1 Vaidya Spacetime

The solution to Einstein's equation which describe a spherically symmetric collapse of null dust is called Vaidya spacetime [31], which can be explicitly written as

$$ds^2 = -\Big(1 - \frac{2M}{r}\Theta(w - w_0)\Big)dw^2 - 2\eta\, dw dr + r^2 d\Omega^2, \tag{2.3.1}$$

where $\Theta(z)$ is the Heaviside step function, $w = w_0$ identifies an expanding or contracting shell, with

$$w = \begin{cases} u, & \eta = +1 \\ v, & \eta = -1 \end{cases} \tag{2.3.2}$$

The coordinates u and v are the advanced and retarded Eddington-Finkelstein coordinates, while M is the energy of the shell[3]. As in the case of massive homogeneous dust, a MOTS forms as the shell crosses the hypersurface $r = 2G_N M$ before clashing with the singularity at $r = 0$. For this model, it is possible to construct an exact quantum theory starting from the canonical description of a null shell, and show that no spacetime singularity will appear at the end of the collapse.

[3] In this section, we will explicitly write G_N only where needed and set $c = \hbar = 1$.

2.3.2 Classical dynamics

Any spherically symmetric solution with a null shell of dust is composed of a flat spacetime inside the shell and of a Scharzschild spacetime outside, as showed in (2.3.2). Moreover, the two geometries must match on a null hypersurface corresponding to the shell. We can describe all physical solutions with three parameters $(\eta, M, w_\pm)$: $\eta \in \{-1, +1\}$ identify a collapsing shell ($\eta = -1$) and an expanding shell ($\eta = +1$); $w_+ = u$ and $w_- = v$ are the asymptotic retarded and advanced times for an expanding and collapsing shell respectively at $\partial_+\mathcal{M}$ and $\partial_-\mathcal{M}$; $0 < M < \infty$ identify the metric field. As will be later more clear, $(M, w_\pm)$ define two coordinate charts, one for each of the two disconnected regions $\tilde{\Gamma}_+$ and $\tilde{\Gamma}_-$ of the phase space of the system corresponding to all two possible dynamics of the shell.

From spherical symmetry, the manifold $\mathcal{M} = \Sigma \times \mathbb{R}$ reduces to $\mathcal{M} = \mathbb{R}_+ \times \mathbb{R}$, since given that $\Sigma = \mathbb{R}^3$ and fixed adapted coordinates (ρ, θ, ϕ) on Σ, we can integrate over θ and ϕ in the action and effectively reduce the dimension of the manifold.

At this point, we have to fix a gauge, that is a unique representative metric field for any physical solution given by $(\eta, M, w_\pm)$. In double null coordinates (U, V), the metric field can be expressed as

$$ds^2 = -A(U,V)dUdV + R^2(U,V)(d\theta^2 + sin\theta^2 d\phi^2), \tag{2.3.3}$$

where the functions

$$A(\eta, M, w_\pm; U, V), \quad R(\eta, M, w_\pm; U, V), \tag{2.3.4}$$

are uniquely defined for each solution requiring regularity conditions at the centre $\partial_0\mathcal{M}$, which is given by $U = V$ with coordinate $T_0 := (U+V)/2$, and continuity at the null surface representing the collapsing shell. The trajectory for the outgoing shell is fixed by $U = w_+ = u$, while for the ingoing shell by $V = w_- = v$, being u and v measurable parameters from asymptotic observers at $\partial_+\mathcal{M} = \mathcal{I}^+$ and $\partial_-\mathcal{M} = \mathcal{I}^-$. These two one-dimensional asymptotic regions are shared by all solutions and defined by equation

$$\mathcal{I}^+ = \{(U,V) | V \to +\infty, \text{ with } U = U_\infty\}, \tag{2.3.5}$$

$$\mathcal{I}^- = \{(U,V) | U \to -\infty, \text{ with } V = V_\infty\}. \tag{2.3.6}$$

The group of four-dimensional diffeomorphisms is restricted by requiring that they must commute with rotations, which is denoted as usual Diff($\mathcal{M}$), where $\mathcal{M}$ is now two-dimensional. From the restricted group of diffeomorphism, we will only consider transformations which preserve the central boundary $\partial_0\mathcal{M}$ and infinity $\partial_\infty\mathcal{M} = \partial_+\mathcal{M} \cup \partial_-\mathcal{M}$, which together define the gauge group $\text{Diff}_{0,\infty}(\mathcal{M})$. Those transformations which change the asymptotic boundaries of the space-time manifold $\mathcal{M}$ are excluded from the gauge group, because they have physical significance and turn to be useful to define the most important observables of the system. As an example, the diffeomorphism

$$\varphi_t : (U, V) \to (U + t, V + t) \tag{2.3.7}$$

sends the expanding and contracting shells $U = u$ and $V = v$ to $U = u + t$ and $V = v + t$, which acts clearly on the boundary $\partial_0\mathcal{M}$ and $\partial_\infty\mathcal{M}$. Its action on the space of solutions is

$$\varphi_t : (M, w) \to (M, w + t), \tag{2.3.8}$$

independently on $\eta \in \{-1, +1\}$, and since the double null coordinates appears in

$$A(U,V), \quad R^2(U,V), \tag{2.3.9}$$

only in the form

$$V-U, \quad U-\omega, \quad V-\omega, \tag{2.3.10}$$

each pair of solution (M,ω) and $(M,\omega+t)$ will represents the same geometry (isometric spacetimes). However, this is a transformation which sends a solution to another different physical solution, since it can be distinguished by observers which are able to measure the shell arrival (departure) retard (advanced) time $w = u$ ($w = v$). Therefore, we will not regard this transformation as a gauge one, but as a physical symmetry, and later use this group in the quantum theory to generate time evolution.

To construct the canonical theory, we need to derive the dynamics of a collapsing (or expanding) shell from an Hamiltonian action principle, which is given by the following action functional:

$$S = \int \mathrm{d}\tau \Big[p_s \dot{r}_s + \int \mathrm{d}\rho (P_\Lambda \dot{\Lambda} + P_R \dot{R} - N\mathcal{H}_0 - N^\rho \mathcal{H}_\rho - N_\infty E_\infty) \Big], \tag{2.3.11}$$

where the spherically symmetric metric in the ADM decomposition is written as

$$ds^2 = -N^2 \mathrm{d}\tau^2 + \Lambda^2 (\mathrm{d}\rho + N^\rho \mathrm{d}\tau)^2 + R^2 \mathrm{d}\Omega^2, \tag{2.3.12}$$

where $\rho = r_s(\tau)$ is the areal radius of the collapsing shell, $N_\infty = \lim_{\rho\to\infty} N^\rho(\rho)$ and E_∞ is the ADM mass[4]. As usual, N and N^ρ are the lapse and shift functions, while $\mathcal{H}_0$ and $\mathcal{H}_\rho$ identify the super-Hamiltonian and super-momentum constraints, whose analytical expression is known. The action (2.3.11) can now be transformed in new variables through a Kuchař decomposition. We will not show in detail how to compute the new variables, but essentially it is a two-step procedure as described before: the first part is a transformation on the constraint surface $\tilde{\Gamma}$ from the ADM phase space

$$(r_s, p_s, \Lambda, P_\Lambda, R, P_R) \to (u, p_u, v, p_v, U(\rho), V(\rho)) \tag{2.3.13}$$

where $U = U(\rho)$ and $V = V(\rho)$ are embedding variables satisfying some regularity and boundary conditions, and $p_u = -M$ for $\eta = 1$ and $p_v = -M$ for $\eta = -1$ on $\tilde{\Gamma}$; in the second part this transformation is extended out of the constraint surface to include the conjugate momenta P_U and P_V, which are defined to vanish on the constraint surface, i.e. $P_U, P_V \approx 0$ are the new constraints. As we pointed out before, since the phase space is actually composed of two disconnected regions $\tilde{\Gamma}_+$ and $\tilde{\Gamma}_-$, we should more precisely define a transformation, and also an action $S_\pm$, for each region. However, it is possible to prove that both dynamics can be derived from a single action functional S,

$$S = \int_{-\infty}^{+\infty} \mathrm{d}\tau (p_u \dot{u} + p_v \dot{v} - n p_u p_v) + \int_{-\infty}^{+\infty} \mathrm{d}\tau \int_0^{+\infty} \mathrm{d}\rho (P_U \dot{U} + P_V \dot{V} - N^U P_U - N^V P_V), \tag{2.3.14}$$

[4] A dot denotes a derivative with respect to the shell proper time τ.

where both outgoing and ingoing solutions are given by equation $p_u p_v = 0$, while n is a new Lagrange multiplier, which is satisfied by $p_v = 0$ if $\eta = +1$ and $p_u = 0$ if $\eta = -1$, and now $-M = p_u + p_v$ (on-shell, i.e. on the constraint surface). This last relation is well-defined since p_u and p_v can never be simultaneously different from zero on the two solutions. Moreover, the separations between embedding variables U, V, P_U, P_V and physical degrees of freedom is now obvious. It is possible to understand how to merge the two solutions if we consider an expanding shell whose trajectory is $u(\tau) = const.$ In this case, $v(\tau)$ will be an arbitrary parameter depending only on τ; it is not different from an embedding variable, being not dynamical, and the conjugated momentum p_v can be set to vanish introducing an appropriate Lagrange multiplier (the same apply for a collapsing shell, exchanging $u \to v$). In the new coordinates, the phase space has non-trivial boundaries, given by expressions

$$p_u \leq 0, \quad p_v \leq 0 \quad \frac{v-u}{2} > 0. \tag{2.3.15}$$

2.3.3 Quantisation

Any function $\tilde{\mathcal{O}} : \tilde{\Gamma} \to \mathbb{R}$ defined on the constraint surface $\tilde{\Gamma}$ which commutes with the Hamiltonian constraints,

$$\{\tilde{\mathcal{O}}, \mathcal{H}[N]\} \approx 0, \quad \{\tilde{\mathcal{O}}, \mathcal{H}[N^i]\} \approx 0, \tag{2.3.16}$$

is called *Dirac observable*. Actually, a Dirac observable is what usually in any Hamiltonian theory is simply called an *observable*, since it has the property to be independent of the action of the Hamiltonian constraints. However, since the Hamiltonian is also expected to generate the time evolution of the system, from (2.3.16) we may conclude that the dynamics of any observable is trivial. This apparent problem is historically called the problem of *frozen time* or *frozen dynamics*, whose wrong conclusion follows from assuming that weak commutativity with the Hamiltonian constraints necessarily leads to constants of motion. Starting point for the quantisation is the action (2.3.14), whose physical degrees of freedom u, p_u, v, p_v can be quantised using the *group quantisation* method. This method is based on the construction of a Lie algebra of Dirac observables, which generates a transformation that preserves the non-trivial boundaries of (2.3.15) of the phase space. The main advantage of this method is that it leads automatically to self-adjoint operators representing observables. Defining $D_u := up_u$ and $D_v := vp_v$, indeed they are Dirac observables

$$\{D_u, p_u p_v\} = 0, \quad \{D_v, p_u p_v\} = 0 \tag{2.3.17}$$

which define the Lie algebra

$$\{D_u, p_u\} = p_u, \quad \{D_v, p_v\} = p_v, \quad \{D_u, D_v\} = \{p_u, p_v\} = 0, \tag{2.3.18}$$

as follows from the canonical commutation relations

$$\{u, p_u\} = 1, \quad \{v, p_v\} = 1. \tag{2.3.19}$$

As required, the algebra (2.3.18) generates a group of transformations of the phase space which leaves the boundaries $p_u = 0$ and $p_v = 0$ unchanged. Now, as in the canonical quantisation, we

promote p_u, D_u, p_v, D_v to self-adjoint operators, acting on smooth functions $\psi_u, \psi_v \in \mathcal{H}$ as

$$(\hat{p}_w\psi_w)(p) = -p\psi_w(p), \quad (\hat{D}_w\psi_w)(p) = -ip\frac{d\psi_w(p)}{dp}, \quad \text{with} \quad w \in \{u, v\}, \tag{2.3.20}$$

where $\mathcal{H}$ is the Hilbert space of the physical states. The last boundary conditions (2.3.15) can be made explicit by means of another canonical transformation

$$t = \frac{v+u}{2}, \qquad r = \frac{v-u}{2}, \tag{2.3.21}$$

$$p_t = p_u + p_v, \qquad p_r = p_v - p_u, \tag{2.3.22}$$

which now becomes $r > 0$, a relation which is expected if we look at the variable r as the areal radius of the shell. However, this variable is not a Dirac observable,

$$\{r, p_u p_v\} = \frac{1}{2}\{v-u, p_u p_v\} \neq 0, \tag{2.3.23}$$

reason why the construction of an operator which serves as position operator is actually more involved and not without serious shortcomings, since the procedure is not unique and exclusively formal[5]. Besides that, the operator

$$\hat{r}^2 := -\sqrt{p}\frac{d^2}{dp^2}\frac{1}{\sqrt{p}} \tag{2.3.24}$$

can be extended to a self-adjoint operator whose eigenfunctions are

$$\psi(r, p) = \sqrt{\frac{2p}{\pi}}sin(rp), \quad r \geq 0. \tag{2.3.25}$$

As we observed before, time can be introduced in the quantum theory since $-(\hat{p}_u + \hat{p}_v) = -\hat{p}_t$ acts as the generator of time evolution, with t being the same parameter which generate transformations (2.3.8), and it results to be a self-adjoint operator with a positive spectrum. [6] Since in the canonical theory $-p_u - p_v = M$, the operator $-\hat{p}_t$ represents the energy of the system.

The last observable we need in order to understand the implications of the model is the direction of motion of the shell at time $t = 0$, which is represented by the operator $\hat{\eta}_0$, whose action on $\psi \in \mathcal{H}$ [7] is

$$(\hat{\eta}_0\psi)(p) = \int_0^\infty dp' \, [P_+(p, p') - P_-(p, p')]\psi(p'), \tag{2.3.26}$$

where $P_\pm(p, p')$ denotes the kernels of the projectors $\hat{P}_\pm$ on outgoing and ingoing states, which are defined as eigenfunctions of $\hat{\eta}_0$ with eigenvalues $\eta_0 = +1$ and $\eta_0 = -1$ respectively.

[5] Every observable in principle should be measurable. As well as we measure the position of particles with scattering experiments, where particle couple with an external radiation, we could try to couple an external field to the collapsing shell. At this point, asymptotic observers could detect quanta emitted through the interactions, which may provide information about the dynamics of the system.

[6] The time introduced is a classical variable, therefore corresponds to a *time before quantisation*.

[7] Technically, ψ_w and ψ belong to different representations of the Lie group which preserves the phase space boundaries. While ψ_u and ψ_v describes two independent degrees of freedom, in the ψ representation the system has only one degree of freedom (in- and out- going motions have been coupled).

2.3.4 Motion of wave packets

Having developed the full quantum mechanical theory for a null shell, we can apply it to study the dynamics of a family of normalised wave packets defined by

$$\psi_{k\lambda}(p) = \frac{(2\lambda)^{k+1/2}}{\sqrt{(2k)!}} p^{k+1/2} e^{-\lambda p}, \tag{2.3.27}$$

where $k = 1, 2, ...$ and $\lambda > 0$ defines the expected energy and energy width of each packet, with $[\lambda] = L$. Wave-packets are normalised with respect to the scalar product defined on $\mathcal{H}$,

$$< \phi, \psi >= \int_0^{+\infty} \frac{dp}{p} \phi^*(p)\psi(p). \tag{2.3.28}$$

The time evolution of the packet is generated by the action of the unitary operator $\hat{U}(t) = e^{-i\hat{p}_t t}$,

$$\psi_{k\lambda}(t, p) = \psi_{k\lambda}(p)e^{-ipt}. \tag{2.3.29}$$

In the Schrödinger r-representation, i.e. basis of eigenfunctions $\psi(r, p)$ of the position operator $\hat{r}^2$, the corresponding wave function for the (kλ)-wave packet $\Psi_{k\lambda}(t, r)$ can be defined through the integral transform

$$\Psi_{k\lambda}(t, r) := \int_0^{\infty} \frac{dp}{p} \psi_{k\lambda}(t, p)\psi(r, p), \tag{2.3.30}$$

which can be explicitly computed using properties of Euler's gamma function. As a result, we get

$$\Psi_{k\lambda}(t, r) = \frac{1}{\sqrt{2\pi}} \frac{k!(2\lambda)^{k+1/2}}{\sqrt{(2k)!}} \Big[\frac{i}{(\lambda + it + ir)^{k+1}} - \frac{i}{(\lambda + it - ir)^{k+1}} \Big]. \tag{2.3.31}$$

This analytic formula for the wave function allows us to investigate what happen at the boundary $r = 0$. Suppose that the wave packet starts in the asymptotic region $\mathcal{I}^-$ far away from the (regular) centre $r = 0$, so that $\Psi_{k\lambda}(t, 0) = 0$ for $t \to -\infty$. Then, since from (2.3.31) follows that

$$\lim_{r\to 0} \Psi_{k\lambda}(t, r) = 0 \quad \forall -\infty < t < +\infty, \tag{2.3.32}$$

and if we look at $P = |\Psi_{k\lambda}(t, r)|^2 \, dr$ as the probability to localise the wave-packet representing the shell between r and $r + dr$ at time t, then the wave packet is practically never squeezed up to a point, which we can interpret as the absence of a singularity. The question whether the dynamics of the shell describe a bounce can be addressed if we look at the portion of the packet which moves towards $r = 0$ at different times. The only ingoing part is given by the projection $\hat{P}_-\psi_{k\lambda}$, and with a not-trivial calculation we can prove that

$$||\hat{P}_-\psi_{k\lambda}||^2_{t=0} = 1/2, \quad ||\hat{P}_-\psi_{k\lambda}||^2_{t\to-\infty} = 1, \quad ||\hat{P}_-\psi_{k\lambda}||^2_{t\to+\infty} = 0. \tag{2.3.33}$$

At the time $t = 0$, the packet is equally divided into a collapsing and expanding shell, while there is only an ingoing shell at $t = -\infty$ and an outgoing one at $t = +\infty$. In the standard picture of a black hole, the event horizon acts as a one directional membrane in spacetime. However, a priori nothing prevent the wave packet to be confined within its Schwarzschild

radius, a situation which would be hardly conceivable in the classical picture, and in answer to this question we could compare the minimum expected radius $\langle r_0\rangle_{k\lambda}$ with the expected gravitational radius $\langle r_H\rangle_{k\lambda}$, where

$$\langle r_H\rangle_{k\lambda} = 2G_N\langle M\rangle_{k\lambda} = 2G_N\int_0^{+\infty}\frac{dp}{p}p\,\psi_{k\lambda}(p)^2, \tag{2.3.34}$$

and $\langle M\rangle_{k\lambda}$ is the expected energy of the wave-packet. Requiring that

$$\langle r_0\rangle_{k\lambda} + \langle\Delta r_0\rangle_{k\lambda} < \langle r_H\rangle_{k\lambda} - \langle\Delta r_H\rangle_{k\lambda}, \tag{2.3.35}$$

the inequality holds approximatively for all energies $\langle M\rangle_{k\lambda} \gtrsim m_p$[8], independently on k and λ.

2.3.5 Grey horizons

Outside the Planck regime, the shell will bounce before it reaches its expected Schwarzschild radius $\langle r_H\rangle$, while for energies starting from the Planck mass it could cross it. However, this quantum mechanical model is only a semiclassical approximation, since the dynamics of a null shell is constructed over a fixed background manifold $\mathcal{M}$, and it could be hardly trust in this regime. On the other side, since it is a self consistent mathematical model, it should be able at least to provide a mechanism to overcome the previous contradiction.

If we consider a spherical distribution of matter inside its Schwarzschild radius, the outside geometry is not unique and may correspond to that of a black hole or a white hole[9], each one characterised by a different horizon which will be called *black horizon* and *white horizon*. In our model, the metric field is determined by the physical degrees of freedom through the constraints, and it identifies the colour c and position of the Schwarzschild radius $R_H(\rho)$ outside the shell. In particular, if M is the energy of the shell, the position of the horizon is $R_H(\rho) = 2G_NM$, while the colour is determined by the direction of motion of the expanding (collapsing) shell $c = \eta$. At this point, if we move to the quantum theory, it is possible to express these quantities in terms of the operators which describes the shell, and to determine the expected position of the horizon $2G_N\langle M\rangle$ with the expected colour $\langle\eta\rangle$. Since $\hat\eta$ is determined by the difference of the projectors $\hat P_+ - \hat P_-$, from (2.3.33) the horizon will be almost black ($\langle\eta\rangle \approx -1$) when the shell crosses the horizon inwards, grey ($\langle\eta\rangle = 0$) at the time of the bounce and white ($\langle\eta\rangle \approx 1$) at the time of the outwards crossing.

2.4 LTB and OS quantum collapse models

2.4.1 Quantum Lemaĭtre-Tolman-Bondi model

The same approach towards quantisation can be extended to the LTB and OS model. Starting from the solutions to the Einstein's equations for inhomogeneous dust (1.2.7), if each shell is

[8] In units $c = \hbar = 1$, we can set $G_N = \ell_p^2 = m_p^{-2}$.

[9] This statement is a consequence of Birkhoff's theorem [19].

considered individually[10], the classical dynamics of the outermost shell can be generated with the action functional,

$$S = -\frac{1}{2}\int d\tau\, R\dot{R}^2, \tag{2.4.1}$$

where τ represents dust proper time and R is the areal radius as usual [6]. Thus, the momentum conjugate to R and the canonical Hamiltonian are,

$$P = \frac{\partial L}{\partial \dot{R}} = -R\dot{R}, \tag{2.4.2}$$

$$H = \dot{R}P - L = -\frac{P^2}{2R}, \tag{2.4.3}$$

and they set the starting point to construct the corresponding quantum theory. Differently for the null shell, in this problem it is possible to apply the standard Dirac's canonical quantisation procedure,

$$P \to \hat{P} = -i\hbar\frac{\mathrm{d}}{\mathrm{d}R}. \tag{2.4.4}$$

Then, taking care of possible ordering ambiguities, the Hamiltonian operator reads

$$\hat{H} = \frac{\hbar^2}{2}R^{-1+a+b}\frac{d}{dR}R^{-a}\frac{d}{dR}R^{-b}, \tag{2.4.5}$$

which is chosen to act on the Hilbert space endowed with the scalar product

$$\langle\psi_1,\psi_2\rangle = \int_0^{+\infty} dR\, R^{1-a-2b}\psi_1(R)\psi_2(R). \tag{2.4.6}$$

With an oculate choice of a and b, the Hamiltonian operator $\hat{H}$ can be made self-adjoint [6]. As a consequence, wave-functions will evolve unitary according to $\hat{H}$, which means that probability will be conserved with respect to dust proper time.

Energy wave packets

As in the null dust collapse, it is possible to describe the dynamics of energy wave-packets, which are constructed by superposing stationary modes ϕ_E of different energies, defined by

$$\hat{H}\phi_E = -E\phi_E, \tag{2.4.7}$$

and properly normalised in the scalar product (2.4.6). In analogy to (2.3.30), a wave-packet is defined by

$$\Psi(R,\tau) = \int_0^{+\infty} \mathrm{d}\sqrt{E}\,\phi_E(R)e^{iE\tau}A(\sqrt{E}), \tag{2.4.8}$$

where the function $A(\sqrt{E})$ is chosen to be a Poisson-like distribution, exactly as (2.3.27),

$$A(\sqrt{E}) = \frac{\sqrt{2}\lambda^{\frac{1}{2}(k+1)}}{\sqrt{\Gamma(k+1)}}\sqrt{E}^{k+\frac{1}{2}}e^{-\frac{\lambda}{2}\sqrt{E}^2}, \tag{2.4.9}$$

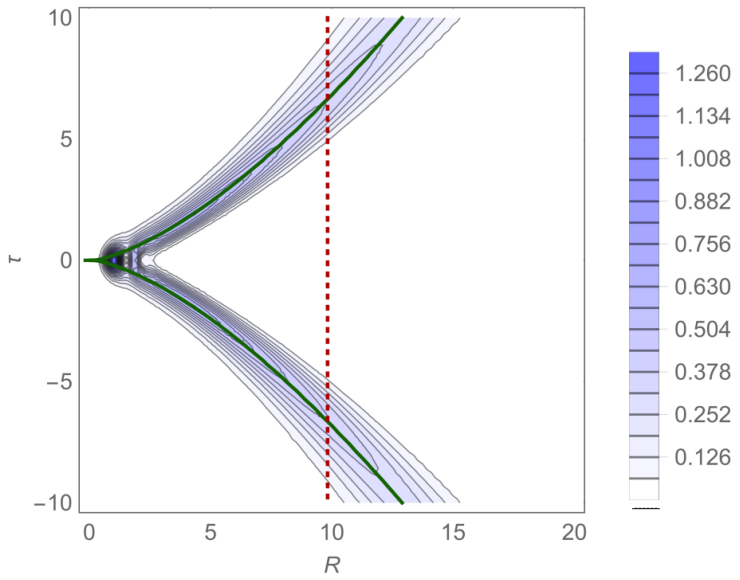

Figure 2.1: Probability to localise the shell of areal radius R at comoving time τ given by $\rho = R^{1-a-2b}|\Psi(\tau, R)|^2$. In full green line is represented the classical trajectory and in dotted red line the apparent horizon $R = 2\bar{E}$, with $a = 2$, $b = 1$ and $\lambda = 2, 2$, $k = 9.8$ (from [6]).

where $k \geq 0$ and $\lambda > 0$, with $[\lambda] = L$. Actually, the wave-packet (2.4.8) can be written in a closed form in terms of Kummer's hypergeometric function (see Appendix A for their definition). Even in this case, by looking at the probability density $\rho = R^{1-a-2b}|\Psi(R, \tau)|^2$, for which the packet representing the outermost shell bounces before reaching the singularity. In particular, for some values of λ and k the dust shell bounces inside the apparent horizon, as shown in Figure 2.1. Here, the probability distribution for R oscillates near $\tau = 0$, since the two packets corresponding to collapse and re-expansion are superimposed, which agrees with the *grey horizon* interpretation. In fact, as in the previous case, the singularity avoidance can be described as a destructive interference between two packets representing a black hole and a white hole. Unfortunately, the wave packet is too complex to compute the expectation value $\langle R \rangle = \bar{R}$ of the areal radius to get an estimate of the energy at which the collapsing configuration will start the re-expansion. An approximate expression for $\bar{R}$ can be found if we fix k, which is equal to fix the relative width of the packet,

$$\frac{\Delta\sqrt{E}}{\sqrt{\bar{E}}} \lesssim 0.53, \tag{2.4.10}$$

which still depends on the factor ordering parameter a. As a result, $\bar{R}(\tau)$ is symmetric in τ and reaches a global minimum at $\tau = 0$, which scales with $\bar{E}$ as

$$\bar{R}(\tau = 0) \propto \bar{E}^{-\frac{1}{3}}. \tag{2.4.11}$$

[10] In the full general settlement, the functional form of the Hamiltonian constraints would make it impossible to investigate whether the singularity is avoided or not at the end of the collapse.

In particular, for a solar-mass collapsing cloud, $\bar{E} \approx 10^{38} m_p$ and the expected width $\bar{R}$ at the bouncing time, results

$$\bar{R}(0) \approx 10^{-13} \ell_p. \tag{2.4.12}$$

At first sight, this result shows that the outermost shell will re-expand at sub-Planckian scales. However, in this case our attention in only in the outermost shell, and nothing prevents that during the bounce the order of the shells might be reversed.[11]. In this perspective, the window for a re-expanding phase at higher scale than the sub-Planckian $10^{-13}\ell_p$ is still open.

2.4.2 Quantum Oppenheimer-Snyder model

As for the LTB model, it is also possible the construction of a quantum theory for the collapse of spherically symmetric homogeneous dust [32]. In particular, the quantisation is extended to an OS model with a flat interior, corresponding to $k = 0$ in (1.2.20), where it is possible to construct two unitary quantum theories: one for a comoving observer, the other one for a stationary observer[12]. The detail of the quantisation, which is based on the construction of proper coherent states [32], will be omitted, since the interest of this work is to investigate if these systems could describe physical black holes, and the mechanism through which the central singularity is avoided. From the point of view of the comoving observer, the dynamics is described by the Hamiltonian,

$$H = -\frac{P}{2R^2}, \tag{2.4.13}$$

which not surprisingly is exactly the Hamiltonian of the LTB model (2.4.3), with P being the momentum conjugate to the areal radius R. After quantising the system, the modified equation of motion for a shell of areal radius R is

$$R(\tau) = \left(\frac{\hbar^2\delta}{M} + \frac{9M}{2}(\tau - \tau_0)^2\right)^{\frac{1}{3}}. \tag{2.4.14}$$

Remarkably, the second term reproduces the classical solution (1.2.13) for $k = 0$[13], while at $\tau = \tau_0$ the $\bar{E}^{-\frac{1}{3}}$ dependence on the energy of a wave packet is reproduced, modulo quantisation ambiguities which are encoded in the parameter $\delta > 0$. The dynamics for a static observer is instead generated by the multivalued Hamiltonian,

$$H = -\sqrt{\frac{A}{2}} \begin{cases} \tanh^2 P_A \\ \coth^2 P_A \end{cases}, \tag{2.4.15}$$

where A and P_A are defined through the canonical transformations,

$$A = \frac{R^2}{2}, \quad P_A = \frac{P}{R}. \tag{2.4.16}$$

[11] A scrambling of the shell would be signalled by a change of sign in R'.

[12] Each observer provides a different clock through which the unitary evolution of the quantum system can be ensured.

[13] In this chapter G_N is set to one.

In the Hamiltonian (2.4.15), the two branching points are localised at $P_A \to \pm\infty$, since

$$\lim_{P_A\to\pm\infty}\left(\tanh^2 P_A\right) = \lim_{P_A\to\pm\infty}\left(\coth^2 P_A\right) = \pm 1. \tag{2.4.17}$$

A quantisation of a multivalued hamiltonian would require multivalued quantum states, each evolving with respect to the corresponding branch of the Hamiltonian operator. Even if this construction can be formally achieved, for the present model it is not really necessary, since the two branches of the Hamiltonian will be proved to describe two completely different quantum systems. Besides that, the Hamiltonian operators in the stationary observer system make impossible finding explicitly the energy eigenfunctions. Hopefully, it is still possible to construct a quantum corrected dynamics for each branch, which is described by the "approximated" Hamiltonian operators $\hat{H}_\pm(P_A, A)$ defined as

$$M = -\frac{\Gamma(2\beta-1)\Gamma(2\beta)}{\Gamma(2\beta+1/2)\Gamma(2\beta-3/2)}\hat{H}_\pm(P_A, A), \tag{2.4.18}$$

where M is the mass of the quantum corrected dust cloud, while the branch described by $\hat{H}_+$ is called *outside branch* and the one by $\hat{H}_+$ *inside branch*[14]. Again, β is a positive real parameter which encodes quantisation ambiguities. In Figure 2.2 the dust cloud is shown to bounce when collapsing from infinity, and to re-collapse when expanding from the horizon, where the latter is a slower process than the bounce. Actually, the quantum dynamics describe also collapsing trajectories from infinity which approach the horizon from inside (outside) for the inner (outer) branches [7]. Moreover, as pointed out before, it is now evident that the two branching points at $P_A \to \pm\infty$ can never be reached in a finite time. Therefore, it is not necessary to explicitly construct multivalued quantum states. To see how transitions between these behaviours depend on M and β, it is possible to look at Figure 2.3 and 2.4. Here is represented the phase portrait at $P_A = 0$ as a function of M for different values of β. There could happen that, for fixed M and β, there exist two values of the areal radius A for which the conjugated momentum $P_A = 0$. These points correspond to classical *inversion points*, where the "velocity" of the system vanishes. Clearly, in this case, a stop can occur only in correspondence to a bounce or a re-collapse. On the opposite, when there exist no value of A for which P_A, the corresponding solution will describe an asymptotic approach to the horizon. Then, whatever branch is considered, for every β all configurations with $M \lesssim M_{crit}$ will bounce and re-collapse, while all above it not. More seriously, the bounce of the dust always happens outside the photon sphere $M = (2A)^{\frac{1}{2}}/3$, while the re-collapse between the photon sphere and the horizon $M = (A/2)^{\frac{1}{2}}$. Since everything which occur outside the photon sphere is visible from external observers, this quantum model does not reproduce anything like a black hole. Quantisation ambiguities introduce even less pleasing features. In fact, there is not a fixed value of β for which dust bounces for all M, and the two quantum theories of the comoving and static observers are not unitarily equivalent.

[14] Actually, these approximated Hamiltonian operators are lower symbols of the multivalued Hamiltonian (2.4.15). See [7] for details.

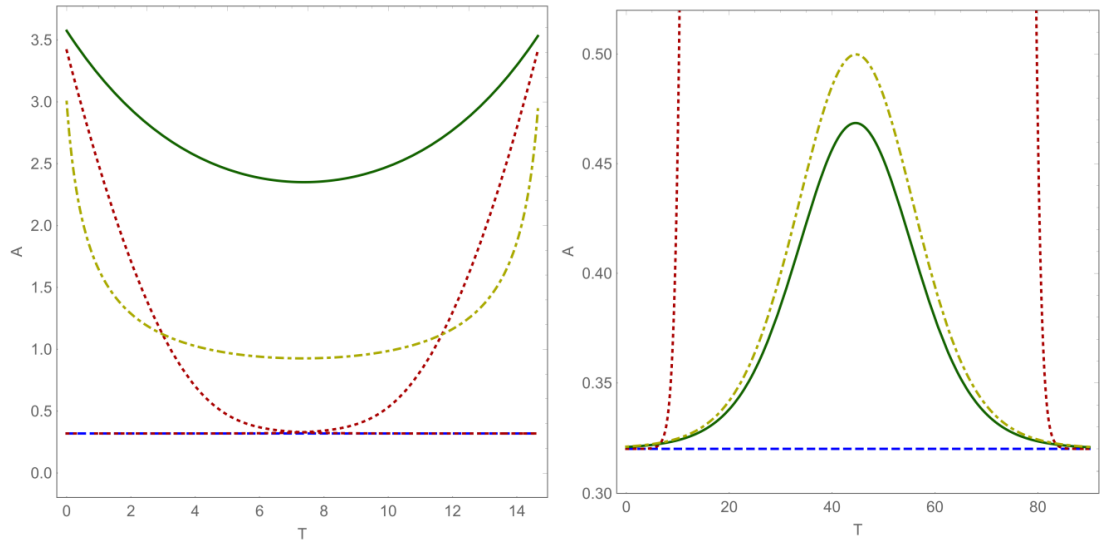

Figure 2.2: Bouncing and re-collapsing quantum corrected trajectories compared to classical expansion away and collapse towards the horizon. Green lines represent the outside branch, yellow dotted lines represent the inside branch, while the dotted red lines represent classical trajectories. The horizon $M = (A/2)^{\frac{1}{2}}$ is represented by dashed blue lines. $M = 0.4$ and $\beta = 5$, in Planck units (from [7]).

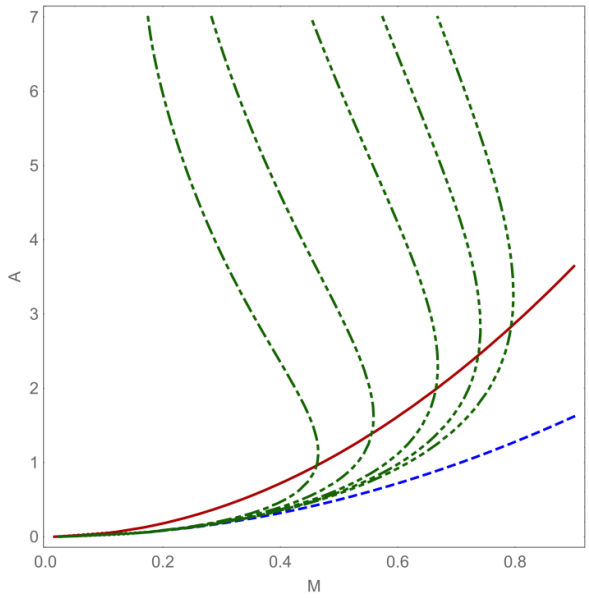

Figure 2.3: Quantum corrected phase space portraits at $P_A = 0$ for the outside branch of the Hamiltonian, for different β (green lines). The horizon $M = (A/2)^{\frac{1}{2}}$ is represented in dashed blue line, while the photon sphere $M = (2A)^{\frac{1}{2}}/3$ is represented in red full line, in Planck units (from [7]).

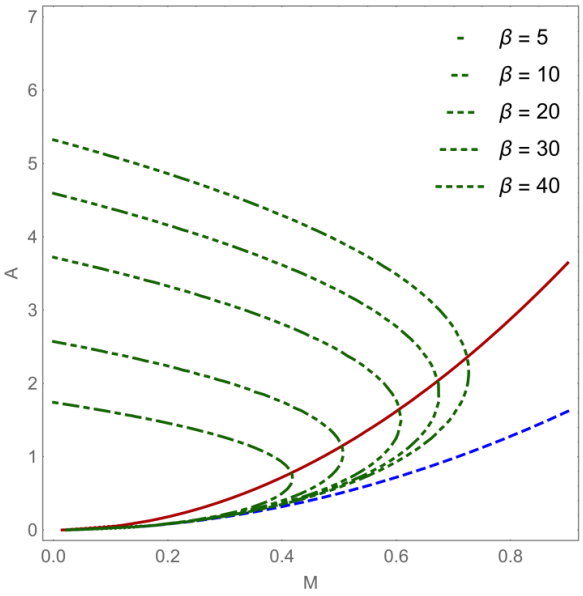

Figure 2.4: Quantum corrected phase space portraits at $P_A = 0$ for the inside branch of the Hamiltonian, for different β (green lines). The horizon $M = (A/2)^{\frac{1}{2}}$ is represented in dashed blue line, while the photon sphere $M = (2A)^{\frac{1}{2}}/3$ is represented in red full line, in Planck units (from [7]).

Chapter 3

Quantum ball of dust

In this chapter, an alternative quantisation procedure to the canonical approach of the Oppenheimer-Snyder collapse is presented [1]. In particular, the main objective is to extend it to an isotropic distribution of dust particles discretised into N arbitrary layers.

3.1 Gravitational collapse of N-layers of dust

As a starting point, let us consider the gravitational collapse of a spherically symmetric distribution of dust with ADM mass M. Since dust interacts only gravitationally, the shell of areal radius $R = R(\tau)$ will follow a radial time-like geodesic in the Schwarzschild spacetime

$$\mathrm{d}s^2 = -\Big(1 - \frac{2G_N M}{r}\Big)\mathrm{d}t^2 + \Big(1 - \frac{2G_N M}{r}\Big)^{-1}\mathrm{d}r^2 + r^2\mathrm{d}\Omega^2, \tag{3.1.1}$$

where τ is time as measured by a clock comoving with dust, and $\mathrm{d}\Omega = \mathrm{d}\theta^2 + \sin^2\theta\mathrm{d}\phi^2$ is the line element for a 2-sphere of areal radius r. Instead of proceeding with the quantisation of a single layer of dust, as in [1], we can generalise this model to an isotropic distribution of dust (a ball) discretized in N nested shells with areal radii R_i, $i = 1, 2, ..., N+1$, surrounding a central core of ADM mass $M_1 = \mu_0$ and areal radius $r = R_1(\tau)$. We can assume these layers to be ordered, i.e. $R_{i+1} > R_i$, $\forall\, i = 1, ..., N$, and to carry only a fraction $\mu_i = \epsilon_i M$ of the total ADM mass M. The fraction contained inside a shell of radius $r < R_i$ is thus

$$M_i = \sum_{k=0}^{i-1} \mu_k, \tag{3.1.2}$$

with the total mass being

$$M_{N+1} = \sum_{i=0}^{N} \mu_i \equiv M. \tag{3.1.3}$$

Each layer will fall freely along radial geodesics of the metric

$$\mathrm{d}s^2 = -\Big(1 - \frac{2G_N m}{r}\Big)\mathrm{d}t^2 + \Big(1 - \frac{2G_N m}{r}\Big)^{-1}\mathrm{d}r^2 + r^2\mathrm{d}\Omega^2\,, \tag{3.1.4}$$

where $m = m(r)$ is the fraction of total ADM mass inside each sphere of radius $r = R_i(\tau)$. The radial geodesic equation for $R_i(\tau)$ is (see Appendix C)

$$\Big(\frac{\mathrm{d}R_i}{\mathrm{d}\tau}\Big)^2 - \frac{2G_N M_i}{R_i} = \frac{E_i^2}{M_i^2} - 1, \quad i = 1, ..., N \tag{3.1.5}$$

where E_i is the conserved momentum conjugate to $t = t_i(\tau)$; this equation can be cast in the form of the Newtonian equation of conservation of energy by defining $P_i = \mu_i dR_i/d\tau$,

$$H \equiv \frac{P_i^2}{2\mu_i} - \frac{G_N \mu_i M_i}{R_i} = \frac{\mu_i}{2}\Big(\frac{E_i^2}{\mu_i^2} - 1\Big), \quad i = 1, ..., N\,, \tag{3.1.6}$$

where P_i is the momentum conjugated to $r = R_i(\tau)$. As a consequence of isotropy the momenta L_i conjugated to $\phi = \phi_i(\tau)$ are also conserved, but since we are now interested only in the quantisation of non-rotating infalling dust, we have set $L_i = 0$, $\forall i = 1, ..., N$.

3.1.1 Quantisation

In the framework of canonical quantisation, the observable areal radius R_i and its conjugated momentum P_i are represented by non-commuting hermitian operators $\hat{R}_i$ and $\hat{P}_i$, where the commutation relation

$$\big[\hat{R}_i, \hat{P}_j\big] = i\hbar\delta_{i,j}\hat{\mathbb{1}} \tag{3.1.7}$$

encodes the uncertainty relation between R_i and P_i separately for each dust layer. With the canonical quantisation prescription $\hat{P}_i = -i\hbar\partial_{R_i}$, equations (3.1.6) become time-independent Schrödinger equations, one for each shell:

$$\hat{H}_i\psi_{n_i} = \Big[-\frac{\hbar^2}{2\mu_i}\Big(\frac{\mathrm{d}^2}{\mathrm{d}R_i^2} + \frac{2}{R_i}\frac{\mathrm{d}}{\mathrm{d}R_i}\Big) - \frac{G_N\mu_i M_i}{R_i}\Big]\psi_{n_i} = \mathcal{E}_{n_i}\psi_{n_i}. \tag{3.1.8}$$

By solving these Schrödinger equations (see Appendix A), and expressing the Newton constant $G_N = \ell_p/m_p$ and the reduced Planck constant $\hbar = \ell_p m_p$, the eigenvalues of the Hamiltonian can be computed, and they are given by the expression

$$\mathcal{E}_{n_i} = -\frac{G_N^2 {\mu_i}^3 M_i^2}{2\hbar^2}\frac{1}{{n_i}^2} = -\frac{\mu_i^3 M_i^2}{2m_p^4}\frac{1}{n_i^2}. \tag{3.1.9}$$

The eigenfunctions $\psi_{n_i}(r)$ associated to the eigenvalues $\mathcal{E}_{n_i}$ are

$$\psi_{n_i}(R_i) = \Big(\frac{\mu_i^6 M_i^3}{\pi\,\ell_p^3\, m_p^9\, n_i^5}\Big)^{\frac{1}{2}} \exp\Big\{-\frac{\mu_i^2\, M_i\, R_i}{\ell_p\, m_p^3\, n_i}\Big\}\, L^{(1)}_{n_i-1}\Big(\frac{2\,\mu_i^2\, M_i\, R_i}{\ell_p\, m_p^3\, n_i}\Big), \tag{3.1.10}$$

where $n_i = 1, 2...$, and they define a complete set of eigenfunctions in the Hilbert space $\mathcal{H}_i^L$ of a single dust layer, with the scalar product defined as

$$< \psi_{n_i}, \psi_{n_i'} >= 4\pi \int_0^{+\infty} \mathrm{d}R_i\, \psi^*_{n_i}(R_i)\psi_{n_i'}(R_i) = \delta_{n_i,n_i'} \tag{3.1.11}$$

and $i = 1, ..., N$. The eigenvalues of the Hamiltonian are not independent of the conserved quantities E_i; therefore, the only allowed states are those with a well-defined energy, and they must satisfy the condition

$$0 \leq \frac{E_i^2}{\mu_i^2} = \frac{2\mathcal{E}_{n_i}}{\mu_i} + 1 \tag{3.1.12}$$

which introduce a lower bound on the quantum number n_i

$$\frac{\mu_i M_i}{m_p^2} \leq n_i. \tag{3.1.13}$$

Since the left-hand side of (3.1.13) depends on M_i, the lower bound on n_i depend on how the dust is distributed among the inner layers, thus the ground state of a single layer, which is defined by the lowest allowed value of n_i

$$n_i \equiv n_{0,i} = \frac{\mu_i M_i}{m_p^2}, \tag{3.1.14}$$

will depend on the inner distribution of dust among the N layers and the core. The same is true for energy eigenvalues $\mathcal{E}_{n_i}$ and eigenfunctions ψ_{n_i}, which are not completely specified until a criterion to determine the mass fractions μ_i is found.

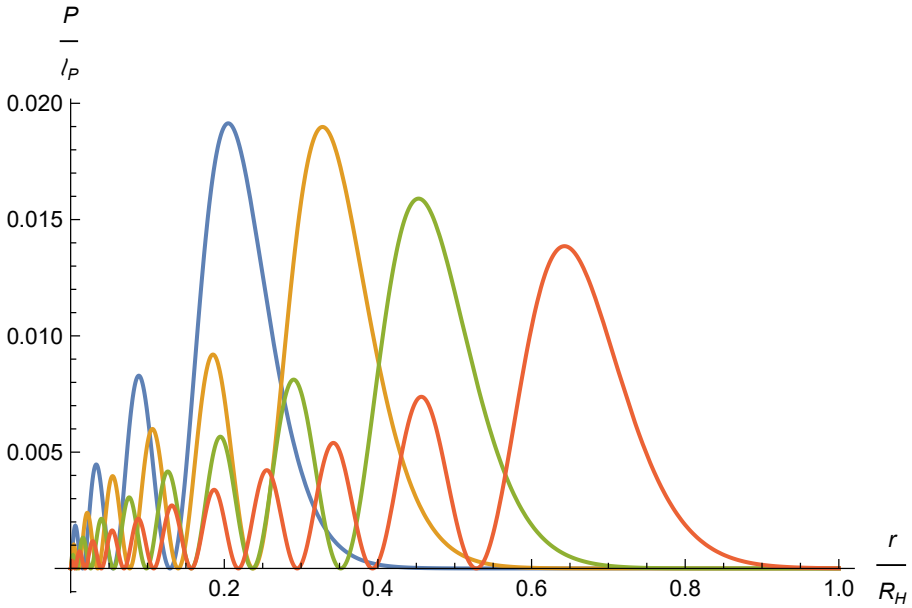

Figure 3.1: Ground state probability density $|\psi_i|^2$ for a black hole of total ADM mass $M \approx 150\, m_p$, $\mu = m_p/10$ and $R_H = 300\, \ell_p$. The number of layer is $N = 4$.

3.1.2 Fuzzy quantum layers

The expectation value and uncertainty for the areal radius of the i-th shell are (see Appendix A)

$$\bar{R}_{n_i} = \langle \psi_{n_i}, \hat{R}_{n_i} \psi_{n_i} \rangle = \frac{3\ell_p m_p^3}{2\mu_i^2 M_i} n_i^2, \tag{3.1.15}$$

$$\frac{\Delta R_{n_i}}{\bar{R}_{n_i}} = \frac{\sqrt{2+n_i^2}}{3n_i}. \tag{3.1.16}$$

The collapse of a pressureless distribution of matter can only collapse towards the central singularity, since there is no force that can withstand the gravitational attraction, as in the classical Oppenheimer-Snyder model. However, if the areal radii are subjected to the quantisation prescription (3.1.7), which prescribes that conjugated variables must obey the Heisenberg uncertainty relation, the expected areal radius (3.1.15) of each shell becomes finite. With a careful look, the width and energy of the lowest state $n_N = 1$ for the outermost shell $i = N$ will be approximately

$$\bar{R}_1 \sim \left(\frac{m_p}{M}\right)^3 \ell_p, \quad \mathcal{E}_1 \sim -M\left(\frac{M}{m_p}\right)^4, \tag{3.1.17}$$

where μ_i is assumed to be an arbitrary fraction of M, approximately of the same order of magnitude. For a black hole with ADM mass $M = M_\odot$, $M/m_p \approx 10^{38}$, and this state is not much different from a classical singularity. However, since not all energy eigenstates can represent physical states, the average radius for a shell is minimum when it is in the ground state (3.1.14),

$$\bar{R}_{n_i} \geq \bar{R}_{n_{0,i}} = \frac{3}{2}\ell_p \frac{M_i}{m_p} = \frac{3}{2} G_N M_i. \tag{3.1.18}$$

If instead a singular configuration is identified by means of its areal radius, and not the quantum number n_i, by looking at Figure 3.1 the probability to localise a shell in the ground near the centre of symmetry is shown to vanish. In this perspective, the bound (3.1.13) select these states for which each shell almost surely will not be found near the centre. This is the bound found in [1], which would not emerge in the Newtonian theory, since in this case $\mathcal{E}_i = E_i$ and the full spectrum would be physically allowed. In the quantum theory, each areal radius can a priori assume every possible value in the range $0 < R_i < +\infty$ and nothing can prevent the assumption $R_{i+1} > R_i$ from being respected during the collapse. Therefore, to guarantee that the nesting of dust shells is conserved, we have to impose that for each pair of layers, the mean radius of the outermost must be greater or equal to the mean innermost radius; this requirement would result in the same former assumption in terms of averages, but since each radius R_{n_i} fluctuate around $\bar{R}_{n_i}$, well-defined nested layers must satisfy

$$\bar{R}_{n_{i+1}} - \bar{R}_{n_i} \gtrsim \Delta R_{n_i}, \tag{3.1.19}$$

$\forall i = 1, \ldots, N$. In other words, in each pair, the outermost radius must be outside a thick shell with average radius $\bar{R}_{n_i}$ and thickness ΔR_{n_i}. This requirement allows us to constraint the dust

distribution among each layer, and in fact, as we will see later, this inequality determines a criterion to fix M_{i+1} in terms of M_i for a dust layer in the ground state. Using the equations (3.1.15) and (3.1.16), (3.1.19) can be written as

$$\bar{R}_{n_{i+1}} \gtrsim \bar{R}_{n_i}\Big(1 + \frac{\Delta R_{n_i}}{\bar{R}_{n_i}}\Big), \tag{3.1.20}$$

$$\bar{R}_{n_{i+1}} \gtrsim \bar{R}_{n_i}\Big(1 + \frac{\sqrt{2+n_i^2}}{3n_i}\Big). \tag{3.1.21}$$

If we assume $n_i \gg 1$, this bound becomes

$$\bar{R}_{n_{i+1}} \gtrsim \frac{4}{3}\bar{R}_{n_i}, \tag{3.1.22}$$

and using the value $\bar{R}_{n_i}$ in (3.1.15) yields

$$\frac{\mu_i^2 M_i}{\mu_{i+1}^2 M_{i+1}} \frac{n_{i+1}^2}{n_i^2} \gtrsim \frac{4}{3}. \tag{3.1.23}$$

For layers in the ground state $n_i = n_{0,i} = \mu_i M_i/m_p^2$, we obtain

$$M_{i+1} \gtrsim \frac{4}{3}M_i, \tag{3.1.24}$$

which is the relation previously mentioned, and it implies $\mu_i \gtrsim M_i/3$ from the defining relation (3.1.2), $\forall i = 1, \ldots, N$. The hyphotesis on quantum numbers $n_{0,i} \gg 1$ is then equivalent to require that $M_i \gg m_p$, which can be met by macroscopic black holes.

3.2 Global ground state

Each set of energy eigenfunctions $\{\psi_{n_i}\}_{n_i=0}^{+\infty}$ is a complete orthonormal set in the Hilbert space $\mathcal{H}_i^L$ of a single layer, as is the case of the hydrogen atom energy states. Moreover, each layer carries a different fraction of total mass μ_i, and since a priori they are all different, each layer is distinguishable from the others and the total Hilbert space $\mathcal{H}$ is

$$\mathcal{H} = \mathcal{H}_1^L \otimes \mathcal{H}_2^L \cdots \otimes \mathcal{H}_N^L. \tag{3.2.1}$$

Any quantum state representing the collapsing ball will be described by a linear superposition of basis element of $\mathcal{H}$ naturally given by the tensor product of the energy eigenstates of $\mathcal{H}_i$, namely each state $|\Psi\rangle$ can be written as

$$|\Psi\rangle = \sum_{n_1=0}^{+\infty} \sum_{n_2=0}^{+\infty} \cdots \sum_{n_N=0}^{+\infty} C_{n_1,n_2,\ldots,n_N} |n_1, n_2, \ldots, n_N\rangle, \tag{3.2.2}$$

where $|n_1, n_2, \ldots, n_N\rangle$ is the tensor product

$$\bigotimes_{i=1}^{N} |n_i\rangle = |n_1, n_2, \ldots, n_N\rangle \tag{3.2.3}$$

and $C_{n_1,n_2,\ldots,n_N} = \langle n_1, n_2, \ldots, n_N|\Psi\rangle \in \mathbb{C}$. Furthermore, to represent properly a quantum state $|\Psi\rangle$ must be normalized, i.e $\langle\Psi|\Psi\rangle = 1$. The ground state of the quantum ball is represented by the tensor product of single layer ground states

$$|n_0\rangle = |n_{0,1}, n_{0,2}, \ldots, n_{0,N}\rangle, \tag{3.2.4}$$

with $|n_0\rangle$ solution of the Schrödinger equation

$$\hat{H}|n_0\rangle = \mathcal{E}_0|n_0\rangle \tag{3.2.5}$$

with eigenvalue $\mathcal{E}_0 = \sum_{i=1}^{N} \mathcal{E}_{n_{0,i}}$. The operator $\hat{H}$ is defined as the hermitian operator acting on the Hilbert space $\mathcal{H}$ given by the tensor product of hamiltonians $\hat{H}_i$, i.e. $\hat{H} = \hat{H}_1 \otimes \hat{H}_2 \cdots \otimes \hat{H}_N$. In the ground state, the average areal radius of the ball R corresponds, up to quantum fluctuations, to the outer radius of the outermost shell $\bar{R}_{n_{0,N}}$, which from (3.1.18) reads

$$R_s := \bar{R}_{n_{0,N}} + \Delta R_{n_{0,N}} \approx \frac{3}{2} G_N M, \tag{3.2.6}$$

and clearly results that $R_s \lesssim R_H = 2G_N M$, where $r = R_H$ is the gravitational radius of the spherical distribution of dust. The quantum numbers labelling the ground state of the ball $|n_0\rangle$ depend only on N and M, in fact if we set $\mu_i \approx M_i/3$ in (3.1.14) we get

$$\begin{aligned} n_{0,i} &\approx \frac{1}{3}\frac{M_i^2}{m_p^2} \\ &\approx \frac{1}{3}\left(\frac{3}{4}\right)^{2N-2i+2} \frac{M^2}{m_p^2}, \end{aligned} \tag{3.2.7}$$

where we expressed M_i in terms of $M = M_{N+1}$, namely

$$M_i \approx \left(\frac{3}{4}\right)^{N+1-i} M, \quad \forall i = 1, \dots, N+1. \tag{3.2.8}$$

Moreover, for the outer layer of the outermost shell corresponding to $i = N+1$, both quantum number $n_{0,N+1}$ and radius $R_{N+1} \approx R$ are totally independent on the number of layers, which determines only the inner structure of the ball, and the only parameter left free is M. Equation (3.2.8) holds also for radiuses $\bar{R}_i$, upon replacing M with R, and since nothing has yet been said abou the mass M_1 and mean radius $\bar{R}_1$ of the inner core, we can now write them as

$$\bar{R}_1 \approx \left(\frac{3}{4}\right)^{N} R_s \tag{3.2.9}$$

$$M_1 \approx \left(\frac{3}{4}\right)^{N} M, \tag{3.2.10}$$

which confirm that N determines how we describe the inner structure of the ball, and thus the inner core.

3.2.1 Multi-particle quantum states

Up to now, we have completely neglected the dust particles of which the collapsing ball is composed of. We can extend our model by requiring that each layer contain $\nu_i = \mu_i/\mu$ dust particles falling freely along the radial geodesics $r = R_i(\tau)$, each one with equal proper mass μ. Formally, everything said hold with the only substitution $\mu_i \to \mu$. In particular, the wave functions (3.1.10) will describe the ground state of the ν_i particles in each layer, which is now defined by $n_{0,i} = \mu M/m_p^2$, under the requirement $\bar{R}_{n_{i+1}} \gtrsim \bar{R}_{n_i} + \Delta R_{n_i}$, which means that dust particles of the same layer will be in the same quantum state. The single layer Hilbert space $\mathcal{H}_i^L$ is given by the tensor product of copies of the single-particle Hilbert space $\mathcal{H}_i$

$$\mathcal{H}_i^L = \bigotimes_{k=1}^{\nu_i} \mathcal{H}_i \tag{3.2.11}$$

where the total number of dust particles $\sum_{i=0}^{N} \nu_i = M/\mu$ is fixed, as required by any well-defined quantum mechanical system. Dust particles are not distinguishable, but since in our analysis we are not interested in their statistical properties, we will assume them to be distinguishable. Therefore, the multi-particles state $|\{n_1, \nu_1\}, \dots, \{n_N, \nu_N\}\rangle$ is now defined as

$$\bigotimes_{i=1}^{N} \left(\bigotimes_{k=1}^{\nu_i} |n_k\rangle \right) := |\{n_1, \nu_1\}, \dots, \{n_N, \nu_N\}\rangle, \tag{3.2.12}$$

while the global ground state of the ball is identified with the ket

$$|\{n_{1,0}, \nu_1\}, \dots, \{n_{N,0}, \nu_N\}\rangle \tag{3.2.13}$$

and $|n_k\rangle \in \mathcal{H}_k$, with $k = 1, 2, \ldots$ labelling layers. Remarkably, by looking at the expression for the ground state quantum number $n_{0,N} := N_s$ for the inner layer of the outermost shell $(i = N)$,

$$N_s = \frac{\mu M_N}{m_p^2} = \frac{3}{4}\frac{\mu M}{m_p^2}, \tag{3.2.14}$$

the black hole area quantisation [12, 14] is recovered by multiplying the corresponding quantum number with the total number of dust particles M/μ

$$\frac{M}{\mu} N_s \approx \frac{R_H^2}{\ell_p^2} \approx \frac{M}{m_p^2}. \tag{3.2.15}$$

The same law can be also recovered from the quantisation of the radius of each layer; in fact, by using (3.2.7), the area law becomes

$$N_s \approx \frac{R_H^2}{\ell_p^2} \approx \frac{M^2}{m_p^2}, \tag{3.2.16}$$

where the matter degrees of freedom are not explicitly counted, exactly as in the one-body model [1]. The formula (3.2.15) is reproduced by the corpuscolar description of black holes [33]. From the perspective of corpuscolar gravity, a black hole is composed of N_G soft-gravitons marginally bound on their own gravitational potential U_{GG}, which form a condensate with Compton-de Broglie wavelength $\lambda_G \approx R_H$. The above scaling relation can be recovered assuming that the gravitational interaction can be approximated by the Newtonian potential

$$V_N(r) = -\frac{G_N M}{r}. \tag{3.2.17}$$

From the quantum field theory point of view, in the Newtonian approximation the confined gravitons could superimpose within a finite volume of width $\lambda_G \approx R_H$. Assuming that the total mass of a black hole $M \approx N_G \varepsilon_G$, that is interactions among low energy gravitons are still negligible, where $\varepsilon_G \sim \hbar/\lambda_G$ is the energy scale of graviton, relation (3.2.15) is readily

$$N_G \sim \frac{M}{\varepsilon_G} \sim \frac{M^2}{m_p^2} \sim \frac{R_H^2}{\ell_p^2}, \tag{3.2.18}$$

provided that $N_G \approx N_s M/\mu$. However, in the original formulation of the corpuscolar description, matter degrees of freedom were considered to be subdominant to the gravitational ones, and their role essentially neglected. This conclusion is not supported by this model, since the existence of a macroscopic core (3.2.6) hidden behind the gravitational radius R_H is a consequence of the quantum description of the collapsed dust. On the contrary, it is supported the idea that the matter core inside the black hole defines its interior structure, since the ball average radius R_s is determined through the expectation value of the position operator $\hat{R}_N$ on the quantum state (3.2.14).

Besides that, a spherically symmetric compact core in the ground state is expected to produce deviations, or *quantum hair*, from the Schwarzschild solution in the exterior of the black hole [34, 35], a fact which would disprove the traditional *No-hair* conjecture. This last

point is clarified by considering the gravitational energy of a spherical matter distribution of mass M enclosed in a ball of radius R_s,

$$U_N(R_s) \approx M V_N(R_s) \approx -\frac{G_N M^2}{R_s}. \tag{3.2.19}$$

Now, the gravitational potential can be represented by the expectation value of a scalar field $\hat{\Phi}$ on the coherent state $|g\rangle$ [34],

$$\langle g|\hat{\Phi}|g\rangle \approx V_N, \tag{3.2.20}$$

where the normalisation of $|g\rangle$ gives the number of soft-gravitons (3.2.18) generated by matter inside the sphere of radius R_s. If is assumed that gravitons has the same wave-length λ_G, the energy of each graviton will be

$$\varepsilon_G \approx \frac{U_N}{N_G} \sim -\frac{\hbar}{\lambda_G}, \tag{3.2.21}$$

and gravitons self-interactions reproduce the post-Newtonian energy

$$U_{GG}(R_s) \approx N_G \varepsilon_G V_N(R_s) \sim \frac{G_N^2 M^3}{R_s^2}. \tag{3.2.22}$$

This simple argument shows how non-linearities, encoded in the self-interacting gravitons, can be employed to determine quantum corrections to the Newtonian potential of a spherical source of mass M, and allow us to identify N_G with the number of soft gravitons in the coherent state $|g\rangle$ representing the gravitational potential generated by the source.

For this Oppenheimer-Snyder based model, quantum corrections could be computed for the metric potential V_N which appears in the Schwarzschild metric[1],

$$\mathrm{d}s^2 = -(1+2V_N)^2\mathrm{d}t^2 + (1+2V_N)^{-1}\mathrm{d}r^2 + r^2\mathrm{d}\Omega^2, \tag{3.2.23}$$

and which plays the role of a potential in the geodesic equations (3.1.5). In order to make contact with observations, a long-lasting successful working hypothesis is based on the assumption that there exist a classical background solution $(\mathcal{M}^{cl}, \mathbf{g}^{cl})$ to the Einstein's equation [36, 37]. From the point of view that the quantum theory should provide the most fundamental description of every physical observable, which is supported all along this work, the classical geometry should be reproduced by the expectation value of a quantum operator on suitable quantum states $|\phi\rangle$,

$$\langle\phi|\,\hat{\mathbf{g}}\,|\phi\rangle \approx \mathbf{g}^{cl}. \tag{3.2.24}$$

The criteria to select these quantum states is provided by the same assumption, in that the Schwarzschild background geometry, which is determined by the only function V_N (3.2.23), should be reproduced as close as possible by these states. For a static and spherically symmetric compact source, a choice of coherent state $|\phi\rangle = |g\rangle$ has been proved to effectively reproduce the black hole outer classical geometry and to explicitly give quantum corrections V_{QN} to the potential V_N [38]. These corrections are called quantum hair, since they depend on macroscopic

[1] In general, V_N is a Newtonian potential only for observers very far from the source.

properties of the source, namely the radius R_s, which in our model is determined by the expectation value of the quantum operator $\hat{R}_i$. Moreover, the explicit form of V_{QN} is determined by a choice of a UV cut-off for the momenta of the modes which generate the effective geometry, and for each choice different hair are predicted. For example, a hard cut-off $k < 1/R_s$ gives,

$$V_{QN} \approx V_N\Big(1 - \Big[1 - \frac{2}{\pi}\mathrm{Si}\Big(\frac{r}{R_s}\Big)\Big]\Big). \tag{3.2.25}$$

Therefore, since the mode population is expected to be related to the mass distribution, it could be interesting to find which hair are associated to this refined quantum model.

3.3 Excited states

The last two sections gave insights into the properties of the ground state of the collapsed quantum ball. This state is expected to be stable, and thus to reproduce the final end-state of the collapse. In the previous work [39], a measure of the stability of a simpler quantum core was provided by Shannon's information entropy, and it was showed that isotropic exited states shared a higher information entropy, and thus instability, when compared to the ground state. Moreover, the value predicted for the width of the ball $R_s \approx 3/2G_N M$ holds only for the global ground state, and by no means it is expected to represent the dimension of the core when dust get excited. To have a more precise description of the core, even when that some dust degrees of freedom are not in the ground state, let us consider a ball of dust where in the outermost shell a fraction $0 \leq x \leq 1$ of dust particles are in the ground state $|N_s, 0, 0\rangle$ and the remaining $1-x$ in any excited state $|n, l, m_l\rangle$, where $N_s := n_{0,N}$. We may distinguish between two classes of excited states: a first one with $n = N_s + k > N_s$ and $l = 0$, with $k = 1, 2, \ldots$, in which the spherical symmetry is preserved, and a second one identified by $n = N_s$ and $l > 0$. States with $l \neq 0$ and/or $m_l \neq 0$ are no more spherically symmetric, and the probability to localise a particle will depend in general on the spherical angles θ and ϕ. The physical information about the ensemble of dust particles we described is encoded in the density operator

$$\hat{\rho} = x\,|N_s, 0, 0\rangle\langle N_s, 0, 0| + (1-x)\,|n, l, m_l\rangle\langle n, l, m_l|. \tag{3.3.1}$$

The conservation of the number of particles is expressed by the property

$$\begin{aligned} Tr[\hat{\rho}] &= x \int_{\mathbb{R}^+ \times \mathrm{S}^2} \mathrm{d}^3x\,|\psi_{N_s,0,0}(r)|^2 + (1-x) \int_{\mathbb{R}^+ \times \mathrm{S}^2} \mathrm{d}^3x\,|\psi_{n,l,m_l}(r,\theta,\phi)|^2 \\ &= 1, \end{aligned} \tag{3.3.2}$$

which results from the orthonormality of the eigenfunctions

$$<\psi_{n,l,m_l}, \psi_{n',l',m_l'}> = \int_{\mathbb{R}^+ \times \mathrm{S}^2} \mathrm{d}^3x\,\psi^*_{n,l,m_l}\psi_{n',l',m_l'} = \delta_{n,n'}\delta_{l,l'}\delta_{m_l,m_l'}, \tag{3.3.3}$$

where in the coordinate representation $\langle r, \theta, \phi | n, l, m_l\rangle = \psi_{n,l,m_l}(r, \theta, \phi)$, and the full wave function $\psi_{n,l,m_l}(r, \theta, \phi)$ is obtained including the angular momentum operator in the Schrödinger equation (see Appendix A). The probability to localise a particle of the outermost N-layer within a shell of areal radius $r \in [r', r' + dr']$ and within a solid angle $(\theta, \phi) \in [\theta', \theta' + d\theta'] \times [\phi', \phi' + d\phi']$ is thus

$$dP_N = (x\,|\psi_{N_s,0,0}|^2 + (1-x)\,|\psi_{n,l,m_l}|^2) r'^2 sin(\theta') d\phi' d\theta' dr', \tag{3.3.4}$$

and from this expression we can define the density function

$$\rho_N(r, \theta, \phi) = \mu_N(x\,|\psi_{N_s,0,0}|^2 + (1-x)\,|\psi_{n,l,m_l}|^2), \tag{3.3.5}$$

which describes the distribution of dust particle in the outermost shell, and it yields the total ADM mass M if now integrated in $[0, R_s] \times \mathrm{S}^2$. The Einstein's equations and the continuity

equations of the energy-momentum tensor provide the expressions for the effective radial and transverse pressures determined by the dust density distribution (see Appendix C):

$$p_r(r,\theta,\phi) = -\rho_N(r,\theta,\phi), \tag{3.3.6}$$

$$p_\perp(r,\theta,\phi) = -\Big(\frac{r}{2}\partial_r\rho_N(r,\theta,\phi) + \rho_N(r,\theta,\phi)\Big). \tag{3.3.7}$$

For a mixed ensemble described by (3.3.1), since the azimuthal angle ϕ enters the full energy eigenfunctions ψ_{n,l,m_l} only as a phase, the density distribution ρ_N and pressures p_r and $p_\perp$ will depend only on r and θ (cylindrical symmetry).

Let us now first focus on states with $n = N_s$ and $l > 0$. As noted before, for these states the matter distribution is not isotropic, and consequently the pressures will not be any more constant over hypersurfaces $r > 0$, as in (3.3.6) and (3.3.7). The average radius of the N-layer for a mixture of dust particle described by (3.3.1) is

$$\begin{aligned}\bar{R}_{l,N} &= x\bar{R}_{N_s} + (1-x)\bar{R}_i \\ &= \bar{R}_{N_s} + (1-x)\,\delta\bar{R}_{l,N},\end{aligned} \tag{3.3.8}$$

where the average radius for excited states is given by the equation (see Appendix A)

$$\begin{aligned}\bar{R}_i &= \bar{R}_{n_{0,i}} - \frac{m_p^3\ell_p}{2\mu^2 M_i}l(l+1) \\ &:= \bar{R}_{n_{0,i}} + \delta\bar{R}_{l,i},\end{aligned} \tag{3.3.9}$$

The thickness $\Delta R_{l,N}$ of the N-layer of inner average radius R_N can be written as (see Appendix A)

$$\begin{aligned}\Delta R^2_{l,N} &= \Delta R^2_{N_s} + (1-x)\delta(\Delta R^2_{l,N}) \\ &= \Delta R^2_{N_s} - (1-x)\frac{m_p^2\ell_p^2}{\mu^2}\Big[\frac{3}{2}x + \frac{4}{9}\frac{m_p^4}{\mu^2M^2}\Big]l(l+1)\end{aligned} \tag{3.3.10}$$

and together with (3.3.8) it yields the global ball radius

$$\begin{aligned}R_s &= \bar{R}_{l,N} + \Delta R_{l,N} \\ &= \bar{R}_{N_s} + (1-x)\,\delta\bar{R}_{l,N} + \Delta R_{N_s}\sqrt{1 + (1-x)\frac{\delta(\Delta R^2_{l,N})}{\Delta R^2_{N_s}}}.\end{aligned} \tag{3.3.11}$$

As we should expect, if all dust particles are in the ground state $|N_s, 0, 0\rangle$, the fraction x would be exactly one and we would recover the core radius $R_s \approx 3/2G_NM$. Now, the term in the square root is of order

$$\frac{\delta(\Delta R^2_{l,N})}{\Delta R^2_{N_s}} = O\Big(\frac{m_p^4}{\mu^2M^2}\Big), \tag{3.3.12}$$

and we should ask whether there exist physical systems in which it could be neglected. For an astrophysical black hole, $M \gg m_p$ it is safely negligible if $\mu \lesssim m_p$, which is for sure the case of every observed particle. Therefore, the ball radius can be written in the simpler form

$$R_s \approx \bar{R}_{N_s} + \Delta R_{N_s} + (1-x)\,\delta\bar{R}_{l,N} \tag{3.3.13}$$

$$\approx \frac{3}{2}G_N M - \frac{2}{3}(1-x)\frac{m_p^3\ell_p^2}{\mu^2 M}l(l+1), \tag{3.3.14}$$

which shows that even if all particles are in the excited state $|N_s, l, m_l\rangle$, the ball will never cross the event horizon, since the correction $\delta\bar{R}_{l,N}$ to the radius from the excited states is always non-positive for every $0 \leq x \leq 1$ and $\forall l = 0, 1, \ldots, N_s - 1$. The following analysis will provide only an effective description of non-isotropic states, since the collapse of rotating dust particles are properly described by the motion along geodesics in a Kerr-like spacetime. However, while the global ground state corresponds to an isotropic state, those with angular quantum number $l = 2$ effectively describe a quadrupole deformation of the collapsed matter distribution, and a transition between some states (which have to satisfy new hydrogen-like selection rules) could trigger the emission of gravitational waves. The only restriction in this analysis is that only states corresponding to the same value of the ADM mass M has been considered, which means that a transition between any two of those states happen with no emission of energy, as guaranteed by (3.1.6). To describe a real production of energy, a very intriguing idea would be to use the standard perturbation theory in quantum mechanics, an issue which is left for further investigation. The same analysis can now be extended to a mixed ensemble of dust particles where $n = N_s + k$, with $k = 1, 2, \ldots$ and $l = 0$. The ball radius R_s can be cast in the same form as we did previously, namely

$$R_s = \bar{R}_{N_s} + (1-x)\delta\bar{R}_{k,N} + \Delta R_{N_s}\sqrt{1 + (1-x)\frac{\delta(\Delta R^2_{k,N})}{\Delta R^2_{N_s}}}, \tag{3.3.15}$$

where

$$\delta\bar{R}_{k,N} = \frac{2m_p^3\ell_p}{\mu^2 M}\Big[\frac{3}{2}\frac{\mu M}{m_p^2}k + k^2\Big], \tag{3.3.16}$$

$$\frac{\delta(\Delta R^2_{k,N})}{\Delta R^2_{N_s}} = O\Big(\frac{m_p^4}{\mu^2 M^2}\Big). \tag{3.3.17}$$

The correction to the average radius (3.3.16) from the excited states is now always positive, thus we should expect now that only a finite number of energy states (3.1.10) with $n = N_s + k$ and $k = 1, 2, \ldots$ will exist inside the event horizon. In fact, from (3.3.15) we have

$$R_s \approx \bar{R}_{N_s} + \Delta R_{N_s} + (1-x)\delta\bar{R}_{k,N}$$

$$\approx \frac{3}{2}G_N M + (1-x)\delta\bar{R}_{k,N}, \tag{3.3.18}$$

and if we use (3.3.16), and require $R_s \lesssim 2G_N M$, we get

$$(1-x)\Big(3k\frac{m_p}{\mu}+2k^2\frac{m_p^3}{\mu^2 M}\Big)\lesssim \frac{1}{2}\frac{M}{m_p}. \tag{3.3.19}$$

For $M >> m_p$ and $\mu \lesssim m_p$, which we already assumed, finally we have

$$k(1-x)\lesssim \frac{1}{6}\frac{\mu M}{m_p^2}=\frac{2}{9}N_s, \tag{3.3.20}$$

where we used

$$N_s = n_{0,N}=\frac{3}{4}\Big(\frac{\mu M}{m_p^2}\Big) \tag{3.3.21}$$

from (3.1.14). For $x = 1$ it is always satisfied, while for $x \neq 1$ there are non-zero values of k for which the core could be found outside the horizon, namely those for k equal to a fraction of N_s. In this case, the black hole picture would break down. Both cases can be summarized in the most general situation where a fraction of particles is the excited state $n = N_s + k$, with $k = 0, 1, 2, \ldots$ and $l > 0$, and if we repeat the same analysis we made for the other two cases, the equation for the core radius is shown to preserve the same form

$$R_s = \bar{R}_{N_s} + (1-x)\delta\bar{R}_{l,k} + \Delta R_{N_s}\sqrt{1+(1-x)\frac{\delta(\Delta R^2_{l,k})}{\Delta R^2_{N_s}}}, \tag{3.3.22}$$

where the term under square root can be neglected, as previously assuming that $M \gg m_p$ and $\mu \lesssim m_p$, and the correction to the average radius is now expressed as the sum

$$\delta\bar{R}_{l,k} = \delta\bar{R}_{l,N} + \delta\bar{R}_{k,N}. \tag{3.3.23}$$

Now, since $\bar{R}_{l,N} \leq 0$ for each $l = 0, 1, \ldots, n-1$, and on the contrary $\bar{R}_{k,N} \geq 0$ for each $k = 0, 1, 2, \ldots$, non-isotropic states are pushed towards the centre of the core and some of the states which does not satisfy the bound (3.3.20) in general could be found in the interior of the horizon. In formulas, for a mixture of dust particles as described by the density operator (3.3.1), $R_s \lesssim 2G_N M$ for those value of $0 \leq x \leq 1$, k and l such that

$$(1-x)\Big[3k\frac{m_p}{\mu}+\big(2k^2-\frac{2}{3}l(l+1)\big)\frac{m_p^3}{\mu^2 M}\Big]\lesssim \frac{1}{2}\frac{M}{m_p}. \tag{3.3.24}$$

However, corrections to (3.3.20) are of order $O(m_p^4/\mu^2 M^2)$, and since in most realistic scenarios can be discarded, non-isotropic states do not give any significant contribution to the radius R_s.

3.3.1 Entropy

The density operator (3.3.1) is a positive semidefinite and hermitian operator on a single particle Hilbert space. It encodes the incomplete knowledge of the state of each particle in the N^{th} layer, where a fraction x is characterised by the state $|N_s, 0, 0\rangle$ and a fraction $1-x$ by $|n, l, m_l\rangle$. Being an operator, $\hat{\rho}$ can be represented in different basis, and by looking at its realisations to measure

our uncertainty about the system could be misleading. In fact, our ignorance of the system is better quantified by the Von-Neumann's entropy, which is defined as

$$S(\hat{\rho}) := -\mathrm{Tr}(\hat{\rho}\log\hat{\rho}).^{2} \tag{3.3.25}$$

Since $\hat{\rho}$ is hermitian, it can be always diagonalised, and if $\{\lambda_i\}$ are the eigenvalues of $\hat{\rho}$ with respect to any complete orthonormal basis $\{|\phi_i\rangle\}_{i\in I}$, (3.3.25) becomes

$$S(\hat{\rho}) = -\sum_{i\in I}\lambda_i \log\lambda_i, \tag{3.3.26}$$

where we set $0\cdot\log 0 = 0$. In this form, (3.3.26) can be immediately recognised as the Shannon's entropy S_{Sh} for an information source whose realisations $x_i \in \chi$ can occur with probability $\lambda_i = p(x_i) = p_i$,

$$S_{Sh} = -\sum_{x_i\in\chi} p_i \log p_i. \tag{3.3.27}$$

where χ defines an alphabet of symbols. In our definition, the logarithm is not expressed in base two, which means that entropy is not measured in bit but in *nat*, where 1nat $= (1/\log 2)$bit. It is worth noting that the Von Neumann's entropy (3.3.25) could be interpreted as information entropy only for the ensemble $|\phi_i\rangle$ of orthonormal eigenstates of $\hat{\rho}$. Even if formally Shannon's and Von-Neumann's entropies look the same, them do not share the same properties in general. In fact, the classical Shannon's entropy departs from the quantum Von-Neumann entropy when we consider the interaction of more subsystems (or information sources).

Now, the entropy $S(\hat{\rho})$ quantifies our ignorance about the state of the system in the sense that, if $\hat{\rho}$ is a *pure* state, i.e. all members of the ensemble are in the same state $|\psi\rangle$, then

$$\hat{\rho} = |\psi\rangle\langle\psi| := \hat{P}_\psi \implies S(\hat{\rho}) = 0. \tag{3.3.28}$$

This is what we would expect, since after we measure the state of the system, we would found it in $|\psi\rangle$ without any uncertainty. On the opposite, if the ensemble is completely random, i.e. each member has equal probability $x_\psi = x$ to be found in every (accessible) quantum state $|\psi\rangle \in \mathcal{H}_\psi$, the entropy will be maximum

$$\hat{\rho} = \sum_{\psi} x_\psi \hat{P}_\psi \implies S(\hat{\rho}) = \log(d), \tag{3.3.29}$$

where d is the number of accessible states from the system, and $\sum_\psi x_\psi = 1$ with $x_\psi \geq 0$ since they represent fractional populations. In our case, the density operator would represent a pure state if all dust particles in the N^{th} layer were in the ground state $|N_s, 0, 0\rangle$, i.e. $x = 1$, or in the same excited state $|n, l, m_l\rangle$, i.e. $x = 0$, while the entropy would reach the maximum for $x = 1/2$, and since each particle has only two states at its disposal, then $S_{max} = \log 2$. For any two-state system, the entropy is equal to,

$$S(\hat{\rho}) = \begin{cases} 0, & \text{if } x = 0, 1, \\ x\log x + (1-x)\log(1-x), & \text{if } 0 < x < 1, \end{cases} \tag{3.3.30}$$

[2]The Boltzmann's constant k_b gives entropy its natural units, which here is ignored to recover the Shannon's information entropy definition.

which we can prove to be the right entropy with a direct computation using the orthonormal basis $\{|n,l,ml\rangle\}$. In fact, diagonalising $\hat{\rho}$,

$$\hat{\rho}|n',l',m_l'\rangle = (x\,\delta_{N_s,n'}\delta_{0,l'}\delta_{0,m_l'} + (1-x)\,\delta_{n,n'}\delta_{l,l'}\delta_{m_l,m_l'})|n',l',m_l'\rangle \tag{3.3.31}$$

$$:= \lambda_{n',l',m_l'}|n',l',m_l'\rangle, \tag{3.3.32}$$

we can use directly (3.3.26),

$$S(\hat{\rho}) = -\sum_{n'=N_s}^{\infty}\sum_{l'=0}^{n'-1}\sum_{m_l'=-l'}^{l'}\lambda_{n',l',m_l'}\log\lambda_{n',l',m_l'} \tag{3.3.33}$$

which gives the entropy in (3.3.30). In this simple case, the equivalence between Shannon's and Von-Neumann's entropy provides a different interpretation of the entropy from $\exp(S)$ estimating the number of accessible quantum states for the system. In fact, according to Shannon's *source coding theorem* [40], S_{Sh} is the minimum number of bits (per source symbol) required to store information being produced by the source and which can be at later time reconstructed without information loss. Therefore, to store the information of the state $\hat{\rho}$,without any successive loss, we only need at maximum one bit, and this would the entropy for the N^{th} layer if we were to neglect all the fundamental matter degrees of freedom. In fact, the quantum state of the N^{th} layer is described by the composite density matrix

$$\hat{\rho}_N = \bigotimes_{i=1}^{\nu_N}\hat{\rho}, \tag{3.3.34}$$

and the total entropy for the whole composite system (N^{th} layer populated by ν_N dust particles) is

$$\begin{aligned} S(\hat{\rho}_N) &= -\operatorname{Tr}(\hat{\rho}_N\log\hat{\rho}_N) \\ &= -\sum_{i=1}^{\nu_N}\operatorname{Tr}(\hat{\rho}\log\hat{\rho}) \\ &= \nu_N S(\hat{\rho}), \end{aligned} \tag{3.3.35}$$

where the trace on the first line is computed on $\mathcal{H}_N^L$ as defined in (3.2.11). The maximum ignorance of the system is quantified by the total entropy $S_{max} = \nu_N\log 2$, or as we said the maximum number of accessible quantum states is $exp(S_{max}) = 2^{\nu_N} \approx 2^{M/4\mu}$, where ν_N correspond to the number of bit needed to successfully encode the state of the N^{th} layer, as described by (3.3.34). The number of accessible quantum state is exponential in the ADM mass M, and hence in the volume of the collapsed ball, a property which is shared by any system whose independent degrees of freedom are additive in the volume, and which is expected for matter. Gravitational degrees of freedom are instead expected to grow with the horizon area, which instead is proportional to M^2, as prescribed by the Bekenstein's area law.

3.4 Core surface

Remarkably, in the ground state the discretized mass function M_i grows linearly with the mean areal radius $\bar{R}_{n_{0,i}}$; in fact using equation (3.2.8) for both masses and radiuses we get

$$M_i = \frac{2m_p}{3\ell_p}\bar{R}_{n_{0,i}}. \tag{3.4.1}$$

Since this relation is independent on N, we can extend it to a continuos mass function

$$m(r) \approx \frac{2m_p}{3\ell_p}r, \tag{3.4.2}$$

which is consistently the Misner-Sharp-Hernandez mass function

$$m(r) = 4\pi \int_0^r \mathrm{d}r'\, r'^2 \rho(r') \tag{3.4.3}$$

determined by the energy density

$$\rho(r) = \frac{M}{4\pi R r^2} \approx \frac{m_p}{6\pi\ell_p r^2}, \tag{3.4.4}$$

required that $m(R_s) = M$, where M is the total ADM mass. Anyway, even if the function

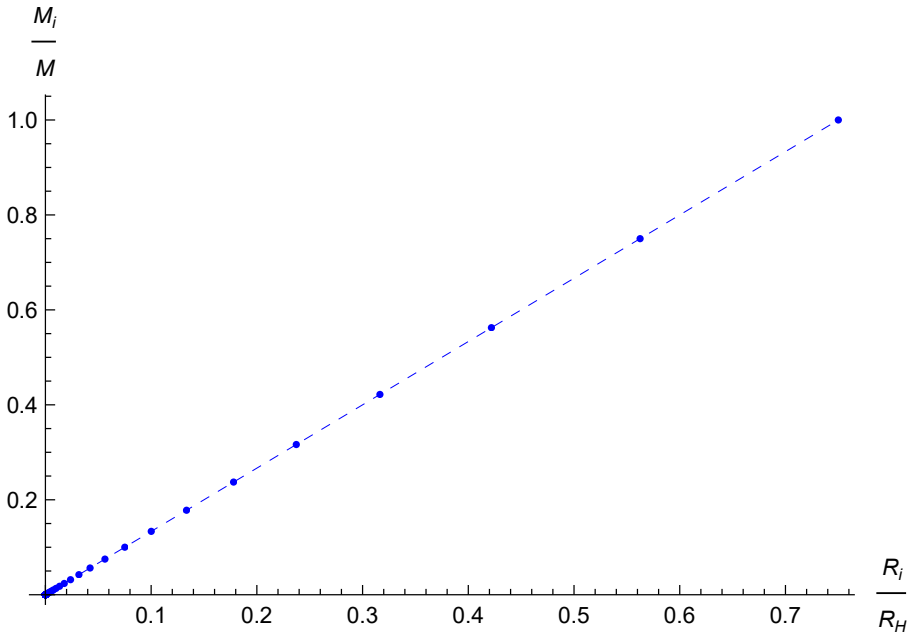

Figure 3.2: Discrete and approximated continuos mass distribution for a black hole of total ADM mass $M \approx 150\, m_p$, $\mu = m_p/10$ and $R_H = 300\, \ell_p$. The number of layer is $N = 200$.

matches the outer Schwarzschild geometry, its first order derivative seems to be discontinuos

at the surface and non-vanishing from the enterior of the ball, namely for $r \to R_s^-$, a picture which makes hard to conceive the quantum core in equilibrium, as it should be in the ground state. The fuzzyness of quantum layers, which is effectively described by the thickness $\Delta R_{n_{0,i}}$, is responsible for this issue; in fact, the outermost shell with thickness $\Delta R_{N_s} \approx R_s/4$ contains one fourth of the total mass M,

$$\mu_N = M_{N+1} - M_N \approx \frac{M}{4}. \tag{3.4.5}$$

Therefore the mass function is expected to vanish on the surface of this "halo" of dust particles, and not on the ball of average radius R_s. What we have just said should not sound mysterious, since in the classical picture M_i described the mass contribution of the only dust inside $r = R_i$, but after the quantisation each particle can access every layer and contribute to the mass of every one of them. A better description of the mass distribution inside each layer should be given by $\rho_i(r) = \mu_i |\psi_{n_{0,i}}(r)|^2$, because $|\psi_{n_{0,i}}(r)|^2$ gives the probability density to localize a particle of the i-layer, which is also expected to show a non-zero probability to find a particle in a different $j \neq i$ layer. In particular, the mass distribution in the outermost shell is determined by $\rho_N(r)$, which does not depend on the number of layers N, and it is expected to match smoothly the outer Schwarzschild geometry with total ADM mass M, which is only possible if the behaviour of ρ_N deviates from being linear in r as in (3.4.3), as expected from the analytical expression of the wave functions (3.1.10). In summary, we seek a mass function $m(r)$, which is linear for $r \lesssim r_0$ and non-linear for $r \gtrsim r_0$, where $r_0 = \bar{R}_{N_s}$, matching smoothly the outer geometry $m(r_1) = M$ on the surface of the outermost shell $r_1 = \bar{R}_{N_s} + \Delta R_{N_s}$. Clearly, r_0 and r_1 parametrize the boundaries of this outer transitional shell. We can write it as

$$m(r) = \begin{cases} \alpha\, r & r \leq r_0 \\ B(r) & r_0 \leq r \leq r_1 \\ M & r \geq r_1 \end{cases} \tag{3.4.6}$$

with α a constant to be fixed and $B(r)$ a non-linear function. Since almost all the information we need to properly describe the outermost shell is encoded in $\rho_N(r)$, $B(r)$ could be chosen to interpolate the profile of that density distribution. In addition, $B(r)$, $B'(r)$ and $B''(r)$ must be continuos at the boundary $r = r_0$ and $r = r_1$ to ensure the continuity of all components of the energy-momentum tensor at both ends, namely

$$\alpha\, r_0 = B(r_0). \qquad B(r_1) = M. \tag{3.4.7}$$

$$\alpha = B'(r_0). \qquad B'(r_1) = 0. \tag{3.4.8}$$

$$0 = B''(r_0). \qquad B''(r_1) = 0. \tag{3.4.9}$$

Even if $B(r)$ is expected to be non-linear, we can still try to find an interpolating function which approximates $m(r)$ without introducing any more constraints. Requiring B,B',B'' to be continuos we have introduced 6 conditions to be fulfilled, which can be done using an $M = 5$ order polynomial which has clearly $M + 1$ coefficients that can be used to satisfy them. A polynomial $B(r)$ of degree M such that (3.4.7), (3.4.8) and (3.4.9) hold exists and it is called osculating polynomial (see Appendix B for details and the analytic expression). Using

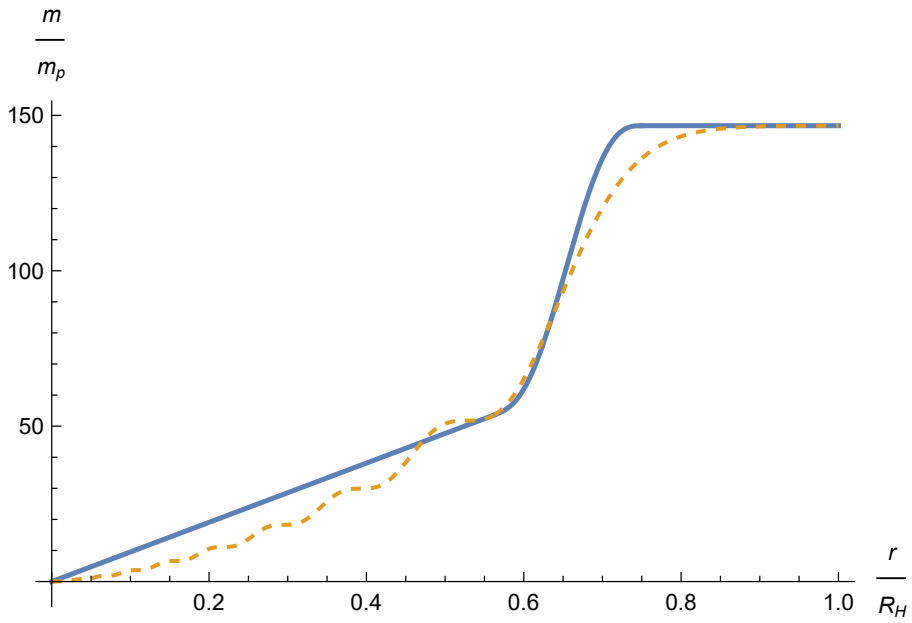

Figure 3.3: Misner-Sharp-Hernandez function m for a black hole of total ADM mass $M \approx 150\, m_p$, $\mu = m_p/10$ and $R_H = 300\, \ell_p$. In dashed line is represented the mass function determined by $\rho_N(r)$, while in solid line is represented the interpolated mass function.

adimensional units $x = r/R_H$, in Fig.(3.2) is represented the mass function (3.4.6) with respect to the Misner-Sharp-Hernandez mass given by $\rho_N(r)$. Boundaries of the transitional layer are explicitly

$$r_0 = \frac{16}{9} R_H, \tag{3.4.10}$$

$$r_1 = \frac{3}{4} R_H, \tag{3.4.11}$$

while the value of α is fixed by the condition

$$\alpha = \frac{4\pi M}{r_0} \int_0^{r_0} \mathrm{d}r\, r^2 \rho_N(r), \tag{3.4.12}$$

which ensures the matching between the linear and non-linear regime. For a spacetime described by the metric (3.1.1), radial and transverse pressure functions can be computed [41] (see Appendix C) and they are given by the equations

$$p_r(r) = -\frac{m'(r)}{4\pi r^2}, \tag{3.4.13}$$

$$p_\perp(r) = -\frac{m''(r)}{8\pi r}, \tag{3.4.14}$$

and represented in Fig.(3.4) and Fig.(3.5). In this model $m(r)$ matches as required the outer Schwarzschild geometry, with continuos first and second order derivatives. The radial pressure

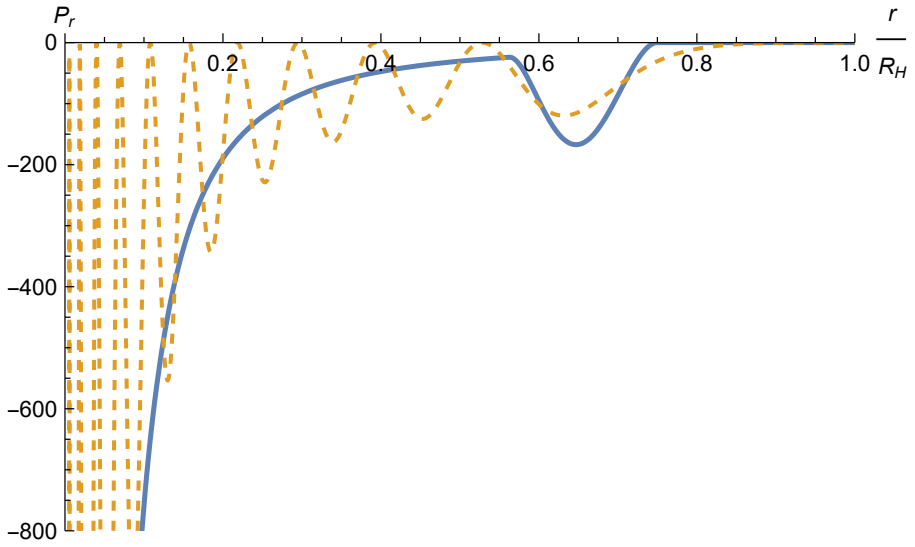

Figure 3.4: Radial pressure p_r corresponding to a black hole of total ADM mass $M \approx 150\, m_p$, $\mu = m_p/10$ and $R_H = 300\, \ell_p$. In dashed line is represented the radial pressure determined by ρ_N.

is approximately zero near the external boundary of the outermost shell, while the tangential pressure (tension) is non-vanishing across this outer transitional layer and oscillating. Although high degree polynomials could introduce spurious oscillations, in this case the only side effect introduced in the interpolation could be the increasing of the height of peaks, while the oscillating behaviour is clearly still present in the mass function determined by $|\psi_{N_s}|^2$. In Fig.(3.5) clearly $p_\perp$ is everywhere continuos but not its first derivative, as we imposed continuity of $B(r)$ at most at second order. Three more conditions can be introduced to ensure the continuity of the energy-momentum tensor up to first derivatives of the components, but at the price of a more complex osculating polynomial $B(r)$. Moreover, this model is independent on the number of layer N we use to describe the inner core, so it can be used in the full general setting of the problem. However, limitations are still present since it improves only the description of the outermost core surface while still using the linear approximation in the interior region, and furthermore it cannot be used with arbitrary value of M and μ, in particular it is impossible to compute $|\psi_{N_s}(r)|^2$ for astrophysical sources.

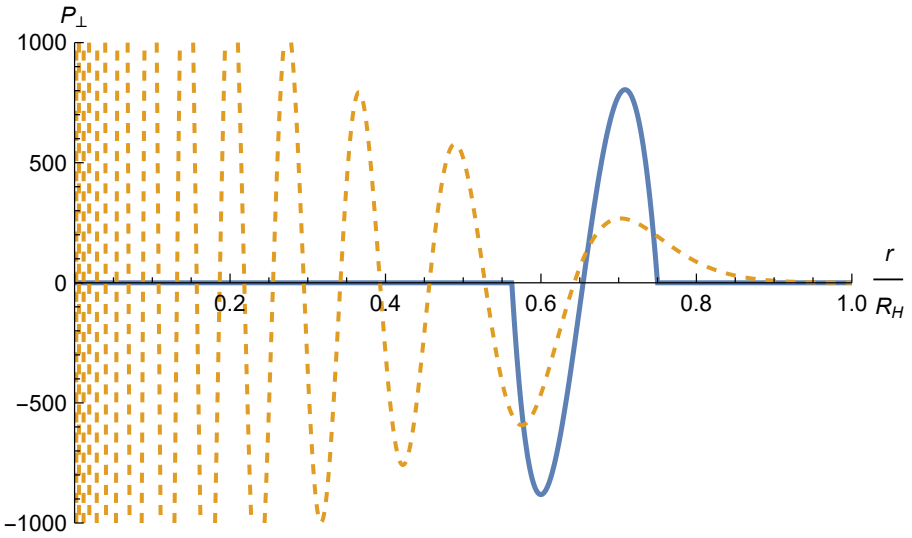

Figure 3.5: Tangential pressure $p_\perp$ corresponding to a black hole of total ADM mass $M \approx 150\, m_p$, $\mu = m_p/10$ and $R_H = 300\, \ell_p$. In dashed line is represented the tangential pressure determined by ρ_N.

3.4.1 Integrable singularity

Since in Einstein's theory every matter distribution sourcing gravity will curve spacetime, the trajectories of an observer falling freely will be determined by matter itself. A measure of the spacetime curvature is given by scalar polynomials constructed of out the Riemann tensor, like the Kretschmann scalar and the Ricci scalar,

$$K = R_{\alpha\beta\gamma\delta} R^{\alpha\beta\gamma\delta}, \quad R = g^{\mu\nu} R_{\mu\nu}, \tag{3.4.15}$$

where $R_{\mu\nu}$ are the components of the Ricci tensor in the coordinate chart $\{x^\mu\}$. In particular, for the quantum core, near the centre of symmetry matter distribution is well approximate by a linear law (3.4.3) (Appendix C). Then, if we look at the Kretschamnn scalar for this distribution, which is

$$K \sim \frac{64}{3} r^{-4}, \quad R \sim \frac{8}{3} r^{-2}, \quad \text{for} \quad r \to 0, \tag{3.4.16}$$

clearly the $K \sim r^{-6}$ behaviour near the singularity of a Schwarzschild black hole is smoothed by the quantum matter. In particular, by looking at the geodesic deviation of two test particles which fall radially along two nearby geodesic, if $\vec{\xi} = (\delta r, 0, 0)$ is the spatial vector field joining the two points, from (Appendix C) results that

$$\frac{1}{\delta r} \frac{\mathrm{d}^2 \delta r}{\mathrm{d}\tau^2} = -R^1{}_{010} \approx 0 \quad \text{for} \quad r \to 0, \tag{3.4.17}$$

where τ is the time measures by a clock attached to one of the test particles. Therefore, even if the scalar polynomials are still divergent near the singularity, there exist preferred directions along which an observer falling freely will not experience any infinite stretching or compression,

but could even reach the singularity and pass through it [42]. This is just a direct proof of a more general result (Appendix C). In fact, it is a consequence of the vanishing of the Misner-Sharp-Hernandez mass function at the centre $m(0) = 0$ and of $m \sim r$, which is enforced by the L^2-integrability of the wave-function,

$$\int_0^r \mathrm{d}r'\, r'^2 |\psi(r')|^2 < \infty. \tag{3.4.18}$$

again a feature of the quantum description of matter. Therefore, a singularity of this time is called *integrable singularity*, since while the scalar polynomials and the effective energy-momentum tensor still diverge near this region, their volume integrals remain finite.

3.4.2 Angular perturbations of the core surface

Dust distribution is assumed from the very beginning to be isotropic and particles radially infalling, therefore we could look at the radial distribution determined by $\psi(r)$ to properly describe the collapsed matter. We can therefore marginalize the probability density in equation (3.3.5) with respect to angles to obtain the radial probability distribution, namely

$$\begin{aligned} \rho_{l,N}(r) &= \int_0^\pi d\theta\, sin\theta \int_0^{2\pi} \mathrm{d}\phi\, r^2 |\psi(r,\theta,\phi)|^2 \\ &= 4\pi r^2 |\tilde{\psi}_l(r)|^2, \end{aligned} \tag{3.4.19}$$

where now we denote the radial wave function $\tilde{\psi}_l(r)$ since it still depends on l (but not on m_l), and the symbol $\sim$ remind us the different convenction used for the normalisation, in particular $\tilde{\psi} = \psi/\sqrt{4\pi}$. From this equality, we recover the probability density for the ground state used in Section 3.4 from $\rho_{0,N}(r) = \rho_N(r)$.
The main result that introduced the first section was the linear relation between $\bar{R}_i$ and M_i in the ground state, which is reasonably expected if during the collapse dust layers preserve their nested structure, i.e. $\bar{R}_{i+1} \approx \bar{R}_i + \Delta R_i$. If we now suppose that a fraction of dust particles are in a different excited state, the nested structure could be partially lost, since the average areal radius $\bar{R}_i$ will depend also on those excited states. In fact, the average radius for the N-layer when dust is in the quantum state (3.3.1), the areal radius is the weighted average expressed by (3.3.8). Moreover, as in the hydrogen atom, we should expect a lower probability to find excited particles in the innermost core for $l > 0$. Therefore, the linear approximation is not expected to hold for all possible fractions $0 \leq x \leq 1$ and excited states $l > 0$. However, the non-vanishing tangential pressure $p_\perp(r)$ in the outermost shell could be responsible for resistance against "angular perturbation" with respect to the isotropic dust configuration. In Figures (3.6a) and (3.6b) is represented the Misner-Sharp-Hernandez function $m(r)$ for $l = 5$ and $l = 8$ with different compositions of excited states, which as we already noted should describe accurately the outermost layer. The mass distribution is almost unperturbed from the rest configuration $\rho_{0,N}$ for, $l \lesssim 5$ and "small" significant deviations start to occur for $l \gtrsim 5$.
We can repeat the same analysis made for a collapsing ball in the ground state, using the interpolating function (3.4.6) to reconstruct the mass density $\rho_{l,N}$ in the outermost layer. As

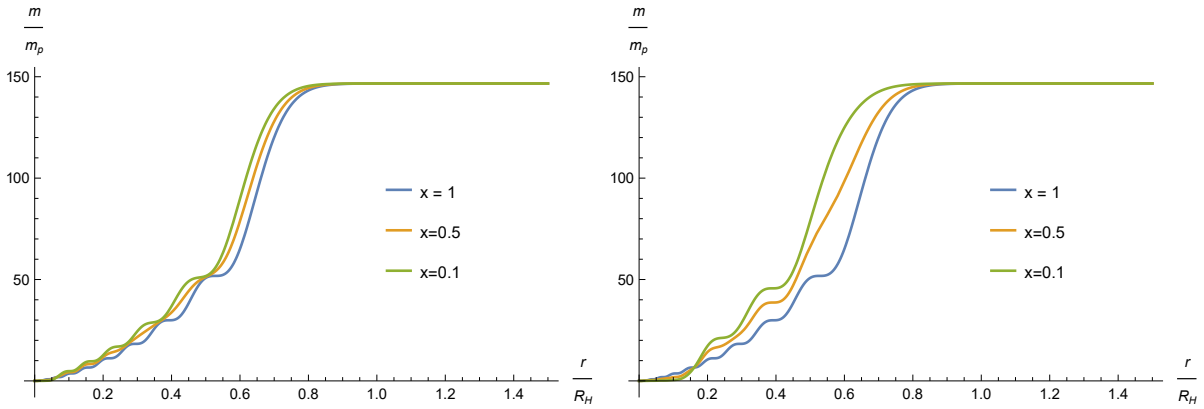

(a) $m(r)$ determined by $\rho_{5,N}(r)$.

(b) $m(r)$ determined by $\rho_{8,N}(r)$.

Figure 3.6: Mass function determined by distributions $\rho_{l,N}(r)$ for different fraction x of particles in the ground state, for a black hole of total ADM mass $M \approx 150\, m_p$, $\mu = m_p/10$ and $R_H = 300\, l_p$.

noted before, the main difficulty now is to determine what are the boundaries of this non-linearity region and how much we can trust our results, since the relation $M_{i+1} \approx 4/3 M_i$ strictly holds only for a nested collapse of dust in its ground state. For $l \lesssim 5$ we can fix r_1 and r_0 to be

$$\begin{aligned} r_0 &= \bar{R}_{n_{0,N}} + \delta\bar{R}_{l,N} \\ &= (\frac{9}{16} - \frac{1}{3}\frac{m_p^4}{\mu^2 M^2} l(l+1))R_H \end{aligned} \tag{3.4.20}$$

$$\begin{aligned} r_1 &= \bar{R}_{n_{0,N+1}} + \delta\bar{R}_{l,N+1} \\ &= (\frac{3}{4} - \frac{1}{4}\frac{m_p^4}{\mu^2 M^2} l(l+1))R_H \end{aligned} \tag{3.4.21}$$

and choose the same α as in (3.4.12) with the appropriate density distribution $\rho_{l,N}(r)$ and point r_0. In Figure (3.8) is represented the interpolated mass function, which again seems to correctly represents the expected dust distribution, and it is not significantly different from the unperturbed mass function. The same conclusions hold for the pressure functions represented in Figures (3.7a) and (3.7b). Those configurations for $l \lesssim 5$, for every fraction x of particles in the ground states does not show significant deviations from the unperturbed configuration, therefore everything we already said is still true. Differently, as we can see in Figures (3.9a), (3.9b) and (3.10), the interpolated mass function and pressures deviates from the outermost core behaviour determined by $\rho_{8,N}(r)$, in this case for $l = 8$.

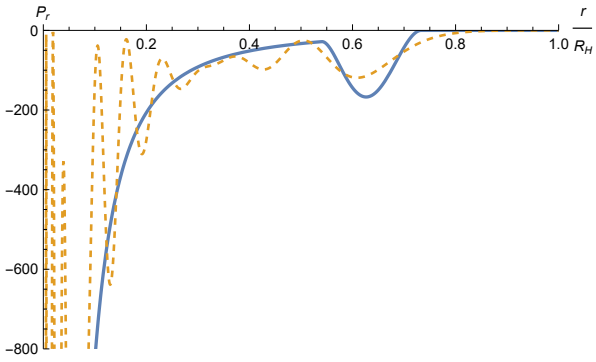

(a) Radial pressure $p_r(r)$.

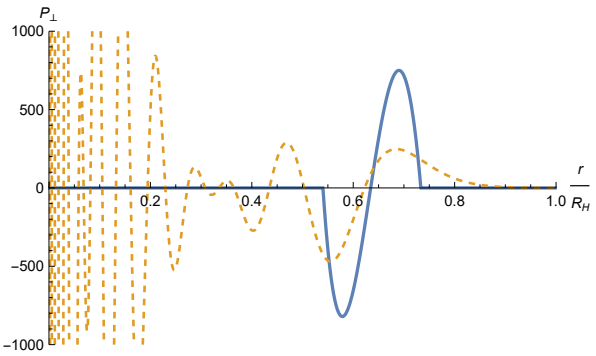

(b) Tangential pressure $p_\perp(r)$.

Figure 3.7: Radial and tangential pressure functions for a black hole of total ADM mass $M \approx 150\, m_p$, $\mu = m_p/10$ and $R_H = 300\, l_p$. In dashed line, pressures are determined by $\rho_{5,N}$, while in solid line dust particles are in the state ψ with $x = 0.5$ and $l = 5$.

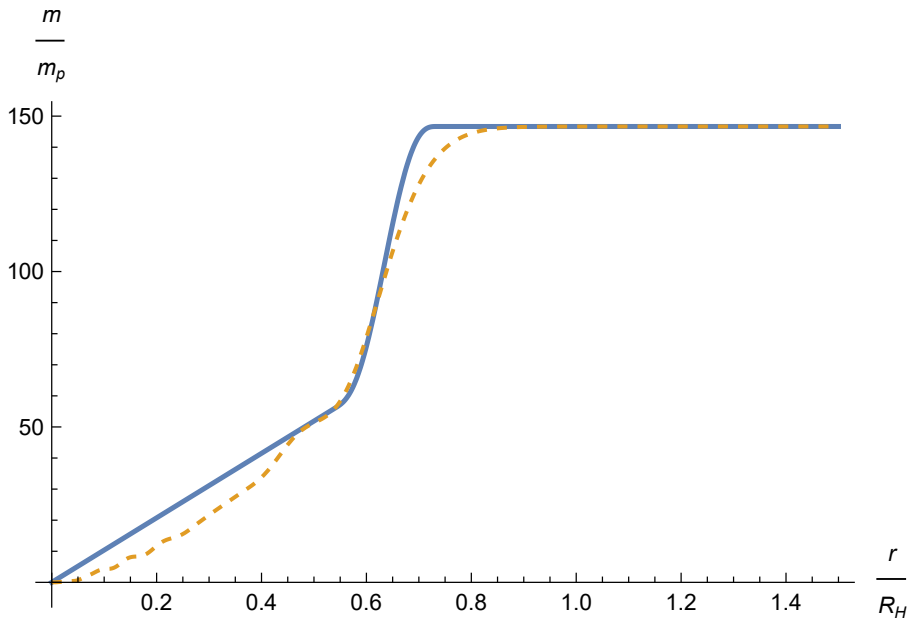

Figure 3.8: Misner-Sharp-Hernandez function m for a black hole of total ADM mass $M \approx 150\, \ell_p$, $\mu = m_p/10$ and $R_H = 300\, \ell_p$. In dashed line is represented the mass function determined by $\rho_{5,N}(r)$, while in solid line is represented the interpolated mass function for dust particles in the state ψ with $x = 0.5$ and $l = 5$.

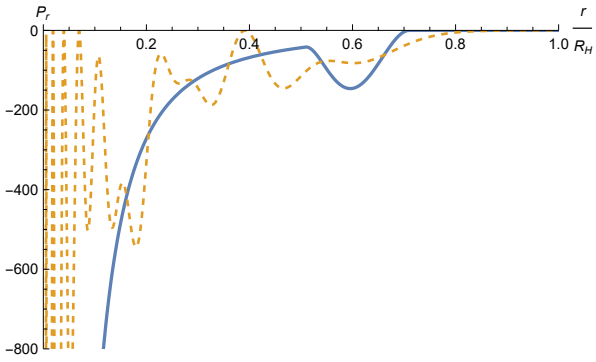

(a) Radial pressure $p_r(r)$.

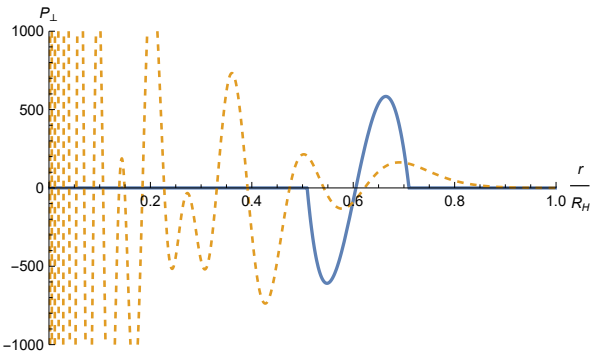

(b) Tangential pressure $p_\perp(r)$.

Figure 3.9: Radial and tangential pressure functions for a black hole of total ADM mass $M \approx 150\, m_p$, $\mu = m_p/10$ and $R_H = 300\, l_p$. In dashed line, pressures are determined by $\rho_{8,N}$, while in solid line dust particles are in the state ψ with $x = 0.5$ and $l = 8$.

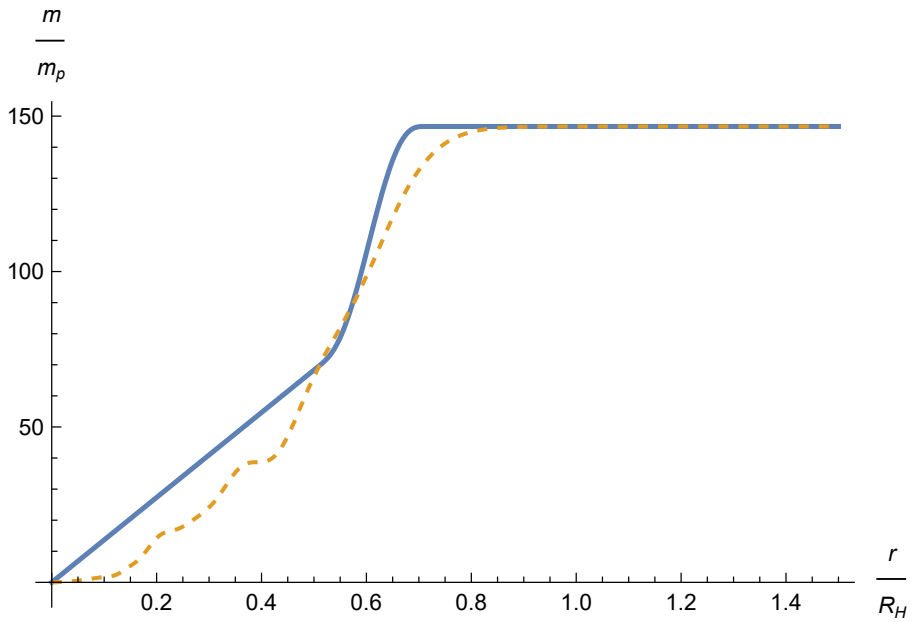

Figure 3.10: Misner-Sharp-Hernandez function m for a black hole of total ADM mass $M \approx 150\, \ell_p$, $\mu = m_p/10$ and $R_H = 300\, \ell_p$. In dashed line is represented the mass function determined by $\rho_{8,N}(r)$, while in solid line is represented the interpolated mass function for dust particles in the state ψ with $x = 0.5$ and $l = 8$.

Chapter 4

Conclusions

In the classical Oppenheimer-Snyder model, for every initial regular configuration, the surface of the collapsing dust becomes trapped at the same time at which it crosses the Schwarzschild radius of the ball. Consequently, the singularity theorems dictate that the shrinking matter must end in a region of spacetime with infinite curvature: a curvature singularity. However, Einstein's theory of gravity is not believed to accurately describe a gravitational collapse up to the very final stages. In fact, the dynamics of a gravitational system is expected to be modified by quantum-gravitational effects, even if a unique quantum theory of gravity is still missing. Many collapse scenarios, where quantum effects modify the classical dynamics, have been depicted within the Hamiltonian theory of gravity. In the canonical approach, this issue is addressed by introducing an effective description of quantum-gravitational systems based on the quantisation of classical equation of motions over a fixed background manifold. In all mini-superspace models described, the quantum modified dynamics prevents the appearance of a singular final state by producing a bounce. Inspecting the behaviour of energy wave packets, in the canonical analysis the re-expanding phase starts when the packet compresses approximately to $E \approx m_p$, in agreement with the common assumption that General Relativity should break down at the Planck scale. A serious limitation of canonical quantisation is that in all descriptions of already idealised spherically symmetric model, only few dynamical quantum degrees of freedom could be included to be able to at least make some prediction, namely just only the areal radius of a collapsing shell. Moreover, the OS model [7] in the canonical picture, does not even seem to describe a black hole.

Employing the quantisation prescription (3.1.7), we have been able to provide a quantum description of the gravitational collapse of a spherically symmetric distribution of dust (OS model), which produces a black hole with a macroscopic matter core as the final end-state of the collapse. In fact, provided that the areal radiuses satisfy the Heisenberg uncertainty principle, the infalling matter does not collapse to a singular final state as in the classical model. In this work, this prescription has been extended to an N-body model of the OS collapse, where dust particles are distributed among N arbitrary layers of areal radius R_i. The ground state radius $R_s \approx 3/2G_N M$ and the quantum number for the outermost layer N_s were shown to be independent of the number of layer N. A macroscopic quantum core $R_s \lesssim R_H$ conflicts with Planck size remnants [9], while still agreeing with the idea that quantum theory

may play a role even at larger distances in gravitational system, and the possibility to detect quantum-gravitational effects at experimentally accessible macroscopic scale is left open.

From (3.2.15) the surface area of the core has been proved to be quantised according to Bekenstein's area law. Consequently, it was possible to identify $N_s M/\mu \approx N_G$, where N_G in the corpuscolar description of black holes represents the number of soft-gravitons generated by a source of mass M. From a simple analogy with the corpuscolar picture, the finite size of the core has been shown to be able to produce deviations from the classical Schwarzschild geometry, and to open up the possibility to compute these corrections for this refined model.

In this extended model, for astrophysical black holes $M \gg m_p$, the width of the core when a fraction $1 - x$ of dust in the outermost layer get excited was shown to consistently describe a compact core hidden behind an event horizon, thus a black hole, only for a finite number of isotropic excited states. When the excited fraction is in a state which is not spherically symmetric, the core radius was found to be approximately equal to the ground state radius R_s. In particular, it was addressed that a de-excitation from states corresponding to a quadrupole deformation $l = 2$ could be associated to the production of gravitational waves. Since in the Oppenheimer-Snyder model, the Hamiltonian constraint (3.1.5) ensures that all states have the same energy, the emission could be described deploying the time-dependent perturbation theory of quantum mechanics, by introducing a time-dependent perturbation $\hat{H}_{int}(t)$ which could induce a transition between states corresponding to different ADM masses.

In the innermost region of the quantum core, a linear approximation for the Misner-Sharp-Hernandez mass function has replaced the central singularity with an integrable singularity, where the Kretschmann's scalar is shown to behave as $K \sim r^{-4}$ as $r \to 0$. However, in the outermost region of the core, the fuzzy layers overlap and the linear approximation is shown to break down. A more accurate description of the surface has been given by interpolating the mass distribution $\rho_{N_s} = |\psi_{N_s}|^2$ in the non-linear region $16/9 R_H < r < 3/4 R_H$. The solution provided is described by a 5-th order polynomial with continuos first and second order derivatives, whose construction does not depend on the number of layer N. An accurate description of the core surface is required when the evaporation and accretion of the quantum core are introduced in this picture, which has been neglected through this work but should be included in a complete description of the collapse.

The effective quantum description of a gravitational collapse depicted in this model is only an approximation of a realistic collapse. Since all stars are rotating, a more precise description would require the quantisation of the geodesic equation in a Kerr spacetime. Moreover, particles should be more fundamentally described by excitations of quantum fields, and all Standard Model interactions should be included. Anyway, from the potential observational signatures provided by this model, it looks very promising to develop more refined quantum pictures of black holes, since they provide physical cosmological signatures that in principle could be detected, and which makes those models appealing to grasp the essential features of a quantum theory of gravity.

Appendix A

Schrödinger equation for a Newtonian potential

It is convenient to formally solve the full Schrödinger equation for a point-like particle with mass μ moving in the Newtonian potential generated by a spherical distribution of total mass M

$$U(r) = -\frac{G_N \mu M}{r}. \tag{A.0.1}$$

The radial Schrödinger equation for a spherically symmetric potential reads

$$\Big[-\frac{\hbar^2}{2\mu}\Big(\frac{\mathrm{d}^2}{\mathrm{d}r^2} + \frac{2}{r}\frac{\mathrm{d}}{\mathrm{d}r}\Big) + \frac{l(l+1)\hbar^2}{2\mu r^2} - \frac{G_N \mu M}{r}\Big] f(r) = \mathcal{E} f(r), \tag{A.0.2}$$

where we already solved the angular part of the equation, whose eigenfunctions are known to be spherical harmonics $Y_l^m(\theta, \phi)$, depending on two integer numbers $l = 0, 1, 2, ...$ and $m = -l, -l+1, ..., l-1, l$. At the end we will set $l = m = 0$ to select only those eigenfunctions representing isotropic states. Furthermore, we expect the energy spectrum to be discrete for $\mathcal{E} < 0$ with normalizable eigenfunctions. The change of function

$$f(r) = \frac{\chi(r)}{r} \tag{A.0.3}$$

simplifies (A.0.2) to

$$\Big[-\frac{\hbar^2}{2\mu}\frac{\mathrm{d}^2}{\mathrm{d}r^2} + \frac{l(l+1)\hbar^2}{2\mu r^2} - \frac{G_N \mu M}{r}\Big] \chi = \mathcal{E}\chi. \tag{A.0.4}$$

This equation must be solved provided the regularity condition

$$\chi(0) = 0, \tag{A.0.5}$$

and requiring each solution $\chi(r)$ to be bounded by a constant in the limit $r \to +\infty$, to guarantee that $\chi(r)$ can be properly normalised. Defining the constant

$$k^2 = -\frac{2\mu\mathcal{E}}{\hbar^2} > 0, \tag{A.0.6}$$

we can rewrite (A.0.4) as

$$\frac{\mathrm{d}^2\chi}{\mathrm{d}r^2} + \Big[-k^2 - \frac{l(l+1)}{r^2} + \frac{2G_N\mu^2 M}{\hbar^2 r}\Big]\chi = 0. \tag{A.0.7}$$

We can tidy up this equation introducing the adimensional radius

$$x = \frac{2\,r}{a\,n}, \tag{A.0.8}$$

where we have redefined $k = k_n$ using a new parameter $n > 0$

$$k = \frac{G_N\mu^2 M}{n\,\hbar^2 a}, \tag{A.0.9}$$

and a is the 'Bohr' radius

$$a = \frac{\hbar^2}{G_N\mu^2 M}. \tag{A.0.10}$$

By using the chain rule

$$\frac{\mathrm{d}g}{\mathrm{d}r} = \frac{x}{r}\frac{\mathrm{d}g}{\mathrm{d}x} = \frac{2}{a\,n}\frac{\mathrm{d}g}{\mathrm{d}x}, \tag{A.0.11}$$

$$\frac{\mathrm{d}^2g}{\mathrm{d}r^2} = \frac{2}{a\,n}\frac{\mathrm{d}x}{\mathrm{d}r}\frac{\mathrm{d}^2g}{\mathrm{d}x^2} = \Big(\frac{2}{a\,n}\Big)^2\frac{\mathrm{d}^2g}{\mathrm{d}x^2}, \tag{A.0.12}$$

with $g(r)$ any differentiable function, the equation (A.0.7) simplifies to

$$\begin{aligned}\Big(\frac{2}{a\,n}\Big)^2\frac{\mathrm{d}^2\chi}{\mathrm{d}x^2} + \Big[-\Big(\frac{1}{a\,n}\Big)^2 - \Big(\frac{2}{a\,n}\Big)^2\frac{l(l+1)}{x^2} + \frac{2}{a}\frac{2}{a\,n}\frac{1}{x}\Big]\chi = 0,\\ \Big(\frac{2}{a\,n}\Big)^2\Big[\frac{\mathrm{d}^2\chi}{\mathrm{d}x^2} + \Big[-\frac{1}{4} - \frac{l(l+1)}{x^2} + \frac{n}{x}\Big]\chi\Big] = 0,\\ \frac{\mathrm{d}^2\chi}{\mathrm{d}x^2} + \Big[-\frac{1}{4} - \frac{l(l+1)}{x^2} + \frac{n}{x}\Big]\chi = 0.\end{aligned} \tag{A.0.13}$$

From the study of the asymptotic form of the solution to this equation in the limit $x \to 0$ and $x \to \infty$, we can try to solve the radial equation using the ansatz

$$\chi(x) = x^{l+1}e^{-x/2}L(x), \tag{A.0.14}$$

and replacing $\chi(x)$ in the equation (A.0.13), we obtain a differential equation for $L(x)$

$$x\frac{\mathrm{d}^2L}{\mathrm{d}x^2} + (2l+2-x)\frac{\mathrm{d}L}{\mathrm{d}x} - (l+1-n)L = 0. \tag{A.0.15}$$

The regularity and boundary condition for χ require that $L(x)$ must be non vanishing for $x \to 0$ and that grows slower than $e^{x/2}$ for $x \to +\infty$. Then, the Kummer differential equation (A.0.15)

has solution provided that the non-negative parameter n is integer with $n \geq 1$, and $l \leq n-1$, and it can be written as

$$L(x) = c\, M(l+1-n; 2l+2; x), \tag{A.0.16}$$

where M is a confluent hypergeometric function of the first kind, called also Kummer's function [43]. This function can be written in terms of generalised Laguerre's polynomials

$$L_p^{(\alpha)} = \frac{(p+\alpha)!}{\alpha! p!}\, M(-p; \alpha+1; x) \tag{A.0.17}$$

where p and α are non negative integer. The functions $L_p^{(\alpha)}$ are polynomials of degree p as can be explicitely seen from the Rodrigues' formula

$$L_p^{(\alpha)} = \frac{x^{-\alpha} e^x}{p!} \frac{d^p}{dx^p}\big(x^{p+\alpha} e^{-x}\big), \tag{A.0.18}$$

and they are orthogonal with the scalar product defined as

$$\int_0^\infty \mathrm{d}x\, x^{\alpha+1} e^{-x} L_{p_1}^{(\alpha)} L_{p_2}^{(\alpha)} = \frac{(\alpha+p_1)!}{p_1!}(\alpha+2p_1+1)\delta_{p_1,p_2}. \tag{A.0.19}$$

Therefore, we can normalize them to define a set of orthonormal polynomials, and express the solution to the Kummer's equation (A.0.15) as

$$L(x) \equiv L_{nl}(x) = \Big[\frac{(n-l-1)!}{2n(n+l)!}\Big]^{1/2} L_{n-l-1}^{(2l+1)}(x), \tag{A.0.20}$$

where the orthonormality follow from (A.0.19) with $p = n-1-l$ and $\alpha = 2l+1$. The eigenvalues of the radial Schrödinger equation are given by (A.0.6) and (A.0.9),

$$\mathcal{E}_n = -\frac{\hbar k_n^2}{2\mu} = -\frac{G_N^2 \mu^3 M^2}{2\hbar^2} \frac{1}{n^2}, \tag{A.0.21}$$

with n non-negative integer, and the energy spectrum is degenerate since they solely depend on n. The spherically symmetric eigenfunctions associated to the eigenvalues $\mathcal{E}_n$ are identified by the quantum numbers $n = 0, 1, 2, ..., l = m = 0$, and their expression is given by (A.0.3), (A.0.8) and (A.0.14),

$$f_n(r) = \Big[\frac{(n-1)!}{2n\, n!}\Big]^{\frac{1}{2}} \Big(\frac{2}{an}\Big) exp\Big\{-\frac{r}{an}\Big\} L_{n-1}^{(1)}\Big(\frac{2r}{an}\Big), \tag{A.0.22}$$

where a is the 'Bohr'radius defined in (A.0.10). Each eigenfunction must be normalizable, since we assume the particle to be localizable somewhere in the space of configurations, and the probability density to find it given by $|f(r)|^2$. Computing the norm

$$\int_{\mathbb{R}^+ x S^2} \mathrm{d}^3x |f(r)|^2 = 4\pi \int_0^{+\infty} \mathrm{d}r r^2 |f(r)|^2 = 1 \tag{A.0.23}$$

we can properly normalise the eigenfunctions expressed in (A.0.22),

$$\psi_n(r) = \frac{f_n(r)}{\sqrt{4\pi}}, \tag{A.0.24}$$

and from the orthogonality relation (A.0.19), the ψ_n will satisfy the condition

$$< \psi_n, \psi_{n'} >:= 4\pi \int_0^{+\infty} \mathrm{d}r\, r^2 \psi_n^*(r)\psi_{n'}(r) = \delta_{n,n'}. \tag{A.0.25}$$

If we define the uncertainty on the observable r as

$$\Delta r := \sqrt{<(r - <r>)^2>} = \sqrt{<r^2> - <r>^2}, \tag{A.0.26}$$

where the expectation of r is given by the weighted average

$$<r> = \bar{r} = \int_0^{+\infty} dr r^2 \psi_n^*(r)\, r\, \psi_n(r), \tag{A.0.27}$$

then they are expressed by the following formulas [44];

$$\bar{r} = \frac{a}{2}[3n^2 - l(l+1)], \tag{A.0.28}$$

$$\begin{aligned} \Delta r^2 &= \Big(\frac{a^2 n^2}{2}\Big)\Big[5n^2 + 1 - 3l(l+1)\Big] \\ &\quad - \Big(\frac{a^2}{4}\Big)\Big[9n^4 + l^2(l+1)^2 - 6n^2 l(l+1)\Big] \qquad \text{(A.0.29)} \\ &= \frac{a^2}{4}\Big(n^4 + 2n^2 - l^2(1+l)^2\Big), \qquad \text{(A.0.30)} \end{aligned}$$

in particular for l=0 we get

$$\bar{r} = \frac{a}{2} 3n^2, \tag{A.0.31}$$

$$\Delta r = \frac{an}{2}\sqrt{2 + n^2}, \tag{A.0.32}$$

$$\frac{\Delta r}{\bar{r}} = \frac{\sqrt{2+n^2}}{3n} = \frac{1}{3} + \mathcal{O}\Big(\frac{1}{n^2}\Big), \quad n \to +\infty. \tag{A.0.33}$$

Appendix B

Hermite interpolation

Osculating polynomials are interpolating polynomials which pass through a set of points with specified derivatives. For the construction of osculating polynomials in full generality we refer to [45, 46]. Given a set of $n+1$ points $\{x_i\}_{i=0}^n$, non-negative numbers $\{m_i\}_{i=0}^n$, with $m_i \in \mathbb{N} \cup \{0\}$, and values to interpolate $\{f_j^{(k)}\}$, with $j = 0, \ldots, n$ and $k = 0, \ldots, m_j$, the osculating polynomial approximating the function $f \in C^m([a, b])$ is the polynomial of least degree such that

$$f^{(k)}(x_j) = f_j^{(k)} \quad \forall j = 0, \ldots, n, \ \forall k = 0, \ldots, m_j. \tag{B.0.1}$$

From these requirements we have $n + 1$ conditions for $f^{(0)} \equiv f$, and $\sum_{j=0}^n m_j$ more conditions to be satisfied for the derivatives; a polynomial of degree

$$M = \sum_{j=0}^{N} m_j + n \tag{B.0.2}$$

has $M + 1$ coefficients that can be used to fulfill these requirements. A general theorem [45] states that a polynomial of degree M such that conditions (B.0.1) are satisfied exist and is given by

$$f(x) = \sum_{j=0}^{n} \sum_{k=0}^{m_j} A_{jk}(x) f_j^{(k)}, \tag{B.0.3}$$

where

$$A_{jk}(x) = p_j(x) \frac{(x - x_j)^k}{k!} \sum_{l=0}^{m_j - k} \frac{1}{l!} g_j^{(l)}(x_j)(x - x_j)^l, \tag{B.0.4}$$

with $p_j(x)$ and $g_j(x)$ defined by

$$p_j(x) = \prod_{\substack{l=0 \\ l \neq j}}^{n} (x - x_l)^{m_l + 1}, \tag{B.0.5}$$

$$g_j(x) = \frac{1}{p_j(x)}. \tag{B.0.6}$$

In the special case $m_j = 1$ for each $j = 0, \ldots, n$ polynomials $f(x)$ are usually called Hermite polynomials and (B.0.3) is called Hermite formula. In our analysis in Section 3.4, we sought the interpolating polynomial $B(x)$ given only two points x_0 and x_1 and which agree up to second derivatives, namely $m_0 = m_1 = 2$. The general formula (B.0.3) simplifies to

$$B(x) = \sum_{j=0}^{1} \sum_{k=0}^{2} A_{jk}(x) B_j^{(k)}, \tag{B.0.7}$$

and $f(x)$ is determined by only six conditions, since it reduces to a polynomial of order $M = 5$ (B.0.2). From now, x refers to $x = r/R_H$, with $x_0 = r_0/R_H$, $x_1 = r_1/R_H$. Taking advantage of the vanishing of

$$B^{(1)}(x_1) = B^{(2)}(x_0) = B^{(2)}(x_1) = 0, \tag{B.0.8}$$

enforced by conditions (3.4.7), (3.4.8) and (3.4.9), where for convenience we use the notation

$$B_j = B^{(0)}(x_j) \quad B'_j = B^{(1)}(x_j) \quad B''_j = B^{(2)}(x_j), \tag{B.0.9}$$

we can set

$$A_{02}(x) = A_{11}(x) = A_{12}(x) = 0. \tag{B.0.10}$$

Therefore the full problem simplifies to determine only three functions $A_{00}(x)$, $A_{01}(x)$ and $A_{10}(x)$. From what we have already said $r_0 = \bar{R}_{n_{0,N}}$ and $r_1 = \bar{R}_{n_{0,N}} + \Delta R_{n_{0,N}}$, and if we define

$$\Delta x = \frac{\Delta R_{n_{0,N}}}{R_H}, \tag{B.0.11}$$

we can express functions (B.0.10) in short form

$$\begin{aligned} A_{00}(x) = & -\frac{1}{\Delta x^3}(x - x_1)^3 - \frac{3}{\Delta x^4}(x - x_1)^3(x - x_0) \\ & - \frac{6}{\Delta x^5}(x - x_1)^3(x - x_0)^2, \end{aligned} \tag{B.0.12}$$

$$A_{01}(x) = -\frac{1}{\Delta x^3}(x - x_1)^3(x - x_0) - \frac{3}{\Delta x^4}(x - x_1)^3(x - x_0)^2, \tag{B.0.13}$$

$$\begin{aligned} A_{10}(x) = & +\frac{1}{\Delta x^3}(x - x_0)^3 - \frac{3}{\Delta x^4}(x - x_0)^3(x - x_1) \\ & + \frac{6}{\Delta x^5}(x - x_1)^2(x - x_0)^3. \end{aligned} \tag{B.0.14}$$

Finally, the full interpolating function $B(x)$ is completely determined and its expression is

$$\begin{aligned} B(x) = & -\frac{\alpha'}{\Delta x^3}(x-x_1)^3 + \frac{M}{\Delta x^3}(x-x_0)^3 \\ & -\Big(\frac{3\alpha'}{\Delta x^4} + \frac{\alpha}{\Delta x^3}\Big)(x-x_1)^3(x-x_0) \\ & -\frac{3M}{\Delta x^4}(x-x_0)^3(x-x_1) \\ & -\Big(\frac{6\alpha'}{\Delta x^5} + \frac{3\alpha}{\Delta x^4}\Big)(x-x_1)^3(x-x_0)^2 \\ & +\frac{6M}{\Delta x^5}(x-x_1)^2(x-x_0)^3, \end{aligned} \tag{B.0.15}$$

with

$$\alpha' = \alpha x_0 = \frac{4\pi M}{R_H}\int_0^{r_0} dr\, r'^2 \rho_N(r). \tag{B.0.16}$$

Appendix C

Schwarzschild spacetime in the tetrad formalism

C.1 Einstein's equations

We considered through this work a spacetime $(\mathcal{M}, \mathbf{g})$ sourced by an isotropic distribution of dust particles, where the line element can be cast in the form

$$\mathrm{d}s^2 = -f(r)\mathrm{d}t^2 + f^{-1}(r)\mathrm{d}r^2 + r^2\mathrm{d}\Omega^2, \tag{C.1.1}$$

if we define

$$f(r) = 1 - \frac{2G_N m(r)}{r}. \tag{C.1.2}$$

The components of the corresponding energy-momentum tensor $T_{\mu\nu}$ are given by the Einstein's equations

$$G_{\mu\nu} = 8\pi G_N T_{\mu\nu}, \tag{C.1.3}$$

where $G_{\mu\nu}$ are the components of the Einstein computed from the metric in (C.1.1). Let us introduce a non-coordinate orthonormal basis (tetrad) $\{\vec{e}_a\}$, whose components in coordinate basis $\{\partial_\mu\}$ are defined as

$$\begin{aligned} e^\mu{}_0 &= (f^{-\frac{1}{2}}, 0, 0, 0), & e^\mu{}_1 &= (0, f^{\frac{1}{2}}, 0, 0), \\ e^\mu{}_2 &= (0, 0, r^{-1}, 0), & e^\mu{}_3 &= (0, 0, 0, (rsin\theta)^{-1}), \end{aligned} \tag{C.1.4}$$

where

$$\vec{e}_a = e_a{}^\mu \partial_\mu \quad \text{and} \quad g(\vec{e}_a, \vec{e}_b) = \eta_{ab}, \tag{C.1.5}$$

and use this tetrad as the proper reference frame of a fluid element with velocity $\vec{u} = \vec{e}_0$, which means that we assume the energy-momentum tensor to be diagonal in this basis,

$$T^{\mu\nu} = \rho e^\mu{}_0 e^\mu{}_0 + p_r e^\mu{}_1 e^\mu{}_1 + p_\theta e^\mu{}_2 e^\mu{}_2 + p_\phi e^\mu{}_3 e^\mu{}_3, \tag{C.1.6}$$

where the proper density ρ and the principal pressure p_r,p_θ,p_ϕ are eigenvalues of $\mathbf{T}$ associated respectively with the eigenvectors $\vec{e}_0$ and $\vec{e}_i$, $i = 1, 2, 3$. The most convenient way to compute the Einstein tensor $\mathbf{g}$ and then the energy-momentum tensor $\mathbf{T}$ is to solve the Cartan structure equations, which allow us to determine the Riemann tensor without using any coordinate basis of vector fields $\{\partial_\mu\}$. That this choice is indeed convenient is a consequence of the Levi-Civita connection being symmetric, or equivalently torsion-free. To pursue our objective, we introduce the basis of one-forms $\{\tilde{\epsilon}^a\}$ dual to $\{\vec{e}_a\}$,

$$\tilde{\epsilon}^a(\vec{e}_b) = \delta^a_b, \tag{C.1.7}$$

whose components in the coordinate basis of one-forms $\{\tilde{dx}^\mu\}$ are

$$\tilde{\epsilon}^a = e^a{}_\mu \tilde{dx}^\mu. \tag{C.1.8}$$

Note that we use greek letters $\mu = 0, \ldots, 3$ to label coordinates x^μ and latin letters $a = 0, \ldots, 3$ to label elements (vector or one-form) in the tetrad, while $\sim$ is used to identify one-forms (in general denoted by a greek letter). The connection coefficients describe how a generic basis element $\vec{e}_a$ fails to be parallely transported along curves tangent to another basis vector field $\vec{e}_b$, and clearly they depend on the basis we choose. In the usual way, they are defined by

$$\nabla_{\vec{e}_c}\vec{e}_b = \gamma_c{}^a{}_b \vec{e}_a = \gamma^a_{cb}\vec{e}_a, \tag{C.1.9}$$

where the odd notation $\gamma_c{}^a{}_b = \gamma(\vec{e}_c)^a{}_b$ is here used to remark that, if we fix c, we get a $4x4$ matrix, while if we fix a and b we obtain locally a map $T_p\mathcal{M} \to C^\infty(\mathcal{M})$ (we consider smooth vector fields and one-form), i.e. a (differential) one-form. Therefore, we can define the matrix valued *connection one-form* as

$$\tilde{\omega}^a{}_b = \gamma_c{}^a{}_b \tilde{\epsilon}^c, \tag{C.1.10}$$

while γ^a_{cb} are usually called *Ricci rotation coefficients*. The definition (C.1.9) differs from the usual one for the Christoffel symbols $\Gamma^\mu_{\nu\sigma}$ only for using a non-coordinate basis, but we can express pointwise the tetrad in the basis $\{\partial_\mu\}$, and consequently find how they are related. That said, we can easily find that

$$\begin{aligned}
\nabla_{\vec{e}_a}\vec{e}_b &= e_a{}^\mu \nabla_\mu (e_b{}^\nu \partial_\nu) \\
&= e_a{}^\mu (\partial_\mu e_b{}^\sigma + e_b{}^\nu \Gamma_\mu{}^\gamma{}_\nu)\partial_\sigma \\
&= \gamma_a{}^c{}_b e_c{}^\sigma \partial_\sigma,
\end{aligned} \tag{C.1.11}$$

and using (C.1.7), which in component is readily $e^a{}_\mu e_b{}^\mu = \delta^a_b$, we obtain the relation

$$\gamma_c{}^a{}_b = e^a{}_\sigma e_c{}^\mu \nabla_\mu e_b{}^\sigma. \tag{C.1.12}$$

Another useful relation which we will use later to derive the components of the energy-momentum tensor in the tetrad is

$$\nabla_\mu e_a{}^\mu = \gamma_b{}^b{}_a. \tag{C.1.13}$$

The proof follow immediately from (C.1.12), in fact

$$\nabla_\mu e_a{}^\sigma = \gamma_c{}^b{}_a e_b{}^\sigma e^c{}_\mu,$$

and contracting with g, since the connection is compatible with the metric tensor, i.e. we can move $g_{\mu\nu}$ inside the covariant derivative, we get

$$\nabla_\mu e_a{}^\mu = \gamma_c{}^b{}_a e_b{}^\mu e^c{}_\mu = \gamma_b{}^b{}_a.$$

Now, the connection one-form is solution of the Cartan's first structure equation, which for a symmetric connection is

$$d\tilde{\epsilon}^a + \tilde{\omega}^a{}_b \wedge \tilde{\epsilon}^b = 0. \tag{C.1.14}$$

Here $d\tilde{\epsilon}^a$ is a two-form, which corresponds to the exterior derivative of the dual basis element $\tilde{\epsilon}^a$, while $\wedge$ is the wedge product. While for a general k-form the exterior derivative may be hard to compute, and equally for the wedge product between, let us say, a k-form and a p-form, it is remarkably easy to compute both for one-forms, and in this peculiar case to solve the first Cartan's equation. Things are made even easier by the property of the connection matrix to be antisymmetric,

$$\tilde{\omega}_{ab} = -\tilde{\omega}_{ba}. \tag{C.1.15}$$

This property follows from the expression of the Ricci coefficients (C.1.12), and with some care in rising and lowering the tetrad indeces with the Minkowski metric tensor $\boldsymbol{\eta}$, as follow from (C.1.5) and (C.1.7). The components of the Riemann tensor in the non-coordinate basis $\{\vec{e}_a\}$ and $\{\tilde{\epsilon}^a\}$ are defined as usual by

$$R^a{}_{bcd} = R(\tilde{\epsilon}^a, \vec{e}_b, \vec{e}_c, \vec{e}_d), \tag{C.1.16}$$

and once again it is worth noting that $R^a{}_{bcd} = (R(\vec{e}_c, \vec{e}_d))^a{}_b$ can be seen, and they are, a matrix valued two-form, which can be expressen in the two-form basis $\{\tilde{\epsilon}^a \wedge \tilde{\epsilon}^b\}_{a,b}$ as

$$\tilde{\Omega}^a{}_b = \frac{1}{2} R^a{}_{bcd} \tilde{\epsilon}^c \wedge \tilde{\epsilon}^d, \tag{C.1.17}$$

where $\tilde{\Omega}^a{}_b$ are called *curvature two-forms*. To be clearer, if we denoted $\Omega^k(\mathcal{M})$ the set of differential k-forms on $\mathcal{M}$, indeed locally $R(\vec{e}_c, \vec{e}_d) \in \Omega^2(\mathcal{M}, End(T_p\mathcal{M}))$. What is still missing is a "connection" between the curvature one-forms $\tilde{\omega}^a{}_b$ and the curvature two-forms $\tilde{\Omega}^a{}_b$, which is given by the Cartan's second structure equation:

$$\tilde{\Omega}^a{}_b = d\tilde{\omega}^a{}_b + \tilde{\omega}^a{}_c \wedge \tilde{\omega}^c{}_b \tag{C.1.18}$$

Now we have all the essential tools to compute the Einstein tensor. To solve the first Cartan's equation, we first write explicitely the one-forms basis element

$$\begin{aligned} \tilde{\epsilon}^0 &= f^{\frac{1}{2}}\, dt, & \tilde{\epsilon}^2 &= r\, d\theta, \\ \tilde{\epsilon}^1 &= f^{-\frac{1}{2}}\, dr, & \tilde{\epsilon}^3 &= r sin\theta\, d\phi. \end{aligned} \tag{C.1.19}$$

The exterior derivative of a k-forms $\tilde{\alpha} = \sum \alpha_I \tilde{dx}^I \in \Omega^k(\mathcal{M})$, where $\alpha_I \in C^\infty(\mathcal{M}, \mathbb{R})$, is defined as

$$d\tilde{\alpha} = \sum{}'_I \, d\alpha_I \wedge \tilde{dx}^I = \sum{}'_I \big(\partial_\alpha \alpha_I \tilde{dx}^\alpha\big) \wedge \tilde{dx}^I, \tag{C.1.20}$$

where $I = (i_1, \ldots, i_k)$ is a multi-index and a primed sum $\sum'$ is only over $1 \leq i_1 < \ldots < i_k \leq n$, and for a one-form $\tilde{\epsilon}^a$ it can be simply expressed in coordinates as

$$d\tilde{\epsilon}^a = \frac{1}{2!}(\partial_\mu e^a{}_\nu - \partial_\nu e^a{}_\mu)\, \tilde{dx}^\mu \wedge \tilde{dx}^\nu. \tag{C.1.21}$$

Doing the computation we get

$$\begin{aligned} d\tilde{\epsilon}^0 &= \frac{1}{2} f^{-\frac{1}{2}} f'\, dr \wedge dt, & d\tilde{\epsilon}^2 &= dr \wedge d\theta, \\ d\tilde{\epsilon}^1 &= 0, & d\tilde{\epsilon}^3 &= sin\theta\, dr \wedge d\phi \\ & & &\quad + r cos\theta\, d\theta \wedge d\phi, \end{aligned} \tag{C.1.22}$$

where from now we use the lighter notation $\tilde{dx}^\mu = dx^\mu$ since it is clear that they are all one-forms. Note that $d\tilde{\epsilon}^1 = 0$ by the anticommunativity of the wedge product $dr \wedge dr = 0$, and we use the notation $f' = \partial_r f$. Our goal now is to find a solution to (C.1.14), where we will show how to solve for $\tilde{\omega}^0{}_1$, and then the same procedure can be extended to find the other solutions. For $a = 0$, (C.1.14) reads

$$d\tilde{\epsilon}^0 = -\tilde{\omega}^0{}_b \wedge \tilde{\epsilon}^b = \frac{1}{2} f^{-\frac{1}{2}} f'\, dr \wedge dt, \tag{C.1.23}$$

from the antisymmetry property (C.1.15) $\tilde{\omega}^0{}_0 = 0$, and then there is only one term which could be proportional to $dr \wedge dt$ on the left hand side, which is $\tilde{\omega}^0{}_1 \wedge \tilde{\epsilon}^1 = f^{\frac{1}{2}}\, \tilde{\omega}^0{}_1 \wedge dr$. Therefore, the one-forms $\tilde{\omega}^0{}_1 = \frac{1}{2} f' dt$ and $\tilde{\omega}^0{}_2 = \tilde{\omega}^0{}_3 = 0$ solve (C.1.23). Iterating this procedure, the only non vanishing one-forms are

$$\begin{aligned} \tilde{\omega}^0{}_1 &= \tilde{\omega}^1{}_0 = \frac{1}{2} f' f^{-\frac{1}{2}}\, \tilde{\epsilon}^0 = \frac{1}{2} f'\, dt & \tilde{\omega}^3{}_1 &= -\tilde{\omega}^1{}_3 = f^{\frac{1}{2}} \frac{1}{r}\, \tilde{\epsilon}^3 = f^{\frac{1}{2}} sin\theta\, d\phi \\ \tilde{\omega}^2{}_1 &= -\tilde{\omega}^1{}_2 = f^{\frac{1}{2}} \frac{1}{r}\, \tilde{\epsilon}^2 = f^{\frac{1}{2}}\, d\theta & \tilde{\omega}^3{}_2 &= -\tilde{\omega}^2{}_3 = \frac{1}{r} \frac{cos\theta}{sin\theta} \tilde{\epsilon}^3 \end{aligned} \tag{C.1.24}$$

To solve the Cartan's second structure equations we need first to compute the exterior derivative $d\tilde{\omega}^a{}_b$, and using the definition (C.1.20) we readily get

$$d\tilde{\omega}^0{}_1 = \frac{1}{2} f''\, \tilde{\epsilon}^1 \wedge \tilde{\epsilon}^0, \qquad d\tilde{\omega}^3{}_1 = \frac{1}{2} \frac{f'}{r}\, \tilde{\epsilon}^1 \wedge \tilde{\epsilon}^3 + f^{\frac{1}{2}} \frac{cos\theta}{r^2 sin\theta}\, \tilde{\epsilon}^2 \wedge \tilde{\epsilon}^3, \tag{C.1.25}$$

$$d\tilde{\omega}^2{}_1 = \frac{1}{2} \frac{f'}{r}\, \tilde{\epsilon}^1 \wedge \tilde{\epsilon}^2, \qquad d\tilde{\omega}^3{}_2 = \frac{1}{r^2}\, \tilde{\epsilon}^3 \wedge \tilde{\epsilon}^2. \tag{C.1.26}$$

Let us now replace the expression for the exterior derivative of $\tilde{\omega}^a{}_b$ inside (C.1.18), from which we can extract the components of the Riemann tensor from (C.1.17) using extensively the

anti-commutative property of $\tilde{\omega}^a{}_b$. At the end, the components in the tetrad are

$$\begin{aligned} R_{0101} &= \frac{1}{2}f'' & R_{0202} &= \frac{1}{2}\frac{f'}{r} & R_{0303} &= \frac{1}{2}\frac{f'}{r}, \\ R_{1212} &= -\frac{1}{2}\frac{f'}{r} & R_{1313} &= -\frac{1}{2}\frac{f'}{r} & R_{2323} &= \frac{1-f}{r^2} \end{aligned} \tag{C.1.27}$$

which can now be used to compute the diagonal components of the Ricci tensor $R_{ab} = \eta^{cd}R_{cadb}$:

$$\begin{aligned} R_{00} &= \frac{1}{2}f'' + \frac{f'}{r} & R_{11} &= -R_{00} \\ R_{22} &= \frac{1}{r^2}\frac{d}{dr}\big[r\big(1-f\big)\big] & R_{33} &= R_{22}. \end{aligned} \tag{C.1.28}$$

We are only one step from the Einstein's equations, as we only miss the scalar curvature

$$R = \eta^{ab}R_{ab} = -2R_{00} + 2R_{22} = 2R_{11} + 2R_{22}, \tag{C.1.29}$$

whose explicit expression is

$$R = 2\frac{m''r + 2m'}{r^2}, \tag{C.1.30}$$

and finally, from (C.1.3), (C.1.6), (C.1.28) and (C.1.29), we obtain a system of four differential equations in the unknown functions f, ρ, p_r, p_θ, p_ϕ, namely

$$G_{00} = \frac{1}{r^2}\frac{d}{dr}\big[r\big(1-f\big)\big] = 8\pi G_N\rho, \tag{C.1.31}$$

$$G_{11} = -G_{00}, \tag{C.1.32}$$

$$G_{22} = \frac{1}{2}f'' + \frac{f'}{r} = 8\pi G_N p_\theta, \tag{C.1.33}$$

$$G_{33} = G_{22}. \tag{C.1.34}$$

The components G_{11} and G_{33} provide the equation of state for the collapsing matter

$$\rho(r) = -p_r(r), \qquad p_\theta(r) = p_\phi(r) := p_\perp(r), \tag{C.1.35}$$

while G_{00} fixes the expression of $m(r)$ to be

$$m(r) = 4\pi\int_0^r dr'\, r'^2\rho(r'). \tag{C.1.36}$$

Therefore, the metric components and the principal pressures are fixed by the model of dust density distribution $\rho(r)$ we use, and in particular the component G_{22} gives the transverse pressure as a function of the density distribution $\rho(r)$. It is worth noting that for positive energy density $\rho > 0$, the radial pressure will be everywhere negative inside the collapsing ball. Whit this quite lengthy analysis we managed to compute the Einstein's equation for spherically distributed dust working directly in the tetrad frame (C.1.4). However, if we are interested only in deriving the pressure functions given the density distribution ρ, it is indeed quicker and

easier to impose the continuity equation for the energy-momentum tensor. In the tetrad frame $\{\vec{e}_a\}$, it gives four differential equations,

$$\nabla_a T^{ab} = 0, \tag{C.1.37}$$

which we can explicitly compute with some extra work. The energy-momentum tensor is expressed in the two basis as

$$T = T^{\mu\nu}\,\partial_\mu \otimes \partial_\nu = T^{ab}\,\vec{e}_a \otimes \vec{e}_b, \tag{C.1.38}$$

where the change of coordinates is given by

$$T^{\mu\nu} = T^{ab} e_a{}^\mu e_b{}^\nu. \tag{C.1.39}$$

In the coordinate basis $\{\partial_\mu\}$ (C.1.37) becomes

$$\begin{aligned} \nabla_\mu T^{\mu\nu} &= \nabla_\mu (T^{ab} e_a{}^\mu e_b{}^\nu) \\ &= T^{ab}\nabla_\mu (e_a{}^\mu e_b{}^\nu) \\ &\quad + e_a{}^\mu \nabla_\mu (T^{ab} e_b{}^\nu) \\ &\quad + e_b{}^\nu \nabla_\mu (T^{ab} e_a{}^\mu). \end{aligned} \tag{C.1.40}$$

If we apply now the Leibniz rule we get six terms symmetric in (ab) and (C.1.40) simplify in

$$\nabla_\mu T^{\mu\nu} = 2\big(T^{ab} e_a{}^\mu \nabla_\mu e_b{}^\nu + T^{ab} e_a{}^\nu \nabla_\mu e_b{}^\mu + e_a{}^\mu e_b{}^\nu \partial_\mu T^{ab}\big) = 0. \tag{C.1.41}$$

At this point we can project the (1,0) tensor $\nabla_\mu T^{\mu\nu}$ on the tetrad, and then if we use the relations between the Ricci coefficients and the Christoffel symbols (C.1.12) and (C.1.13), we get the final form of the continuity equations

$$\begin{aligned} e^c{}_\nu \nabla_\mu T^{\mu\nu} &= 2\big(T^{ab} e^c{}_\nu e_a{}^\mu \nabla_\mu e_b{}^\nu + T^{ab} e^c{}_\nu e_a{}^\nu \nabla_\mu e_b{}^\mu + e^c{}_\nu e_a{}^\mu e_b{}^\nu \partial_\mu T^{\mu\nu}\big) \\ &= 2\big(T^{ab}(\gamma_a)^c{}_b + T^{cb}(\gamma_b)^b{}_a + e_a{}^\mu \partial_\mu T^{ac}\big) = 0. \end{aligned} \tag{C.1.42}$$

Since we are interested in how the density distribution fixes the pressure functions, whose relation is given by the components G_{11} and G_{22}, it is possible to prove [36] that the Einstein's equation $G^{22} = 8\pi G_N T^{22}$ is equivalent to the projected component (C.1.42) corresponding to $c = 1$, from which we have

$$e^1{}_\nu \nabla_\mu T^{\mu\nu} = \frac{1}{2}(\rho + p_r) + \frac{2}{r}(p_r - p_\perp) f + f p_r' = 0 \tag{C.1.43}$$

Now, as $\rho = -p_r$ and $f \neq 0$, the equations of state are explicitly

$$p_r = -\rho = -\frac{m'}{4\pi r^2}, \tag{C.1.44}$$

$$p_\perp = \left(\frac{r}{2} p_r' + p_r\right) = -\frac{m''}{8\pi r}. \tag{C.1.45}$$

C.2 Scalar polynomials

From the components of the Riemann tensor (C.1.27) it is possible to compute the Kretschmann scalar, which is a quadratic scalar invariant defined by

$$K = R_{abcd}R^{abcd} \tag{C.2.1}$$

$$= 4\big(R_{0101}R^{0101} + R_{0202}R^{0202} + R_{0303}R^{0303} \tag{C.2.2}$$

$$+ R_{1212}R^{1212} + R_{1313}R^{1313} + R_{2323}R^{2323}\big). \tag{C.2.3}$$

Since,

$$\begin{aligned} R_{0101}R^{0101} &= \frac{(m'')^2r^4 - 4m'm''r^3 + 4(m'^2 + mm'')R^2}{r^6} \\ &\quad + \frac{-8mm'r + 4m^2}{r^6}, \end{aligned} \tag{C.2.4}$$

$$\begin{aligned} R_{0202}R^{0202} &= R_{0303}R^{0303} = R_{1212}R^{1212} = R_{1313}R^{1313} \\ &= \frac{m'^2r^2 - 2mm'r + m^2}{r^6}, \end{aligned} \tag{C.2.5}$$

$$R_{2323}R^{2323} = 4\frac{m^2}{r^6}, \tag{C.2.6}$$

replacing in the definition (C.2.1) gives the final expression

$$\begin{aligned} K &= 4\frac{(m'')^2r^4 - 4m'm''r^3 + 4(2m'^2 + mm'')r^2}{r^6} \\ &\quad + 4\frac{-16mm'r + 12m^2}{r^6} \end{aligned} \tag{C.2.7}$$

C.3 Geodesic in Schwarzschild spacetime

The parametric equation of a geodesic γ in the Schwarzschild spacetime is determined by solving the geodesic equations for a vector field $\vec{Y}$ in a chart $(U, \phi = x^i)$ on M,

$$\nabla_{\vec{Y}}\vec{Y} = \alpha\vec{Y}, \tag{C.3.1}$$

where $\alpha : \mathcal{M} \to \mathbb{R}$. Since (C.3.1) are a four second-order partial differential equations, they always admit at least locally a solution. In coordinates, the parametric equations of γ are given by

$$x^\mu = x^\mu(\lambda), \tag{C.3.2}$$

and expressing

$$\vec{Y} = \frac{\mathrm{d}x^\mu}{\mathrm{d}\lambda}\partial_\mu, \quad \partial_\mu|_P = \frac{\partial}{\partial x^\mu}\Big|_P \in T_P\mathcal{M}, \tag{C.3.3}$$

the geodesic equations become,

$$\left(\nabla_{\vec{Y}}\vec{Y}\right)^{\mu} = \frac{\mathrm{d}^2 x^{\mu}}{\mathrm{d}\lambda^2} + \Gamma^{\mu}_{\nu\rho}\frac{\mathrm{d}x^{\nu}}{\mathrm{d}\lambda}\frac{\mathrm{d}x^{\rho}}{\mathrm{d}\lambda} = \alpha\frac{\mathrm{d}x^{\mu}}{\mathrm{d}\lambda}, \tag{C.3.4}$$

which is a set of four second-order differential equations for $x^{\mu}(\lambda)$. If $\alpha = 0$, then λ is said to be an affine parameter[1]. Given any affine parameter λ, the geodesic equation (C.3.4) simplifies to

$$\frac{\mathrm{d}^2 x^{\mu}}{\mathrm{d}\lambda^2} + \Gamma^{\mu}_{\nu\rho}\frac{\mathrm{d}x^{\nu}}{\mathrm{d}\lambda}\frac{\mathrm{d}x^{\rho}}{\mathrm{d}\lambda} = 0, \tag{C.3.5}$$

and it is possible to define any new affine parameter by

$$\lambda \to \mu = a\lambda + b, \tag{C.3.6}$$

with $a, b \in \mathbb{R}$.

Geodesics are also known to be curves of local extremal length. The length of a time-like geodesic[2] γ connecting two points P and Q is defined by

$$L(\gamma) = \int_{\lambda_Q}^{\lambda_P} d\lambda\sqrt{-g_{\mu\nu}\dot{x}^{\mu}\dot{x}^{\nu}}, \quad \gamma(\lambda_P) = P,\, \gamma(\lambda_Q) = Q \tag{C.3.7}$$

where $\dot{f} = df/d\lambda$. Since it is possible to think of the argument of the integral as the velocity of a point-like particle with unit mass moving along γ, this definition can also be written as

$$L(\gamma) = \int_{\lambda_Q}^{\lambda_P} d\lambda\sqrt{2T(x,\dot{x})}, \quad T(x,\dot{x}) = -\frac{1}{2}g_{\mu\nu}\dot{x}^{\mu}\dot{x}^{\nu}. \tag{C.3.8}$$

In general, λ is an arbitrary affine parameter different from the time τ of a clock which moves instantaneously with the particle. It is useful to define the *arc-length* function of $\gamma : [\lambda_0, \lambda_1] \to \mathcal{M}$,

$$s(\lambda) = \int_{\lambda_0}^{\lambda} d\lambda'\sqrt{-g_{\mu\nu}\dot{x}^{\mu}\dot{x}^{\nu}}, \tag{C.3.9}$$

whose derivative with respect to λ is equal to the velocity of the particle,

$$\dot{s}(\lambda) = \sqrt{-g_{\mu\nu}(x(\lambda))\dot{x}^{\mu}(\lambda)\dot{x}^{\nu}(\lambda)}. \tag{C.3.10}$$

If the proper time is used as parameter $\lambda = \tau$, the length of the curve will correspond to the time needed to move from $\gamma(\tau_0)$ to $\gamma(\tau) < \gamma(\tau_1)$, and since this distance is exactly the corresponding arc-length, it implies that

$$s(\tau) = \tau - \tau_0 \Longrightarrow \dot{s}(\tau) = 1. \tag{C.3.11}$$

By assuming that $\tau > 0 = \tau_0$, it follows that using the proper time as parameter is equivalent to using the arc-parameter $s = \tau$, which implies that the velocity of the particle for this parametrisation will be equal to one,

$$2T(x(s), \dot{x}(s)) = -g_{\mu\nu}(x(s))\dot{x}^{\mu}(s)\dot{x}^{\nu}(s) = 1. \tag{C.3.12}$$

[1] It is understood that a curve is identified by its parametrisation.

[2] For a space-like geodesic $g_{\mu\nu}\dot{x}^{\mu}\dot{x}^{\nu} > 0$.

From (C.3.9), the arch-length of γ coincide with the action of a test particle with mass μ,

$$S[x^\mu(\tau)] = -\mu \int^\tau d\tau \sqrt{-g_{\mu\nu}\dot{x}^\mu \dot{x}^\nu}, \tag{C.3.13}$$

in which the affine parameter is naturally provided by the proper time τ of the particle. Therefore, extremising the length of geodesic will be equivalent to find extremal curves $x^\mu(\tau)$ for the action (C.3.13), which are given by solutions to the Euler-Lagrange equations

$$\frac{d}{d\tau}\Big(\frac{\partial T}{\partial \dot{x}^\mu}\Big) - \frac{\partial T}{\partial x^\mu} = 0. \tag{C.3.14}$$

For the metric (C.1.1), the kinetic energy function $T(x, \dot{x})$ reads

$$2T = f(r)^2 \dot{t}^2 - f(r)^{-2}\dot{r}^2 - r^2(\dot{\theta}^2 + \sin^2\theta\dot{\phi}^2) = 1, \tag{C.3.15}$$

since for a massive particle parametrised with the proper time $(-g_{\mu\nu}\dot{x}^\mu\dot{x}^\nu)^{\frac{1}{2}} = 1$, as shown in (C.3.12). Moreover, $T(x, \dot{x})$ is independent on t and ϕ, and the two corresponding integral of motions can be defined as

$$E = \mu\frac{\partial L}{\partial \dot{t}} = \mu f(r)\dot{t}, \tag{C.3.16}$$

$$L = -\mu\frac{\partial L}{\partial \dot{\phi}} = \mu r^2 \sin^2\theta\dot{\phi}. \tag{C.3.17}$$

The first integral of motion E corresponds to the proper mass of the particle as measured by an asymptotic observer, for which a weak-field approximation hold, in that

$$E \to \mu, \quad \text{if} \quad r \to +\infty,\, t = \tau. \tag{C.3.18}$$

Instead L corresponds to the conserved angular momentum around the axis which defines ϕ, as can be seen if we set $\theta = \pi/2$, which it is always possible from the arbitrariness in the definition of the axis directions in an isotropic spacetime. With this condition, since $\dot{t}$ is determined by integrating (C.3.17), the only two unknown functions are $r = r(\tau)$ and $\phi = \phi(\tau)$. In particular, the equations for radially in-falling geodesics are determined by setting $\phi = 0$ identically, from which (C.3.15) reduces to

$$f^{-1}\Big(\frac{E^2}{\mu^2} - \dot{r}^2\Big) = 1. \tag{C.3.19}$$

Therefore, the parametric equations $\{t(\tau), r(\tau), \theta(\tau) = \pi/2, \phi(\tau) = 0\}$ for a radially in-falling geodesic are given by solutions of the two differential equations

$$\begin{cases} \dot{r}^2 = \dfrac{2G_N m}{r} + \Big(\dfrac{E^2}{\mu^2} - 1\Big), \\ \dot{t} = \Big(1 - \dfrac{2G_N m}{r}\Big)^{-1}\dfrac{E}{\mu}. \end{cases} \tag{C.3.20}$$

C.4 Integrable singularity

As a final result, we are going to state a theorem which shows how some choices of the Misner-Sharp-Hernandez mass function can modify the motion of radially in-falling observers in a Schwarzschild spacetime. First, let us redefine the function $f(r)$ as,

$$\Phi(r) = \frac{1 - f(r)}{2}. \tag{C.4.1}$$

Th. C.4.1: Integrable singularity

If,

1. $\Phi(0) \in \mathbb{R}$,
2. $\Phi' \sim r^{\alpha}, \quad r \to 0$ with $\alpha \geq 1$,
3. $\Phi''(0) \in \mathbb{R}$,

then tidal forces remain finite on world lines of the matter flow,

$$\frac{1}{\delta r}\frac{\mathrm{d}^2 \delta r}{\mathrm{d}\tau^2} = -R^{1}{}_{010} < \infty, \tag{C.4.2}$$

where δr is the radial component of a space-like three-vector $\vec{\xi} = (\delta r, 0, 0)$ connecting to nearby radial geodesics [42].

Bibliography

[1] Roberto Casadio. "A quantum bound on the compactness". In: *The European Physical Journal C* 82.1 (Jan. 2022). DOI: 10.1140/epjc/s10052-021-09980-2. URL: https://doi.org/10.1140%2Fepjc%2Fs10052-021-09980-2.

[2] Ramesh Narayan and Jeffrey E. McClintock. *Observational Evidence for Black Holes.* 2014. arXiv: 1312.6698 [astro-ph.HE].

[3] Sean A. Hayward. "General laws of black-hole dynamics". In: *Physical Review D* 49.12 (June 1994), pp. 6467–6474. DOI: 10.1103/physrevd.49.6467.

[4] Cosimo Bambi. "Astrophysical Black Holes: A Review". In: *Proceedings of Multifrequency Behaviour of High Energy Cosmic Sources - XIII — PoS(MULTIF2019).* Sissa Medialab, Nov. 2020. DOI: 10.22323/1.362.0028. URL: https://doi.org/10.22323%2F1.362.0028.

[5] P. Hájíček and C. Kiefer. "Singularity Avoidance By Collapsing Shells in Quantum Gravity". In: *International Journal of Modern Physics D* 10.06 (Dec. 2001), pp. 775–779. DOI: 10.1142/s0218271801001578.

[6] Claus Kiefer and Tim Schmitz. "Singularity avoidance for collapsing quantum dust in the Lemaître-Tolman-Bondi model". In: *Phys. Rev. D* 99 (12 June 2019), p. 126010. DOI: 10.1103/PhysRevD.99.126010.

[7] Włodzimierz Piechocki and Tim Schmitz. "Quantum Oppenheimer-Snyder model". In: *Phys. Rev. D* 102.4 (2020), p. 046004. DOI: 10.1103/PhysRevD.102.046004. arXiv: 2004.02939 [gr-qc].

[8] Abhay Ashtekar. "Loop quantum cosmology: an overview". In: *General Relativity and Gravitation* 41.4 (Feb. 2009), pp. 707–741. DOI: 10.1007/s10714-009-0763-4.

[9] Carlo Rovelli and Francesca Vidotto. "Planck stars". In: *International Journal of Modern Physics D* 23.12 (Oct. 2014), p. 1442026. DOI: 10.1142/s0218271814420267.

[10] Hal M. Haggard and Carlo Rovelli. "Quantum-gravity effects outside the horizon spark black to white hole tunneling". In: *Physical Review D* 92.10 (Nov. 2015). DOI: 10.1103/physrevd.92.104020.

[11] Valeri P. Frolov and G. A. Vilkovisky. "Quantum Gravity Removes Classical Singularities and Shortens The Life of Black Holes". In: *The Second Marcel Grossmann Meeting on the Recent Developments of General Relativity (In Honor of Albert Einstein).* July 1979.

[12] Jacob D. Bekenstein. "Black Holes and Entropy". In: *Phys. Rev. D* 7 (8 Apr. 1973), pp. 2333–2346. DOI: 10.1103/PhysRevD.7.2333.

[13] Roberto Casadio. "Quantum dust cores of black holes". In: *Physics Letters B* 843 (Aug. 2023), p. 138055. DOI: 10.1016/j.physletb.2023.138055. URL: https://doi.org/10.1016%2Fj.physletb.2023.138055.

[14] V. F. Mukhanov. "Are black holes quantized?" In: *ZhETF Pisma Redaktsiiu* 44 (July 1986), pp. 50–53.

[15] J. R. Oppenheimer and H. Snyder. "On Continued Gravitational Contraction". In: *Phys. Rev.* 56 (5 Sept. 1939), pp. 455–459. DOI: 10.1103/PhysRev.56.455.

[16] Pankaj S. Joshi and Daniele Malafarina. "Recent Developments in Gravitational Collapse and Spacetime Singularities". In: *International Journal of Modern Physics D* 20.14 (Dec. 2011), pp. 2641–2729. DOI: 10.1142/s0218271811020792.

[17] J. Plebanski and Andrzej Krasinski. *An introduction to general relativity and cosmology*. 2006.

[18] Jos M M Senovilla. "Trapped surfaces, horizons and exact solutions in higher dimensions". In: *Classical and Quantum Gravity* 19.12 (May 2002), pp. L113–L119. DOI: 10.1088/0264-9381/19/12/101. URL: https://doi.org/10.1088%2F0264-9381%2F19%2F12%2F101.

[19] S. W. Hawking and G. F. R. Ellis. *The Large Scale Structure of Space-Time*. Cambridge Monographs on Mathematical Physics. Cambridge University Press, 1973. DOI: 10.1017/CBO9780511524646.

[20] Pankaj S. Joshi and Daniele Malafarina. "Recent Developments in Gravitational Collapse and Spacetime Singularities". In: *International Journal of Modern Physics D* 20.14 (Dec. 2011), pp. 2641–2729. DOI: 10.1142/s0218271811020792.

[21] P. Vaidya. "The Gravitational Field of a Radiating Star". In: *Proc. Natl. Inst. Sci. India A* 33 (1951), p. 264.

[22] Pankaj S Joshi, Daniele Malafarina, and Ramesh Narayan. "Equilibrium configurations from gravitational collapse". In: *Classical and Quantum Gravity* 28.23 (Nov. 2011), p. 235018. DOI: 10.1088/0264-9381/28/23/235018.

[23] Lemaître, G. "L'Univers en expansion". In: *Annales de la Société scientifique de Bruxelles* A53 (1993), pp. 51–85.

[24] Richard C. Tolman. "Effect of Inhomogeneity on Cosmological Models". In: *Proceedings of the National Academy of Sciences of the United States of America* 20.3 (1934), pp. 169–176.

[25] H. Bondi. "Spherically symmetrical models in general relativity". In: 107 (Jan. 1947), p. 410. DOI: 10.1093/mnras/107.5-6.410.

[26] Eric Poisson. *A Relativist's Toolkit: The Mathematics of Black-Hole Mechanics*. Cambridge University Press, 2004. DOI: 10.1017/CBO9780511606601.

[27] Roger Penrose. "Gravitational Collapse and Space-Time Singularities". In: *Phys. Rev. Lett.* 14 (3 Jan. 1965), pp. 57–59. DOI: 10.1103/PhysRevLett.14.57.

[28] Charles Torre. "Is general relativity an "already parametrized" theory?" In: *Physical review. D, Particles and fields* 46 8 (1992), R3231–R3234.

[29] Petr Hajicek. "Choice of Gauge in Quantum Gravity". In: *Nuclear Physics B Proceedings Supplements* (Jan. 2000), pp. 1213–.

[30] Petr Hajicek. "Quantum Theory of Gravitational Collapse (Lecture Notes on Quantum Conchology)". In: *Quantum Gravity*. Springer Berlin Heidelberg, 2003, pp. 255–299. DOI: 10.1007/978-3-540-45230-0_6.

[31] P. Vaidya. "The Gravitational Field of a Radiating Star". In: *Proc. Natl. Inst. Sci. India A* 33 (1951), p. 264.

[32] Włodzimierz Piechocki and Tim Schmitz. "Quantum Oppenheimer-Snyder model". In: *Physical Review D* 102.4 (Aug. 2020). DOI: 10.1103/physrevd.102.046004. URL: https://doi.org/10.1103%2Fphysrevd.102.046004.

[33] Gia Dvali and Cesar Gomez. "Black Hole's Quantum N-Portrait". In: *Fortschritte der Physik* 61 (July 2013). DOI: 10.1002/prop.201300001.

[34] Roberto Casadio et al. "Quantum corpuscular corrections to the Newtonian potential". In: *Physical Review D* 96.4 (Aug. 2017). DOI: 10.1103/physrevd.96.044010. URL: https://doi.org/10.1103%2Fphysrevd.96.044010.

[35] Roberto Casadio. *Geometry and thermodynamics of coherent quantum black holes*. 2022. arXiv: 2103.00183 [gr-qc].

[36] Robert M Wald. *General relativity*. Chicago, IL: Chicago Univ. Press, 1984.

[37] N. D. Birrell and P. C. W. Davies. *Quantum Fields in Curved Space*. Cambridge Monographs on Mathematical Physics. Cambridge University Press, 1982. DOI: 10.1017/CBO9780511622632.

[38] Roberto Casadio. "Quantum Black Holes and (Re)Solution of the Singularity". In: *Universe* 7.12 (2021). ISSN: 2218-1997. DOI: 10.3390/universe7120478.

[39] R Casadio et al. "Configurational entropy of black hole quantum cores". In: *Classical and Quantum Gravity* 40.7 (Mar. 2023), p. 075014. DOI: 10.1088/1361-6382/acbe89. URL: https://doi.org/10.1088%2F1361-6382%2Facbe89.

[40] C. E. Shannon. "A mathematical theory of communication". In: *The Bell System Technical Journal* 27.3 (1948), pp. 379–423. DOI: 10.1002/j.1538-7305.1948.tb01338.x.

[41] Roberto Casadio, Andrea Giusti, and Jorge Ovalle. "Quantum rotating black holes". In: *Journal of High Energy Physics* 2023.5 (May 2023). DOI: 10.1007/jhep05(2023)118.

[42] Vladimir N. Lukash and Vladimir N. Strokov. "Space-Times with Integrable Singularity". In: *Int. J. Mod. Phys. A* 28 (2013), p. 1350007. DOI: 10.1142/S0217751X13500073. arXiv: 1301.5544 [gr-qc].

[43] *NIST Digital Library of Mathematical Functions*. https://dlmf.nist.gov/, Release 1.1.9 of 2023-03-15. F. W. J. Olver, A. B. Olde Daalhuis, D. W. Lozier, B. I. Schneider, R. F. Boisvert, C. W. Clark, B. R. Miller, B. V. Saunders, H. S. Cohl, and M. A. McClain, eds.

[44] J. J. Sakurai and Jim Napolitano. *Modern Quantum Mechanics*. 2nd ed. Cambridge University Press, 2017. DOI: 10.1017/9781108499996.

[45] R.L. Burden, J.D. Faires, and A.M. Burden. *Numerical Analysis*. Cengage Learning, 2015. ISBN: 9781305465350.

[46] A. Spitzbart. "A Generalization of Hermite's Interpolation Formula". In: *The American Mathematical Monthly* 67.1 (1960), pp. 42–46. ISSN: 00029890, 19300972.